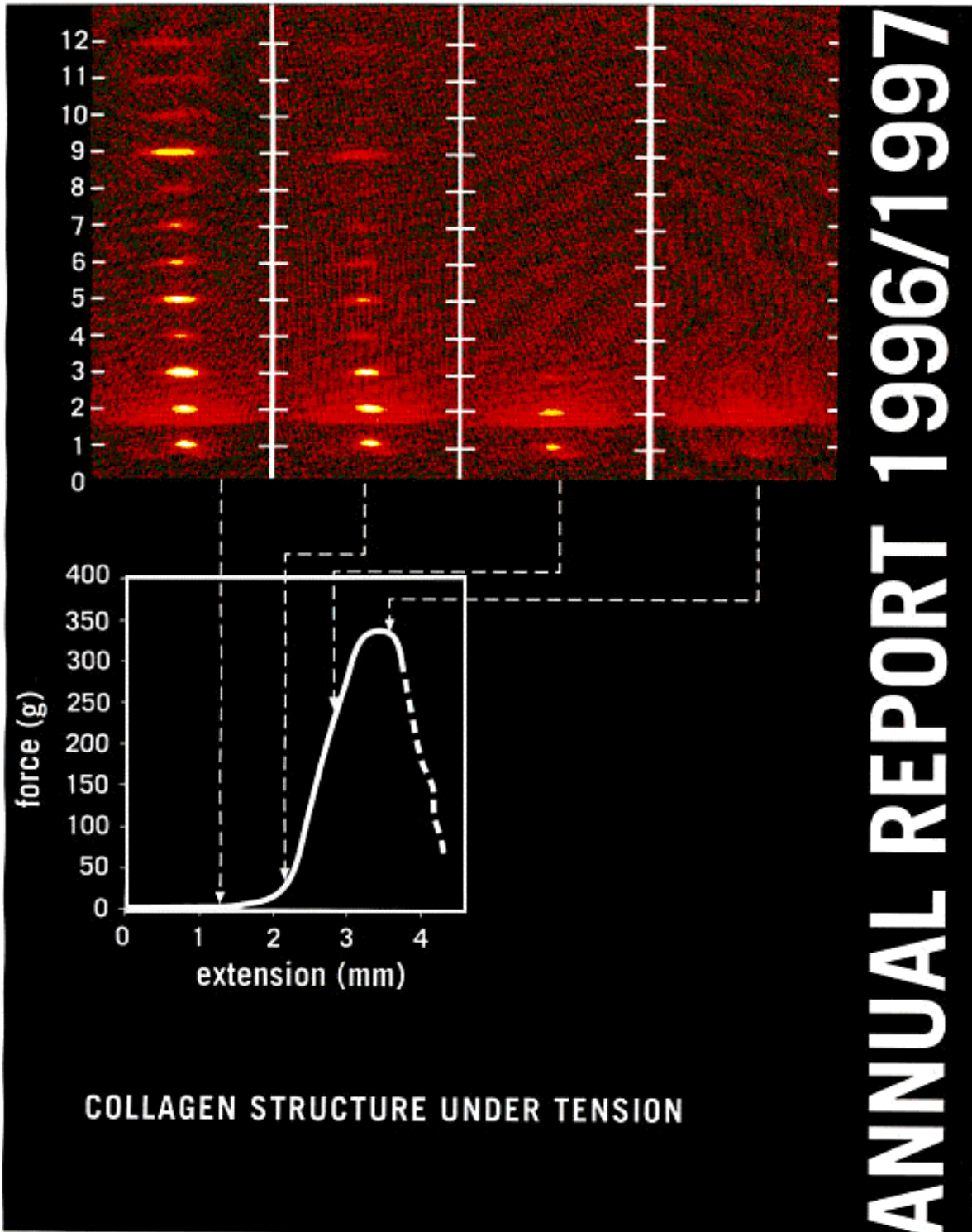


AUSTRIAN SAXS - BEAMLINE AT ELETTRA



ANNUAL REPORT 1996/1997



Extracted from the user contribution P. Fratzl et al.: *In-situ synchrotron x-ray scattering study of the tensile properties of collagen.*

Austrian Small Angle X-ray Scattering (SAXS) Beamline at ELETTRA

Annual Report 1996/1997

Compiled by the SAXS-Group

- for IBR: M. Rappolt and H. Amenitsch
- for ELETTRA: S. Bernstorff

Table of Contents

	<i>page</i>
➤ Preface	<i>1</i>
➤ The SAXS-Group	<i>3</i>
➤ The SAXS-Beamline in General	<i>4</i>
➤ Application for Beamtime at ELETTRA	<i>8</i>
➤ List of Institutes Participating in Experiments	<i>14</i>
➤ List of Performed Experiments	<i>20</i>
➤ User Statistics	<i>26</i>
➤ Technical Developments at the SAXS-beamline	<i>29</i>
1. Installation of the new monochromators (5.4 and 16 keV)	<i>29</i>
2. Installation the of the WAXS port	<i>31</i>
3. Set-up of various sample manipulations stages	<i>35</i>
➤ User Contributions	<i>40</i>
1. Material Sciences	<i>41</i>
2. Life Sciences	<i>52</i>
3. Physics	<i>83</i>
4. Chemistry	<i>89</i>
5. Instrumentation	<i>94</i>
➤ Publications	<i>103</i>
➤ Author Index	<i>115</i>

Preface

It is with a good feeling of gratitude and satisfaction that I can introduce the present, first Annual Report of the Austrian Academy of Sciences SAXS beamline at Elettra. Throughout the time of promoting and, at times, fighting for this new facility aimed at the creation of a competitive, young user community, there was always place for optimism; however, silent fears were there, and they were not related to the promises we made for the technical performance of the line, but much worse, to the possibility that it might fail to attract enough high-quality use right from the start.

As it turns out, and as is clearly documented here, this was not justified. The project is exactly on target. It has proven, already after the first sixteen months of its regular operation, to be a very welcome and popular facility - we have to deal with close to 80 % more time requested than available - for the regional and international community in biophysics and material science, and in many instances a unique tool for cutting-edge research.

What we now can see to emerge at this station is truly encouraging: it is a place, to which creative scientists are keen to come with their ambitious experiments, and where they not only collect data, but also exchange ideas with colleagues and the beam-line scientists. The SAXS hutch is a good place to be, although it sometimes gives the impression of 'life under adverse conditions'. For creating that climate, and for many other achievements throughout all periods from the very beginning of the project, the on-site SAXS team managed by Sigrid and Heinz, deserve my sincerest thanks. Together with the Elettra crew they have done their best to make this a user-friendly and competitive station - and they continue to make it even better. The credit must go to the users, however, for having shown that this investment is successful and provides excellent scientific returns.

For much of the time, for better or worse, I played my role on a different stage, the one where the sometimes frightening dramas of fund-raising, bargaining with partners, industrial and institutional, and negotiations for any thinkable boundary conditions are given. I want to use this present opportunity to thank the many co-actors: the ministerial responsables, my peers at the Austrian Academy of Sciences, our industrial suppliers, and last but not least, the partners at the Elettra management, for all their support, encouragement and endurance. It was worth all the efforts, and I don't regret a minute of it, much less than my wife and daughters understandably did when I was on the road again.

I feel deeply sad that Luciano Fonda, who, apart from the love for sailing, shared with me so much of his early visions and excitement of a synchrotron light source at Trieste, and who has really first triggered my own plans for getting involved with it, will not be there any more.

Peter Laggner
Director
Institute of Biophysics and X-Ray Structure Research,
Austrian Academy of Sciences

Welcome, SAXS!

Watching the Austrian Academy of Sciences SAXS facility on Elettra becoming a world-level resource - very quickly after its commissioning - was a real pleasure. And hosting it is a honor, both for me personally and for the entire Elettra staff and management -- for several reasons.

First of all, this is truly an outstanding facility which opens the way to a huge variety of new experiments. Second, its high technical level means not only excellent performances but also the high reliability that is required to serve a wide user community. In other words, the SAXS facility is a scientific resource not at the Austrian-Italian level, but for Europe and the world science in general.

This success is particularly important for Elettra, because it is also the success of a bold policy of international open doors. Elettra, as it is known, was funded by Italian source and therefore was born as a national facility. Since the very beginning, however, a decision was made to aggressively seek an international status, by opening the door to international users through open competition based on merit.

The SAXS facility is the spearhead of this policy. It is the first truly international beamline commissioned and operating on Elettra, and it opened the way to new initiatives such as the Czech and Slovenian beamlines. And we hope to see many more in the future.

The international vocation of Elettra was recently emphasized by the transfer here of the coordination of the European Round Table for Synchrotron Radiation and Free Electron Lasers. This is a tangible sign of a much broader process, initiated by the SAXS beamline. For this and for many other reasons - chiefly scientific excellence - we feel deeply indebted to the Austrian Academy of Sciences and to all the colleagues who played a role in the SAXS design, construction and commissioning.

A particular note of thanks goes to the leader of this project, Professor Peter Laggner: without his vision, his perseverance in front of formidable obstacle, his dream of a very advanced scientific instrument, SAXS would not be today a wonderful reality.

As to the future, my personal wishes of continuing success: good hunting after an outstanding job!

Giorgio Margaritondo
Director, Elettra Experimental Division
Coordinator, European Round Table for Synchrotron Radiation
and Free Electron Lasers

The SAXS-Group

- HEAD OF PROJECT: Peter Laggner¹⁾
e-mail: fibrlagg@mbox.tu-graz.ac.at
- SCIENTISTS: Heinz Amenitsch^{1), 3)}
e-mail: Amenitsch@Elettra.Trieste.It
Sigrid Bernstorff²⁾
e-mail: Bernstorff@Elettra.Trieste.It
- POSTDOCS: Pavo Dubcek²⁾
e-mail: Pavo.Dubcek@Elettra.Trieste.It
Ralf Menk²⁾
e-mail: Ralf.Menk@Elettra.Trieste.It
Michael Rappolt^{1), 3)}
e-mail: Michael.Rappolt@Elettra.Trieste.It
- PhD-STUDENTS: Georg Pabst^{1), 3)}
e-mail: Georg.Pabst@Elettra.Trieste.It

- 1) Institute for Biophysics and X-ray Structure Research, Austrian Academy of Sciences, Steyrergasse 17, 8010 Graz, Austria.
Tel 0043-316-812 004
Fax 0043-316-812 367
- 2) Sincrotrone Trieste, Strada Statale 14, km 163.5, 34012 Basovizza (TS), Italy.
Tel 0039-040-375 81
Fax 0039-040-938 0902
- 3) Institute for Biophysics and X-ray Structure Research, Austrian Academy of Sciences
c/o Sincrotrone Trieste

The SAXS-Beamline in General

Small Angle X-ray Scattering has become a well known standard method to study the structure of various objects in the spatial range from 1 to 1000 nm, and therefore instruments capable to perform such experiments are installed at most of the synchrotron research centers. The high-flux SAXS beamline at ELETTRA is mainly intended for time-resolved studies on fast structural transitions in the sub-millisecond time region in solutions and partly ordered systems with a SAXS-resolution of 1 to 140 nm in real-space.

The photon source is the 57-pole wiggler whose beam is shared and used simultaneously with a Macromolecular Crystallography beamline. The wiggler delivers a very intense radiation between 4 and 25 keV of which the SAXS-Beamline accepts 3 discrete energies, namely 8 keV and, since spring 1998, also 5.4 and 16 keV are accessible to users. The beamline optics consists of a flat double crystal monochromator and a double focusing toroidal mirror.

A versatile SAXS experimental station has been set-up, and an additional wide-angle X-ray scattering (WAXS) detector has been installed in 1997 monitoring simultaneously diffraction patterns in the range from 0.1 to 0.9 nm. The sample station is mounted move-able onto an optical table for optimizing the sample detector distance with respect to SAXS resolution and sample size.

Besides the foreseen sample surrounding the users have the possibility to install their own specialized sample equipment. In the design phase, besides technical boundary conditions, user friendliness and reliability have been considered as important criteria.

The optimization of the beamline with respect to high-flux and consequently high flux density, allows to perform the following experiments:

- Low Contrast Solution Scattering
- Grazing Incidence Surface Diffraction
- Micro-Spot Scanning
- X-ray Fluorescence Analysis
- Time-Resolved Studies $\geq 11 \mu\text{s}$
- Simultaneously Performed Small- and Wide-Angle Measurements (SWAXS) on:
 - Gels
 - Liquid Crystals
 - (Bio) Polymers
 - Amorphous Materials
 - Muscles

Furthermore, using 5.4 and 16 keV energies, the beamline is widely applicable also to very thin, e.g. single muscle fibers, and optically thick (high Z) specimen, as often used in e.g., material science and solid state physics.

THE INSERTION DEVICE

The wiggler for the SAXS beamline consists of three 1.5 m long segments, each having 19 poles. The device can work with a minimum gap of 20 mm, which corresponds to $K=20$ at 2 GeV. The main parameters of the wiggler are:

- Critical Energy 4.1 keV
- Radiation Power 8.6 kW
- Flux 3.5×10^{14} ph/s/mrad/0.1%BW (at 400 mA)

The wiggler radiation cone has a horizontal width of 9 mrad. From this the SAXS-beamline accepts vertically 0.3 mrad, and horizontally +/-0.5 mrad at a 1.25 mrad off-axis position. The resulting source size for 8 keV photons is 3.9 x 0.26 mm² (horiz. x vert.).

THE OPTICS

The optics common with the diffraction beamline consists of:

- C-Filter and Beryllium window assembly to reduce the power load on the first optical elements by a factor of 2 and to separate the beamline vacuum from the storage ring.
- Beam defining slit chamber which allows to define the SAXS beam on three sides before the monochromator in order to reduce the straylight in the downstream beamline sections.

The SAXS beamline optics consists of:

- A double-crystal monochromator consisting of four individual chambers, in which three interchangeable asymmetric Si(111) crystal pairs are used to select one of three fixed energies. Each of the crystal pairs is optimized for the corresponding energy to accomplish a grazing angle of 2°. The energy resolution $\Delta E/E$ of the monochromator is in the range of $0.7 - 2.5 \cdot 10^{-3}$.
- A baffle chamber after the monochromator is used as an adjustable straylight fenditure.
- A segmented toroidal mirror focuses the light in horizontal and vertical direction with a 1/2.5 magnification onto the SAXS-detector.
- An aperture slit reduces the straylight after the monochromator and the toroidal mirror.
- A guard slit defines the illuminated region around the focal spot.
The spot size on the detector is 1.6 mm horizontally and 0.6 mm vertically. The calculated flux at the sample is in the order of 10^{13} ph/s at 400 mA. For a maximum sample size of 5.4 x 1.8 mm² correspondingly a flux density of 10^{12} ph/s/mm² has been calculated.

SAMPLE STAGE

The multipurpose sample stage allows to perform fast time-resolved relaxation studies based on temperature- or pressure-jumps as well as stopped flow experiments. Shear jump relaxation experiments are planned. Specifically, T-jumps can be induced by an infra-red light pulse (2 ms) from an Erbium-Glass laser, raising the temperature about 10°C in an aqueous sample volume of 10 µl. A newly designed hydrostatic pressure cell with a maximal accessible angular range of 30° for simultaneous SAXS and WAXS measurements is available. P-jumps are realized by switching fast valves between a low and a high pressure reservoir, increasing or decreasing the hydrostatic pressure in the range from 1 bar to 1.7 kbar (in future 3 kbar) within a few ms. Lately also a 1.5 T magnet has been installed. In an overview, the following sample manipulations are possible:

- Temperature Manipulations: Ramps, Jumps and Gradient Scans
 - Pressure Manipulation: Scan and Jumps
 - Stopped Flow Experiments
 - SWAXS Measurements Applying Mechanical Stress
 - SWAXS Measurements Applying Magnetic Fields
- (For further details see also Technical Developments part 3.)

Scientific applications	<p>Low Contrast Solution Scattering, Grazing Incidence Surface Diffraction, Micro-Spot Scanning, X-ray Fluorescence Analysis, Time-Resolved Studies $\geq 11 \mu\text{s}$ and Simultaneously Performed Small- and Wide-Angle Measurements (SWAXS) on:</p> <p>Gels Liquid Crystals (Bio) Polymers Amorphous Materials Muscles</p>
Source characteristics	<p><u>Wiggler (NdFeB Hybrid):</u></p> <p>Period 140 mm No. full poles 57 Gap 20 mm B_{max} 1.607 T Critical Energy ϵ_c 4.27 keV Power (9 mrad) 8.6 kW Effective source size FWHM $3.9 \times 0.26 \text{ mm}^2(\text{HxV})$</p>
Optics	<p><u>Optical elements:</u> Double crystal monochromator: Si (111) asym. cut, water cooled. Mirror: two-segment, toroidal, Pt coated.</p> <p><u>Distance from source:</u> 18.4 m 26.5 m</p> <p>Acceptance 1 mrad/0.3 mrad (HxV) Energy (3 selectable) 5.4, 8, 16 keV (0.077, 0.154, 0.23 nm) Energy resolution $\Delta E/E$ $0.7\text{-}2.5 \times 10^{-3}$ Focal spot size FWHM $1.2 \times 0.6 \text{ mm}^2(\text{HxV})$ Spot at Sample FWHM $5.4 \times 1.8 \text{ mm}^2(\text{HxV})$ Flux at sample $5 \times 10^{12} \text{ ph s}^{-1}(2 \text{ GeV}, 200 \text{ mA}, 8 \text{ keV})$</p>
Experimental apparatus	<p><u>Resolution in real space:</u> 1-140 nm (small-angle), 0.1- 0.9 nm (wide-angle)</p> <p><u>Sample stage:</u> temperature manipulations: ramps, jumps and gradient scans, pressure manipulation: scan and jumps, flow jump experiments, SWAXS measurements applying mechanical stress, SWAXS measurements applying magnetic fields.</p> <p><u>Detectors:</u> 1D gas-filled detectors for simultaneous small- and wide-angle (Gabriel type), 2D CCD-detector for small-angle.</p>
Experiment control	<p><u>Beamline control:</u> Program-units written in LabView for Windows <u>1 D detector control:</u> PC-card and software from Hecus & Braun, Graz.</p>

CURRENT STATUS

The beamline has been built by the Institute for Biophysics and X-ray structure Research (IBR), Austrian Academy of Science, and is now in user operation since September 1996. The set-up of the beamline started at the beginning of January 1995 with the installation of the support structure. Until the end of 1995, the 8 keV single energy system had been realized. The upgrade to the full three energy system was finished in spring 1998. Time resolved experiments require fast X-ray detectors and data acquisition hard- and software. Depending on the desired resolution in time and in reciprocal space, on isotropic or anisotropic scattering of the sample, one-dimensional position sensitive (delay-line type) or two-dimensional area detectors (CCD-type, available since June 1998) are employed.

In conclusion, due to wide tuneability of the beamline and the highly variable kept sample stage, there are nearly no limits for the realization of an experiment, and you are welcome by our team to propose any interesting and highlighting investigation for the benefit of material and life sciences.

Application for Beamtime at ELETTRA

1. Beamtime Policy at SAXS beamline

The agreement of setting-up a collaborating research group, and the co-operation between the Austrian Academy of Sciences and Sincrotrone Trieste concerning the SAXS beamline, has been signed on the 20th March 1998. It defines also the beamtime distribution between the partners and the beamtime policy.

The following points are of interest for users:

The available beamtime of 5000 hours/year is distributed as follows:

- 35% for Austrian Users, type: "CRG" (Collaborating Research Group)
- 50% for Users of Sincrotrone Trieste (ST)
- 15% is reserved for beamline maintenance

In both user beamtime contingents also any industrial, proprietary and confidential research can be performed according to the "General User Policy" of Sincrotrone Trieste.

To apply for CRG and ST user beamtime proposals must be submitted according to the rules of Sincrotrone Trieste. The international review committee at ELETTRA will rank the proposals according to their scientific merit assessment. Based on this decision beamtime will be allocated according to the specific quotes for the beamtimes (CRG/ST).

2. How to apply for beamtime

Users can apply for beamtime every half a year (next deadline will be August 31, 1998) and must send their application forms to:

ELETTRA USERS OFFICE
Strada Statale 14 - km. 163.5
34012 Basovizza (Trieste), ITALY
Tel: +39 040 3758628 - fax: + 39 040 3758565
email: useroffice@elettra.trieste.it

INSTRUCTIONS GIVEN BY THE USERS OFFICE

The Application Form must be completed and sent by normal or express mail to the Users Office. Please note, that PROPOSALS CANNOT BE SUBMITTED BY FAX. Originals together with the requested number of copies must be submitted by the deadline. Late proposals will not be evaluated by the Review Committee.

- Read carefully the following Guidelines.
- Type your proposals in English.
- Respect the available space on the form.
- Include a typed description of the proposed experiment (see page 3 of the Application Form), stating clearly background and objectives.
- Give results of preliminary work carried out with different methods (e.g., in-house X- rays, light scattering, NMR, neutrons, etc.).

- Fill in and sign the section concerning safety aspects.
- In case of continuation proposals:
 - Attach the experimental report of previous measurements. Proposals without such report may not be evaluated.
 - Give your previous proposal number.
- In case of resubmission proposals give previous proposal number.
- The original version must be sent together with 12 additional copies (2-sided), in reduced form, i.e., a photocopy from two A4 pages of the original form reduced to a single A4 page. Different formats will not be accepted.

For further information, e.g., financial support for travel expenses, please have a look into the web-pages of ELETTRA or contact the USERS OFFICE:

<http://www.elettra.trieste.it/Documents/Index/UsersInfo.html>

ELETTRA APPLICATION FORM

SINCROTRONE TRIESTE S.C.p.A. – Users' & European Relations Office
 S.S. 14, km. 163,5 in AREA Science Park – I-34012 Basovizza TS Italy
 tel.:+39 40 3758628 / 8592 / 8538 – email: useroffice@elettra.trieste.it

Experiment title	Proposal number <i>(to be completed by ST)</i>
-------------------------	--

Beamtime is requested as:

- General User

 Research Team (RT)

Please indicate if the research is :

- Non proprietary

 Proprietary

Please indicate if you intend to require financial support through the EU contract "Large Scale Installation Facility":

- Yes

 No

Please indicate the research area of your proposal:

- Physics

 Chemistry

 Medical applications
 Life sciences

 Technology/Instrumentation

 Other areas:.....

Proposer <i>(to whom correspondence will be addressed)</i>	
Name:	
Institution/Company:	
Address:	City:
Mail code:	Country:
Phone:	Fax:
Email:	
Name of local contact at ELETTRA:	

Beamline(s) required	Number of shifts required <i>(1 shift is 8 hours)</i>	Requested starting date
Electron beam requirements:		Unacceptable date (s)
<input type="checkbox"/> Single bunch <input type="checkbox"/> Multibunch		

This proposal is:

- A new proposal
 A continuation proposal
 (please attach a copy of your experimental report and your previous proposal number)
 A resubmission
 (please give previous proposal number)

This proposal is :

- A normal application
 An urgent request
 A long-term project

	Name of other participants	Complete institution/company address	Phone	Telefax	e-mail
1					
2					
3					
4					
5					
6					
7					

Experimental details

Photon energy:

Photon energy resolution:

Other requirements:

Sample environment/treatment

- 1) PLEASE, DESCRIBE THE ENVIRONMENT AND/OR TREATMENT THE SAMPLE WILL BE SUBJECT TO DURING THE EXPERIMENT:

- 2) LIST ALL THE AVAILABLE EQUIPMENT THAT YOU WILL USE FOR THE EXPERIMENT ON THE EXPERIMENTAL STATION (*CHECK IT WITH THE ST BEAMLINE COORDINATOR*)

- 3) LIST ALL THE ADDITIONAL EQUIPMENT THAT YOU NEED TO INSERT IN THE EXPERIMENTAL STATION:

- 4) INDICATE YOUR REQUIREMENTS FOR SPECIAL EQUIPMENT OR FACILITIES TO BE USED OFF-LINE:

Description of the proposed experiment.

The proposal must include: the background, the objectives, the scientific interest of the experiment, the specific need for using synchrotron radiation and ELETTRA's advanced characteristics (the description must not exceed two pages).

To be completed by ST

Proposal n.....

Beamline.....

SAFETY FORM

Sample(s) and chemical substance(s) to be used in this experiment

(in case of more than one sample needed, please attach copies of this page)

If no data sheet is available, please give detailed information about all the samples and chemical substances to be used in the experiment.

Substance:

Chemical formula:

Powder

Liquid

Single Crystal

Multilayer

Biocrystallography

Others:

Size (in mm³):

Mass (in mg):

Surface area:

Space group (if known)

Unit cell dimensions at

T:

a=

b=

c=

α =

β =

γ =

Sample container (capillary, flat plate, pressure cell, etc.):

Safety aspects

If no data sheet is available, please give detailed information about the toxicity of chemical products and potential fire risks

Is there any risk associated with the proposed sample, any preparation at ELETTRA, or sample equipment?

Yes

Uncertain

No

If yes or uncertain, please give details of the risks associated:

the sample is:

Radioactive

Contaminant

Toxic

Inflammable

Explosive

Corrosive

A biological hazard

Oxidising

Combustive

Carcinogene

Exhaust disposal conditions:

Sample disposal: After the experiment the sample will be:

Removed by user

Stored at ELETTRA

Disposed of by ELETTRA

I certify that the above details are complete and correct. I authorize ST to use the above data, including personal data, for all the purposes related to ST activity.

Date:.....

Signature:.....

To be completed by Sincrotrone Trieste Safety Officer

List of Institutes Participating in Experiments

Austria

Austrian Academy of Science, Erich Schmid Institut für
Materialwissenschaft, Leoben

Fratzl Peter

Zizak Ivo

Institut für Metallphysik, Montanuniversität, Leoben

Ortner Balder

Paris Oskar

Austrian Academy of Science, Institute for Biophysics and X-ray Structure
Research, Graz

Amenitsch Heinz

Chemloul Mohammed

Pregetter Magdalena

Krenn Christian

Kriechbaum Manfred

Laggner Peter

Latal Angelika

Lohner Karl

Pabst Georg

Prassl Ruth

Pressl Karin

Rappolt Michael

Schwarzenbacher Robert

Staudegger Erich

Hecus Braun, Graz

Mio Hannes

Weingartner Werner

Ludwig Boltzmann Institut für Osteologie, Wien

Roschger Paul

Ludwig Boltzmann-Institut für Osteologie, und UKH-Meidling & Hanusch-
Krankenhaus, Wien

Klaushofer Klaus

Research Institute for Molecular Pathology, Vienna

Oft Martin

Petritsch Claudia

Universität Graz, Institut für Physikalische Chemie, Graz

Glatter Otto

Universität Linz, Institut für Halbleiterphysik, Linz

Bauer Guenther

Boller H.

Darhuber Anton

Stangl Julian

Universität Wien, Institut für Materialphysik, Wien

Kopacz Ireneusz

Kral Robert

Loidl Dieter

Peterlik Herwig

Schafler Erhard

Zehetbauer Michael

Universität Wien, Institut für Materialphysik & Ludwig Boltzmann Institut für
Osteologie, Wien

Lichtenegger Helga

Misof Klaus

Rinnenthaler Susanne

Croatia

Institute for Physics, Zagreb

Milat Ognjen

"Ruder Boskovic" Institute, Zagreb

Etlinger Bozidar

Gotic Marijan

Ivanda Mile

Music Svetozar

Turkovic Aleksandra

University of Split, Faculty of Technology, Split

Lucic-Lavcevic Magdi

Czech Republic

Academy of Sciences of the Czech Republic, Institute of Macromolecular
Chemistry, Prague

Baldrian Josef

Horky Martin

Plestil Josef

Pospìsil Herman

Steinhart Milos

Vlèek P.

Germany

Forschungszentrum Jülich K.F.A, Institut für Festkörperforschung,
Carsughi Flavio

Max-Planck-Institut für Biochemie, Abtl. Membran- und Neurophysik, Martinsried
Heumann Hermann
Rößle Manfred

Universität Leipzig, Institut für Experimental Physik I, Leipzig
Gutberlet Thomas
Heerklotz Heiko
Klose Gotthard
Mädler Burghard

Universität Mainz, Institut für Biochemie, Mainz
Lauer Iris
Nawroth Thomas

Universität Siegen, Walter Flex Strasse, 57068 Siegen
Meissner Wolff
Sarvestani Amir
Walenta Albert Heinrich

Hungary

Central Research Institute for Physics, Institute of Solid State Physics, Budapest
Borbély S.
Rosta L.

Eötvös University, Institute for General Physics, Budapest
Hanak Peter
Ungár Tamas

Hungarian Academy of Sciences, Biological Research Center, Institute of Plant
Biology, Szeged
Cseh Zoltan
Garab Gyozo
Jávorfi Tamas
Mustárdy L.

Italy

CNR, Istituto Struttura della Materia, Sezione di Trieste
Matteucci Maurizio

ICGEB, Area di Ricerca, Trieste
Kühne Christian

Sincrotrone Trieste, Trieste

Arfelli Fulvia
Bernstorff Sigrid
Dubcek Pavo
Kiskinova Maya
Lonza Diego
Menk Ralf
Pontoni Diego
Prince Kevin C.
Romanzin Luca

Università di Ancona, INFN-Istituto di Scienze Fisiche, Ancona

Bin Yang
Ciuchi Federica
Maccioni Elisabetta
Mariani Paolo
Spinozzi Francesco

Università di Bologna, Dip. di Chimica "G. Ciamician", and C.N.R., Centro di Studio per la Fisica delle Macromolecole, Bologna

Bigi A.
Ferracini Elena
Ferrero Adele
Malta Viscardo
Ottani Stefano
Roveri Norberto

Università di Firenze, Dip. Scienze Fisiologiche, Firenze

Bagni Maria Angela
Cecchi Giovanni
Colombini Barbara
Linari Marco
Lombardi Vincenzo
Lucii Leonardo
Piazzesi Gabriella
Reconditi Massimo

Università di Genova, Istituto di Biofisica, Genova Sestri Ponente

Carrara Sandro
Erokhin Viktor
Nicolini Claudio

Università di Genova, Dip. di Fisica, e INFN, Sez. di Genova, Genova

Ottonello Pasquale
Rottigni G. Antonio

Università di Padova, Dip. di Fisica, e Istituto Nazionale di Fisica Nucleare, Sezione di Padova, Padova

Fantozzi Esme' Maria.Giuliana.
Zannella Giovanni
Zanoni Roberto

Università di Parma, Dip. di Fisica, e INFN Parma
M. Fontana

Università di Torino, Istituto Sperim. Nutrizione Piante, Torino
Marchesini A.

Università di Trieste, Dip. Biochimica, Biofisica, Chimica delle Macromole
(BBCM), Trieste
Rizzo Roberto
Vittur Franco
Gamini Amelia

Japan

Kyoto University, Institute for Chemical Research, Kyoto
Hiragi Yuzuru

Slovenia

Josef Stefan Institute, Ljubljana
Lahajnar G.
Zidanssek A.

University of Maribor, Department of Physics, Faculty of Education, Maribor
Kralj S.

University of Ljubljana, Department of Physics, Faculty of Mathematics and
Physics, Ljubljana
Blinc R.

Russia

Moscow State Univ., Dept. Mechanics, Moscow
Tsaturyan Andreij
Koubassova Natalia

Urals Branch of Russian Acad. Sci., Dept. Biophys., Inst. Pjysiol.,
Popova Yekaterinburg
Sergey Bershitsky

United Kingdom

King's College, Department of Biophysics, Cell and Molecular Biology, London
Ian Dobbie
Irving Malcolm

University of Bristol, H.H. Wills Physics Laboratory, Bristol

Gathercole L.J.
Hollis K.
Shah Jitendra

University Laboratory of Physiology, Oxford
Ashley Chris C
Griffiths Peter J.

USA

Duke University, Medical Center, Durham
Reedy Michael

List of Performed Experiments

1996:

Proposa I	Proposer	Institution	Country	Title	Research Area
Pilot	Laggner Peter, Latal Angelika	Austrian Academy of Sciences, Inst. of Biophysics and X-ray Structure Research, Graz	Austria	Effects of antimicrobial and haemolytic peptides on Phase Behaviour of Biomembranes	Life Sciences
CRG, Pilot	Kriechbaum Manfred, Steinhart Milos	Austrian Academy of Sciences, Inst. of Biophysics and X-ray Structure Research, Graz	Austria	P-scans in Lipids (Test of pressure-cell)	Instrumentation
CRG, Pilot	Zehetbauer Michael	Austrian Academy of Sciences, Inst. of Biophysics and X-ray Structure Research, Graz	Austria	Scanning wide angle micro diffraction on deformed metallic polycrystals I	Material Sciences
CRG	Mio Hannes, Chemloul Mohammed	Austrian Academy of Sciences, Inst. of Biophysics and X-ray Structure Research, Graz	Austria	High count rate performance and time resolution of delay line detector at SAXS beamline	Instrumentation
CRG	Schwarzenbacher Robert	Austrian Academy of Sciences, Inst. of Biophysics and X-ray Structure Research, Graz	Austria	Temperature scans in non-ionic surfactant Brij35	Life Sciences
Pilot	Zanella Giovanni	Univ. of Padova	Italy	Tests of CCD camera system at a high flux SR source	Instrumentation
033/96	Cecchi Giovanni	Univ. di Firenze - Dip. di Scienze Fisiologiche, Firenze	Italy	Time resolved mechanical and x-ray diffraction studies on intact single muscle fibres	Life Sciences
CRG	Fratzl Peter	Univ. of Vienna, Austria	Austria	High resolution scanning SAXS of bone sections	Life Sciences
CRG	Fratzl Peter	Univ. of Vienna, Austria	Austria	Combined SAXS and WAXS of cortical bone	Life Sciences

Pilot	Boller H.	Univ. Linz, Austria	Austria	Diffuse wide angle diffraction on small single crystals	Physics
CRG	Pressl Karin, Laggner Peter	Austrian Academy of Sciences, Inst. of Biophysics and X-ray Structure Research, Graz	Austria	High resolution T-scans in Lipids	Life Sciences
Pilot	Vittur Franco, Di Fonzo Silvia	Univ. Trieste, Sincrotrone Trieste	Italy	Determination of the collagen fibre orientation in different regions of articular cartilage	Life Sciences
Pilot	Rappolt Michael	Sincrotrone Trieste	Italy	T-scans with gradient cell in DPPC	Life Sciences
033/96	Zehetbauer Michael	Austrian Academy of Sciences, Inst. of Biophysics and X-ray Structure Research, Graz	Austria	Scanning wide angle micro diffraction on deformed metallic polycrystals II	Material Sciences
CRG Pilot	Baldrian Josef	Czech Acad. of Sciences Inst. of Macromol. Chemistry Heyrovsky sq. 2 Praha 6 16206 Czech Republic	Austria	Time-resolved SAXS and WAXS studies on macromolecular materials	Material Sciences
031/96	Ferracini Elena	Univ. di Bologna - Dip. di Chimica, Bologna	Italy	Relationships among synthesis, structure and drawability of nascent reactor powders of high molecular weight polyethylene (HMWPE)	Chemistry

1997: January-August

Proposa l	Proposer	Institution	Country	Title	Research Area
CRG	Glatter Otto	Univ. Graz	Austria	Time dependent small angle scattering studies on the refolding process of substrate protein mediated by the E. Coli chaperonin system GroEL-GroES	Life Sciences
076/96	Carrara Sandro	Univ. di Genova, Genova Sestri Ponente	Italy	Small angle scattering study of the shape and size of CdS particles in solution	Physics

077/96	Carrara Sandro	Univ. di Genova, Genova Sestri Ponente	Italy	Small angle scattering study of chromatin in different preparations	Life Sciences
078/96	Carrara Sandro	Univ. di Genova, Genova Sestri Ponente	Italy	Small angle scattering study of protein langmuir-blosgett films	Physics
088/96	Rappolt Michael	Sincrotrone Trieste	Italy	T-scans with gradient cell in DPPC	Life Sciences
CRG	Darhuber Anton	Univ. Linz	Austria	Surface Diffraction on Quantum Dots	Physics
028/96	Lombardi Vincenzo	Univ. di Firenze - Dip. Scienze Fisiologiche Firenze	Italy	Structural changes accompanying of force in single muscle fibres: combined mechanical and diffraction study on the molecular aspect of muscle contraction I	Life Sciences
029/96	Baldrian Josef	Czech Acad. of Sciences Inst. of Macromol. Chemistry Heyrovsky sq. 2 Praha 6 16206 Czech Republic	Austria	Time-resolved SAXS and WAXS studies on macromolecular materials	Material Sciences
152/96	Cecchi Giovanni	Universita di Firenze Dip. di Scienze Fisiologiche, Firenze	Italy	Time resolved mechanical and x-ray diffraction studies on single muscle cell	Life Sciences
155/96	Lombardi Vincenzo	Universita di Firenze Dip. di Scienze Fisiologiche, Firenze	Italy	Structural changes accompanying development of force in single muscle fibres: combined mechanical and diffraction study on the molecular aspect of muscle contraction II	Life Sciences
174/96	Prince Kevin	Sincrotrone Trieste, Trieste	Italy	Test experiment: x-ray fluorescence analysis	Physics
193/96	Turkovic Aleksandra	"Ruder Boskovic" Institute, Zagreb	Croatia	SAXS study of grain sizes and porosity in nanophase TiO ₂	Physics
220/96	Rappolt Michael	Sincrotrone Trieste, Trieste	Italy	Submillisecond time resolved x-ray diffraction on phospho-lipid/water systems by laser temperature-jump	Life Sciences
222/96	Kriechbaum Manfred	Austrian Academy of Sciences Inst. for Biophysics & X-ray Structure Research, Graz	Austria	High pressure time-resolved x-ray diffraction for the study of phase behaviour in lipio dispersion	Life Sciences
239/96	Mariani Paolo	Universita di Ancona Istituto di Scienze Fisiche	Italy	Columnar growth in deoxyguanosine four-stranded helices in isotropic solution	Life Sciences
240/96	Mariani Paolo	Universita di Ancona Istituto di Scienze Fisiche	Italy	And structure and conformation analysis of soluble proteins	Life Sciences

250/96	Latal Angelika	Austrian Academy of Sciences Inst. for Biophysics & X-ray Structure Research, Graz	Austria	Effects of Antimicrobial and Hemolytic Peptides of Phase Behaviour of Biomembranes	Life Sciences
256/96	Kriechbaum Manfred	Austrian Academy of Sciences Inst. for Biophysics & X-ray Structure Research, Graz	Austria	The folding and substrate binding of a multidomain protein	Life Sciences
257/96	Garab Gyozo	Hungarian Academy Sciences Biological Research Center	Hungary	Structure and dynamics of lamellar aggregates of LHCII	Life Sciences
258/96	Baldrian Josef	Czech Academy of Sciences Inst. of Macromolecular Chemistry	Czech Republic	Time resolved SAXS and WAXS studies on macromolecular materials	Chemistry
259/96	Fratzl Peter	Universität Wien Institut für Materialphysik	Austria	High-resolution scanning SAXS of Bone sections	Life Sciences
260/96	Fratzl Peter	Universität Wien Institut für Materialphysik	Austria	In-situ synchrotron x-ray scattering study of the tensile properties of collagen	Life Sciences
263/96	Schwarzenbacher Robert	Austrian Academy of Sciences Inst. for Biophysics & X-ray Structure Research, Graz	Austria	Time resolved structural examinations on the ternary Liquid-crystal-system (Di-tert-butylether/Brij/water)	Chemistry
264/96	Zehetbauer Michael	Universität Wien Institut f. Materialphysik	Austria	X-ray bragg line profile analysis of FCC metals after extreme plastic deformation	Physics
267/96	Amenitsch Heinz	Austrian Academy of Sciences Inst. for Biophysics & X-ray Structure Research, Graz	Italy	Structure determination with SAXS measurements of various modified P70S6kinase at very low concentration	Life Sciences
274/96	Plestil Josef	Academy of Sciences of Czech Republic, Inst. of Macromolecular Chemistry, Prague	Czech Republic	SAXS measurements on solutions of labeled epoxide-monoamine comb-like chains at very low concentrations	Chemistry
276/96	Vittur Franco	Univ. di Trieste, Dip. Biochimica, Biofisica, Chimica delle Macromole, Trieste	Italy	Determination of the collagen fiber orientation in the different regions of articular cartilage	Life Sciences
280/96	Bauer Günther	Universität Linz Institut für Halbleiterphysik, Linz	Austria	x-ray reflection from self-assembled quantum dots and rough superlattices	Physics
281/96	Laggner Peter	Austrian Academy of Sciences Inst. for Biophysics & X-ray Structure Research, Graz	Austria	trapping of structural intermediates in phospholipid phase transitions	Biophysics

282/96	Gailhofer Magdalena	Austrian Academy of Sciences Inst. for Biophysics & X-ray Structure Research, Graz	Austria	Human low density lipoproteins (LDL) - Microphase Separation	Life Sciences
Test	Zannella Giovanni	Univ. Padua	Italy	Tests of CCD-camera system using high flux SR	Instrumentation

1997: September-December

Proposal	Proposer	Institution	Country	Title	Research Area
006/97	Baldrian Josef	Czech Acad. of Sciences, Inst. of Macromol. Chemistry, Czech Republic, Prague	Czech Republic	Time resolved SAXS and WAXS studies on macromolecular materials	Chemistry
030/97	Mariani Paolo	Univ. di Ancona, Istituto di Scienze Fisiche, Ancona	Italy	Structural analysis of ascorbate oxydase	Biophysics
040/97	Shah Jitendra, Roveri Norberto	Univ. of Bristol, H.H. Wills Physics Laboratory, Bristol	United Kingdom	Low Angle Diffraction studies of the intramuscular collagen	Life Sciences
057/97	Nawroth Thomas	Univ. Mainz, Inst. für Biochemie, Mainz	Germany	Transient structural changes and cooperativity during the nucleotide reaction cycle of F1ATPase and ATP synthase	Life Sciences
088/97	Zehetbauer Michael	Universität Wien Institut für Materialphysik, Wien	Austria	Local Dislocation Densities and Internal Stresses by High Lateral Resolution Peak Profile Analysis in Plastically Deformed Polycrystalline Nickel	Physics
101/97	Cecchi Giovanni	Universita di Firenze Dip. di Scienze Fisiologiche, Firenze	Italy	Time resolved mechanical and x-ray diffraction studies on single muscle cell.	Life Sciences
121/97	Rappolt Michael	Austrian Academy of Sciences, Inst. of Biophysics and X-ray Structure Research, Graz	Austria	Simultaneous small and wide angle scattering on the main transition of model-membranes	Biophysics
123/97	Kriechbaum Manfred	Austrian Academy of Sciences, Inst. of Biophysics and X-ray Structure Research, Graz	Austria	Solubilized Na,K-ATPase	Life Sciences

125/97	Schwarzenbacher Robert	Austrian Academy of Sciences, Inst. of Biophysics and X-ray Structure Research, Graz	Austria	Kinetic studies of the silica-based MCM-41 and MCM-48 synthesis	Chemistry
136/97	Ferracini Elena	Univ. di Bologna, Dip. di Chimica "G. Ciamician", Bologna	Italy	Advanced SAXS study on the high-yield isostatic polypropylene transition from the mesomorphic phase to the well crystallized alpha-monoclinic one	Chemistry
139/97	Fratzl Peter	Universität Wien, Institut für Materialphysik, Wien	Austria	In-situ synchrotron x-ray scattering study of the tensile properties of collagen	Life Sciences
141/97	Klose Günther	Univ. Leipzig, Institut für Experimental Physik, Leipzig	Germany	Time-resolved SAXS study of the solubilization of POPC lipid bilayers by the nonionic detergent C12 E8	Life Sciences
Pilot	Menk Ralf	Sincrotrone Trieste, Trieste	Italy	A fast 1-D detector time resolved SAXS experiments	Instrumentation
Pilot	Zidansek A.	J. Stefan Institute, Ljubljana	Slovenia	Smectic ordering in porous glasses: a small angle X-ray scattering study	Material Sciences

User Statistics

1. Overview of all the proposals and assigned shifts from 1995 until December 1997

The Austrian SAXS-beamline at ELETTRA opened to users in September 1996. Since then many experiments have been made related to the fields of life sciences, material sciences, physics, chemistry and instrumentation.

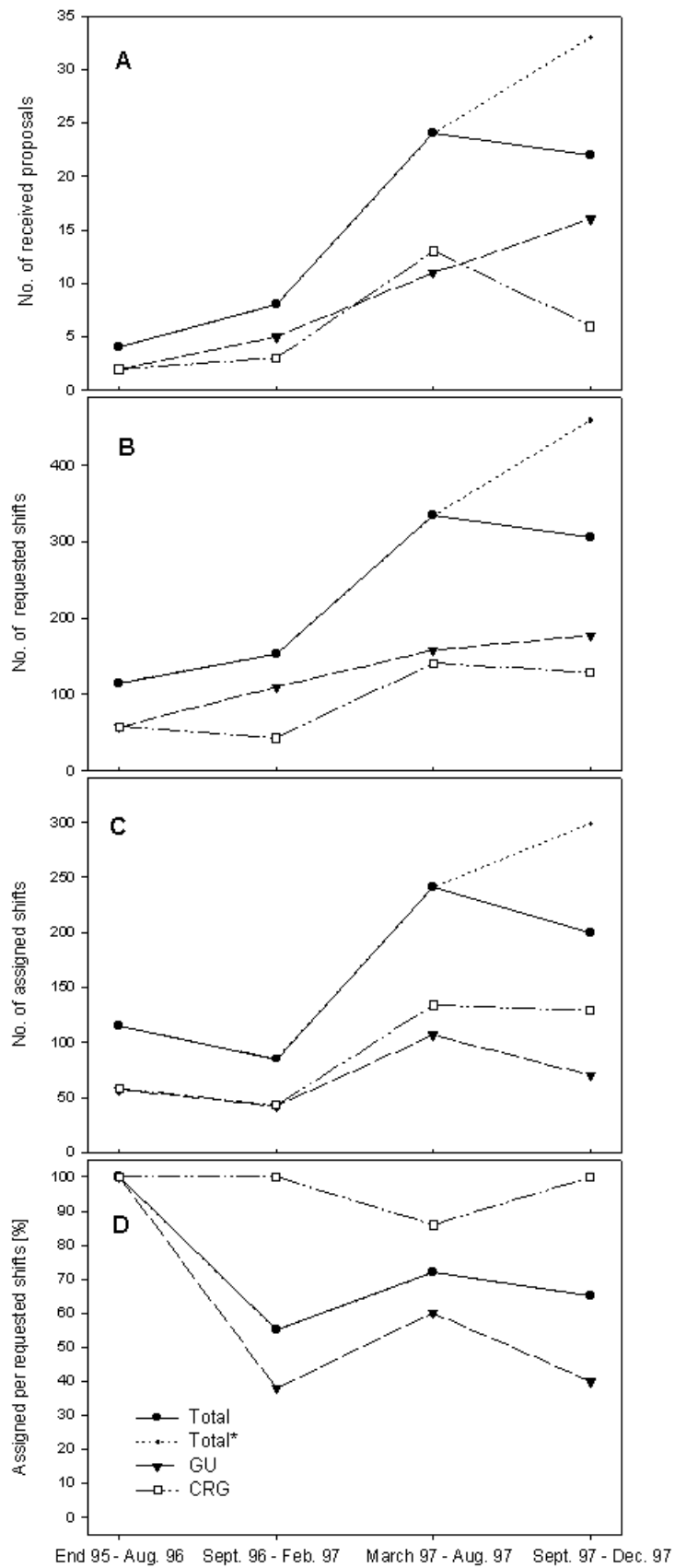
The users gained access to the SAXS-beamline on the basis of the proposals received for the three periods September 1996 - February 1997, March 1997 - August 1997, and September 1997 - December 1997. The assignment of beamtime at this beamline is done separately for the group of "General Users" (GU) and the "Collaborating Research Group" (CRG), i.e., the Research Team of the Austrian Partner. Beamtime was assigned to the proposals of each group in the order of the rating received by the Scientific Committee, and up to the maximum number of shifts available to each group according to the contract between The Austrian Academy of Sciences and the Sincrotrone Trieste. Until December 1997 up to 55 % of the beamtime was given to CRG, up to 30 % to GU, and 15% was reserved for maintenance purposes. From January 1998 on the quota for beamtime will be 35 % for CRG and 50 % for GU.

Fig. 1 gives an overview of the numbers of received proposals, the numbers of requested and assigned shifts, as well as the percentage between assigned and requested shifts. Included in Fig.1 are also the same data for the period End 1995 - August 1996, during which some beamtime had been given already to users in order to perform first pilot- and test-experiments together with the beamline staff. These first experiments during the commissioning phase were not yet based on proposals, since the goal was mostly to evaluate and improve the performance of the beamline and the equipment of its experimental station. As can be seen in Fig.1, the request for beamtime at the SAXS-beamline increased steadily, if one takes into account that the last period was only 4 instead 6 month long, and therefore somewhat less proposals were submitted.

Fig1. (next page): Shown for the 4 beamtime periods, i.e., End of 1995 - January 1996, September 1996 - February 1997, March 1997 - August 1997, and September 1997 - December 1997, respectively, are:

- A: Number of received proposals,
- B: Number of requested shifts,
- C: Number of assigned shifts,
- D: Relation between assigned and requested shifts.

These informations are given both separately for the groups "CRG" (Collaborating Research Group), "GU" (General User) and the sum of both (Total). Since the last period was shorter, for clarity also the an extrapolated value corresponding to a full six-month period is indicated (Total*).



Until December 1997, 132 users from 44 institutes in 11 countries have performed experiments on it. In Fig.2 are shown the origin of these users (top) and of their respective institutes (below). Each user or institute was counted only once, even though most users performed experiments in more than just one of the four given periods.

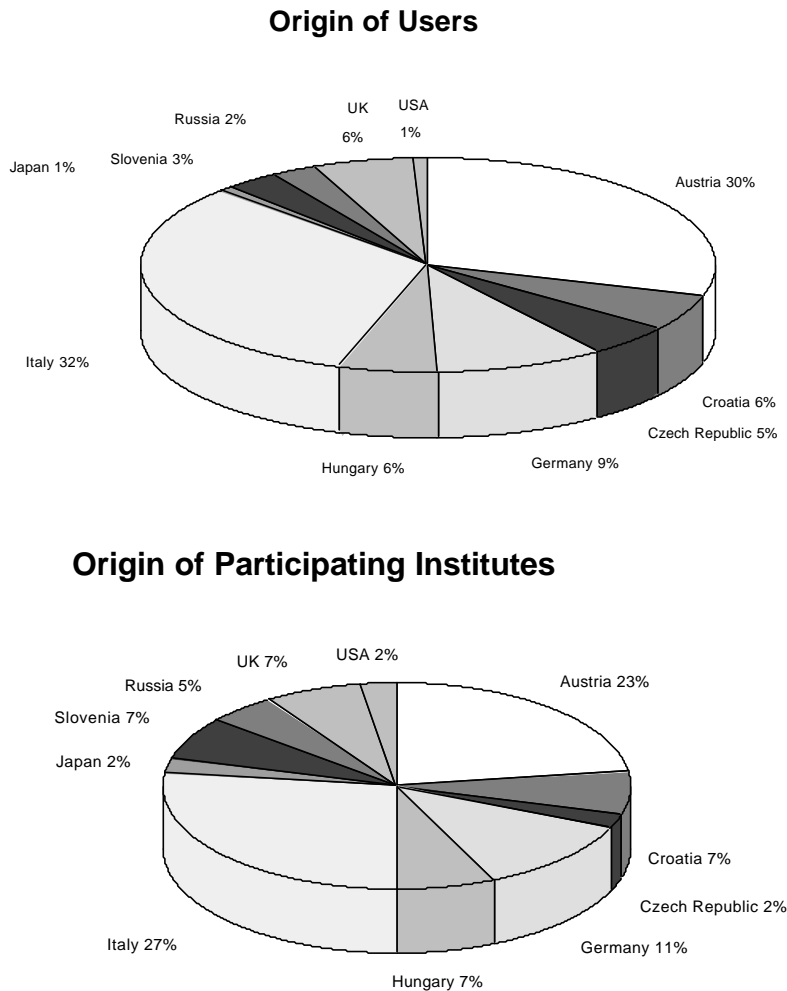


Fig. 2: Origin of users (top) and of their corresponding institutes (below).

2. Documentation of experimental results

Refereed Publications until December 1997:	6			
Refereed Publications, in press:	20			
Non-refereed Publications until December 1997:	8			
Contributions to conferences / workshops until December 1997:				
1993	1994	1995	1996	1997
2	2	3	13	29
PhD Theses until December 1997:	3			
Diploma Theses until December 1997:	2			

Technical Developments at the SAXS-beamline

1. Installation of the new monochromators (5.4 and 16 keV)

The non-dispersive fixed-exit double-crystal monochromator of the SAXS-beamline has three pairs of flat asymmetrically cut Si(111)-crystals interchangeable under vacuum. The crystal pairs are optimised for high-throughput at one of three different discrete and fixed photon energies, namely for 5.4, 8 and 16 keV, respectively. To cope with the severe thermal power load produced by the 57-pole wiggler on the first crystal of each pair (up to 5.4 W/mm² and 700 W under normal incidence, for 400 mA), grazing angles of 2° and optimised backside cooling have been chosen [1]. This solution allows simultaneously a gain of 2.5 - 3.0 in through-put, and accordingly in flux density, with respect to symmetrically-cut double-crystal set-ups.

As can be seen in Fig. 1, the monochromator consists of four vacuum chambers. Chamber I is located about 18 m after the source point and houses the first crystal of each of the three crystal pairs. Due to geometrical constraints and optical considerations [2], we chose to separate the SAXS branch line from the diffraction branch beamline vertically by 1.5 m. Therefore, the second crystals of the three pairs are mounted in three separate chambers (IIa-c). Furthermore, this large vertical separation between incoming and monochromatic photon beam gives a very low parasitic background in the camera.

In the beginning, only chambers I and IIb had been installed, and this 8 keV-single energy system went in operation at the end of 1995. During two longer shut-downs in 1997, two more cooled crystal substrates were added to the crystal holder (see fig.1) in Chamber I, and also the Chambers IIa and IIc were installed.

The first crystal of each pair has a size of 38.5 x 195 x 2.5 mm² (width x length x thickness). The crystals are fixed with their backside to the cooling block via a liquid eutectic In/Ga-alloy layer which enhances the thermal contact. The cooling block has microchannels for water located just underneath the hot surface, which is one of the most effective systems for removal of high power heat loads. Since 2.5 mm thin Si-crystals deform easily, these first crystals have been mounted using in situ a Long Trace Profiler to minimise deformations due to mechanical stress with µm precision over all their surface area [1]. Furthermore, during mounting great care was taken to pre-bent the crystals slightly, so that the unavoidable residual heat-load induced slope errors in working condition (full power load and high water pressure) will remain always smaller than a few arc seconds [3].

The second crystal of each pair has a size of 50 x 195 x 20 mm³ (width x length x thickness). Since the heatload of the monochromatic beam is negligible, no cooling is necessary.

Design analysis using finite element methods had been performed for this system [3], and the crystal behaviour has been tested under heat load. During commissioning it has been demonstrated that the cooling layout functions very satisfyingly, and that up to 5x10¹² ph/s are available at the sample (at 8 keV and 250 mA) as predicted. Since spring 1998 now also the two new photon energies 5.4 and 16 keV are available for user experiments.

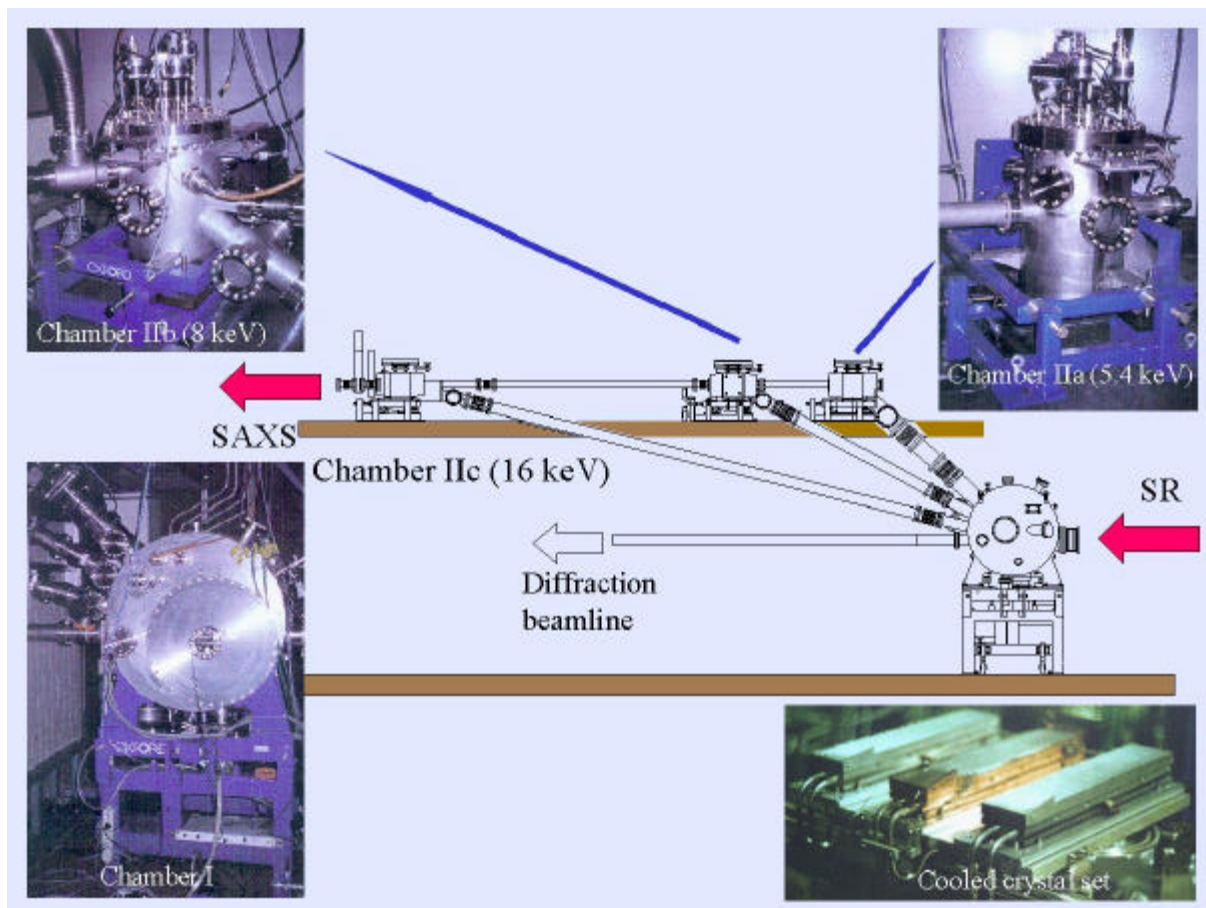


Fig. 1: Center: Side view (in scale) of the SAXS double-crystal monochromator consisting of the chambers I and II a-c. Each crystal has its own alignment unit allowing for 5 degrees of freedom. For the 5.4 or 8 keV set-up, respectively, the crystals in chambers IIb and IIc can be removed under vacuum from the photon beam path. Lower Right: Brazed, fully UHV-compatible crystal substrates. The ramps, which can be seen on the front of the cooling blocks, are for protecting the front and the sides of the crystals from accidental exposure (under quasi normal incidence!), which might occur during e.g. the initial alignment phase.

- [1] S. Bernstorff, H. Amenitsch and P. Laggner
J. Synchrotron Rad. Vol.5, (July 1998), in press
- [2] H. Amenitsch and S. Bernstorff
Sincrotrone Trieste, Technical Note ST/S-TN-93/63 (1993)
- [3] H. Amenitsch, B. Hainisch, P. Laggner and S. Bernstorff
Synchrotron Radiation News 8.4, 22-27 (1995)

2. Installation the of the WAXS port

2.1 Mechanics and Layout

In order to perform simultaneous SAXS- and WAXS-measurements using two linear sensitive detectors (Gabriel type) at the experimental station of the SAXS-beamline at ELETTRA, it was necessary to construct a special vacuum chamber with an installation port for the wide-angle detector and with a standard KF-flange at the small-angle port. The mechanical SWAXS-device, in short the „SWAXS-nose“, has been constructed under the conditions

- to cover a wide range in d-spacing
- and to allow at the same time for a sufficient WAXS-resolution.

This was realized throughout *two concepts*, namely,

- by using both scattering areas below and above the direct beam, respectively
- and by providing four different fixed ports on a quarter arc for the WAXS regime.

As sketch of the SWAXS-nose is given in Fig.1 and possible set-ups are summarized in Table 1. The overall length of the SWAXS-nose in the horizontal direction, measured from the sample position, is 512 mm and the fixed sample to WAXS-detector distance is 324 mm, where the sample-position is given by the midpoint of the WAXS-arc 10 mm in front of the entry window. At the shortest camera-length an overlap in the d-spacings covered by the SAXS- and WAXS-detector, respectively, is possible: then, the common regime lies around 0.9 nm.

d-spacing (Å)				
Range	2q [deg]	8 keV	5.4 keV	16 keV
1	9.4	<i>9.40</i>	14.03	4.27
	27.6	3.23	4.82	1.47
2	27.4	3.25	4.86	1.48
	45.6	1.99	2.97	0.90
3	45.4	2.00	2.98	0.91
	63.6	1.46	2.18	0.66
4	63.4	1.47	2.19	0.67
	81.6	1.18	1.76	0.54

Table 1: Covered d-spacing range in the WAXS-regime under the possible different set-ups at the SAXS-beamline at ELETTRA. As seen in Fig. 1 the WAXS-detector can be mounted at four different fixed positions on the SWAXS-nose (range 1-4), thus, with the three possible energy choices (5.4, 8 and 16 keV) this results in 12 different d-spacing regimes. In italic the most common choice (8 keV, range 1) is highlighted. This range is suited for experiments, e.g., on lipid-systems and (bio)polymers.

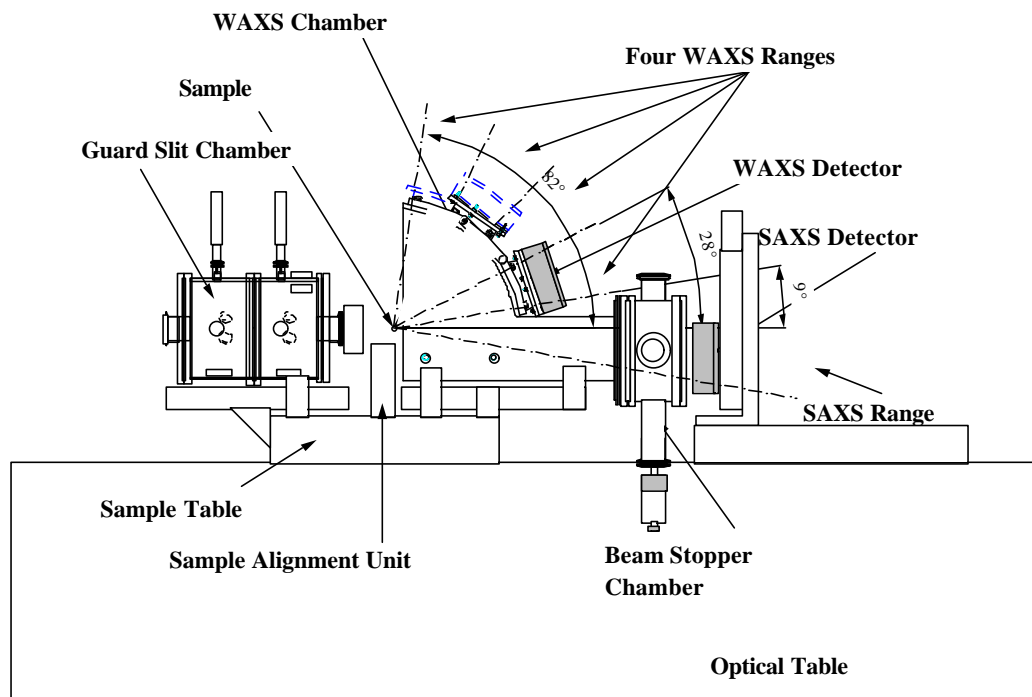


Fig. 1: The SWAXS-nose is sketched in the set-up for the shortest possible camera-length , with the four different WAXS-ranges covering a total angular range (2θ) from $9^{\circ}24'$ up to $81^{\circ}37'$. The SWAXS-nose is in height prealigned relative to the direct beam and can be easily integrated in the beamline directly downstream of the Sample Alignment Unit by means of Bosch-profile connections.

2.2 Parallel Operation of the Dual Detection System

The simultaneous detection of small- and wide angle region (SWAXS) can be easily achieved with two delay line detectors in series. However, special precautions have to be taken to prevent ground loops or interference with other electronic equipment, thereby increasing the noise of the detection system.

An alternative approach for the operation with two delay line detectors in parallel has been developed and tested on the SAXS beamline, which circumvents this problem by connecting the digital signals of the Constant Fraction Discriminator (CFD) of both detectors to one Time-to-Digital Converter (TDC). A similar wiring has been proposed by Rapp et al. [1], however, it turned out to be crucial that non of the two start pulses are delayed. In Fig 2 the detailed schematics of the serial and parallel SWAX detection system is shown, in which the stop signals of the constant fraction discriminators are appropriately delayed and afterwards added on the start and stop signals of the TDC.

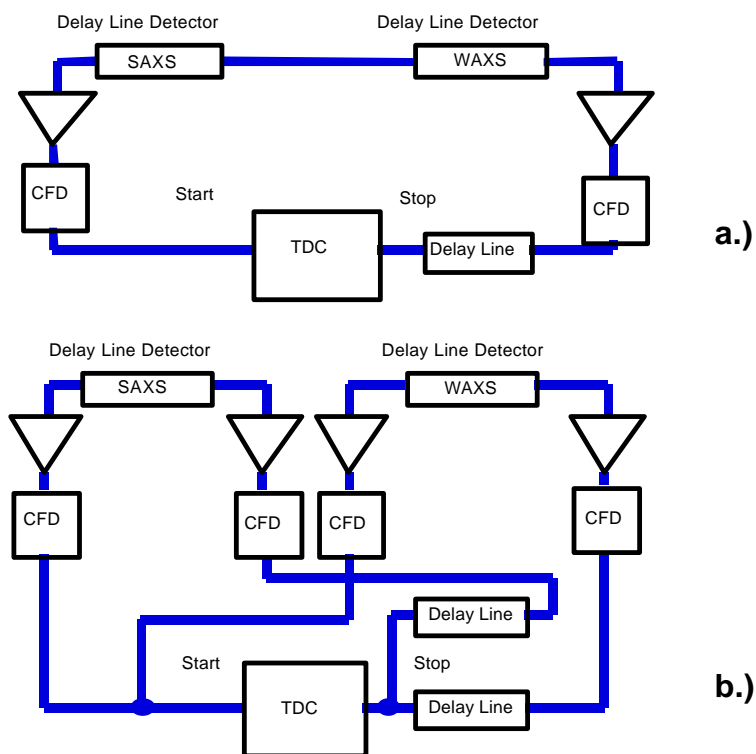


Fig. 2: The schematic wiring diagram of the serial (a.) and the parallel readout system (b.) is shown. From the two delay line detectors the analog signals are amplified and then formed by the constant fraction discriminators (CFD) in fast NIM pulses. The signals must be appropriately delayed and feed into the time to digital converter.

Test measurements in the SWAXS regime have been performed, first, taken with rat tail tendon for SAXS- and second, taken with p-bromo-benzoic acid for the WAXS-regime, both with the complete system in operation. Fig. 3 shows the diffraction patterns of rat tail tendon in which the improvement of the system is in the number and FWHM of resolved peaks, and the reduction of the constant background (incoherent noise on the signal lines). Fig. 4 shows the patterns for the WAXS regime, for which the same is valid as before.

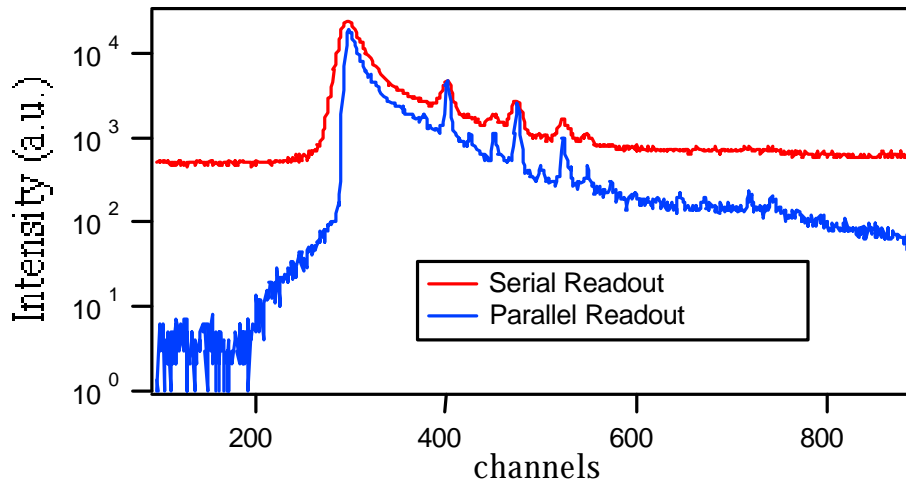


Fig. 3: SAXS regime of the rat tail tendon collagen measured with both set-ups (serial & parallel) demonstrating the improved performance of the latter through less noise and peak resolution

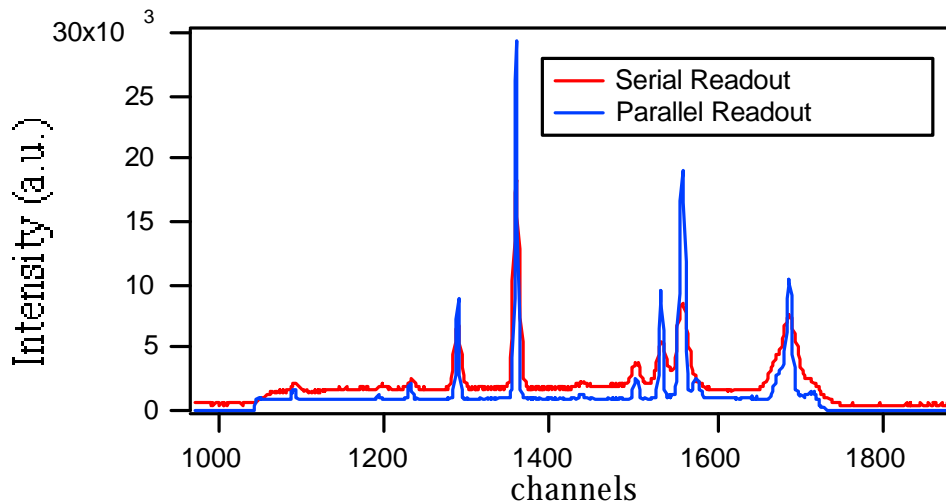


Fig. 4: WAXS regime of para-bromo benzioc acid measured with both set-ups (serial & parallel) demonstrating the improved performance of the latter through less noise and peak resolution.

Reference

[1] Rapp, G., Gabriel, A., Dosière, M. & Koch, M.H.J. (1995). A dual detector single readout system for simultaneous small- (SAXS) and wide-angle X-ray (WAXS) scattering. *Nucl. Instr. Meth. Res. A* **357**: 178-182.

3. Set-up of various sample manipulations stages

3.1 General

Usually the sample is mounted onto the sample alignment stage which allows the user to place the sample into the beam with a precision of 5 μm (resolution: 1 μm). In fig 1 the ranges for vertical and horizontal alignment as well as the maximum dimensions of the sample holders are given. The maximum weight on the sample stage is limited to 10 kg. In case the envelope dimensions of a sophisticated sample station provided by the users are slightly larger than those given in Fig. 3, the user can ask the beamline responsible for a check up of his space requirements. If it does not fit at all to these specifications, user equipment can also be mounted directly onto the optical table, which allows much larger spatial dimensions.

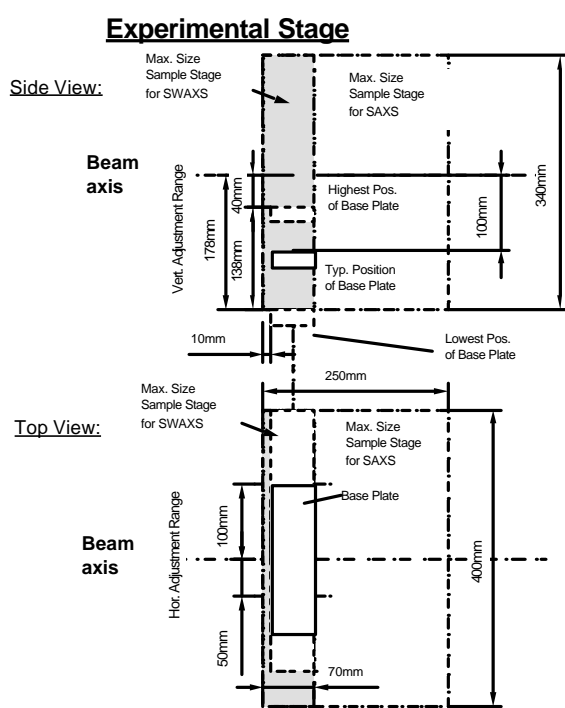


Fig. 3 Maximum dimensions and alignment range of the sample holder to be mounted onto the standard alignment stage

3.2 Sample holders

As standard equipment for liquid samples Paar capillaries (diameter: 1 and 2 mm) are used thermostated with the KHR (electrical heating) or KPR (Peltier heating/cooling) sample holders (Anton Paar, Graz, Austria). For use in these sample holders flow through capillaries and Gel holders are standard equipment.

Temperature scans can be performed with KHR and/or KPR in the range from 0 to 150 $^{\circ}\text{C}$, typically the precision and the stability of this systems is < 0.1 $^{\circ}\text{C}$.

Additionally thermostats for temperature control or cooling proposes can be used at the beamline (0 - 95 $^{\circ}\text{C}$, at present). Helium and Nitrogen gas bottles are available at the beamline, for other gases please contact the beamline responsible.

Multiple sample holders can be mounted onto the standard sample manipulator and various samples can be measured in one run. At present a holder is available for measuring in automatic mode up to 30 solid samples at ambient temperature or up to 4 liquid samples in the temperature range 0 – 95 °C.

3.3 Magnet System

For studying magnetic effects in samples, capillaries or sample holders with suitable dimensions can be mounted inside an electro-magnet. Up to now a sample holder for standard Paar capillaries (Anton Paar, Graz, Austria) is available for ambient temperature only. The alignment of the magnetic field is horizontal or vertical (transversal to the photon beam). For short times the maximum magnetic field is up to 1.8 T, and 1.0 T for continuous operation, respectively, assuming a pole gap of 10 mm for both.

3.4 Stopped Flow Apparatus

A commercial stopped flow apparatus (Unisoku Co., Ltd, Osaka, Japan) is presently available particularly designed for SAXS investigations of conformation changes of proteins, nucleic acids and macromolecules. The process is triggered by the rapid mixing of two solutions and typically the observation time is ranging from ms to minutes.

The main parameters of the system are:

- dead time: about 1 ms
- mixing ratio: 1:1 (at present)
- reservoir volume: 4 ml each
- syringe volume: 0.3 ml each
- shot volume: 0.1 ml - 0.25 ml each solution
- optical path length: 1 mm; X-ray windows: sapphire 2 x 50 μm
- temperature range: by means of a thermostat water bath (0 - 60 °C)

Both solutions are filled in the reservoirs and the syringes are pulled up remote controlled. The syringes are pushed by a pneumatic system and consequently the liquids are rapidly mixed in a sphere mixer and filled into the rectangular observation cell within 1 ms. This process generates the trigger for starting the data acquisition system. The mixing can be repeated about 15 times before the reservoirs must be refilled.

Depending on the diffraction power of the sample time resolutions of up to 10 ms can be obtained.

3.5 Grazing Incidence Small Angle X-ray Scattering

A special set-up has been designed to perform grazing incidence studies on solid samples, thin film samples or Langmuir-Blodgett-films. The samples can be mounted onto a sample holder, which can be rotated around 2 axes transversal to the beam. Furthermore the sample can be aligned by translating it in both directions transversal to the beam.

The precisions are 0.001 deg for the rotations and 5 μm for the translations. Usually the system is set to reflect the beam in the vertical direction. According to the required protocol and the actual assembly of the rotation stages ω , θ , 2θ and ϕ scans can be performed.

For further information see the experimental reports enclosed.

3.6 Temperature Gradient Cell

A temperature gradient cell for X-ray scattering investigations on the thermal behaviour of soft matter manybody-systems, such as in gels, dispersions and solutions, has been developed. Depending on the adjustment of the temperature gradient in the sample, on the focus size of the X-ray beam and on the translational scanning precision an averaged thermal resolution of a few thousands of a degree can be achieved. (see *User Contributions: Instrumentation.*)

3.7 IR-Laser T-Jump System for Time-Resolved X-ray Scattering on Aqueous Solutions and Dispersions.

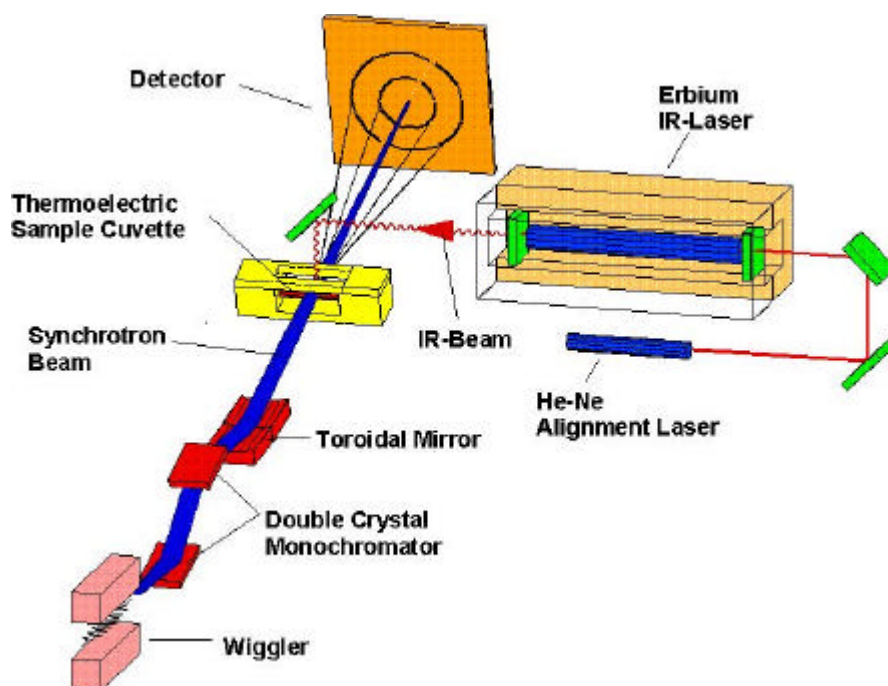


Fig. 2: Sketch of the T-jump set-up.

The IR-Laser System available at the SAXS-beamline (Dr. Rapp Optoelektronik, Hamburg, Germany) [1,2] delivers a maximum of 4 J per pulse (pulse-length = 2 ms) at the sample. The active medium of the laser is an Erbium-Glass rod, which yields a wavelength of 1.54 μm . The laser-beam is guided by one prism onto the sample, which is filled in a glass capillary (1 or 2 mm in diameter) and Peltier or electronically thermostated in a metal sample holder (A. Paar, Graz, Austria). With a spotsize of 7 mm in diameter a sample-volume of 5.5 μl or 22 μl , respectively, is exposed to the laser-radiation. In a water-solutions/dispersions with an absorption coefficient of $A = 6.5 \text{ cm}^{-1}$ T-jumps up to 20 $^{\circ}\text{C}$ are possible. A built-in He-Ne laser is used to adjust the laser optics and second, to align the crossfire between the X-ray and IR-beam. Additionally, 1- or 2-dimensional focussing optics can be installed to achieve smaller IR-spot sizes.

[1] M. Kriechbaum, G. Rapp, J. Hendrix & P. Laggnier (1989). *Rev. Sci. Instrum.* **60(7)**: 2541-2544.

[2] G. Rapp & R.S. Goody (1991): *J. Appl. Cryst.* **24**: 857-865.

3.8 High-Pressure X-Ray Diffraction Cell for Static and Time-Resolved SAXS-Experiments at Hydrostatic Pressures up to 3000 bar.

A compact X-ray sample cell capable of measuring diffraction patterns at hydrostatic pressures up to 3 kbar has been developed. The cell body (5 x 3.5 x 2 cm) consists of high-strength Cr-Ni-Mo-Ti alloy with perpendicular bores for the X-ray beam path and the sample containment, respectively. The exit- and the removable entrance-window for the X-rays are made of 1.5 mm thick Be-discs (3.0 mm diameter), coated with 5 μ m polyimide with a total transmission of 55% for X-rays at a wavelength of 1.54 Å, which is mostly used at conventional X-ray sources. The sample thickness can be 1.5 mm with a volume of approximately 1mm³ completely irradiated by pin-hole collimated (1.0 mm diameter) X-rays. The cone-shaped exit window allows detection of scattered X-rays from the sample within a maximal angular range of 30° (see Fig. 1).

The hydrostatic pressure is generated by a motorized screw-type high-pressure pump using water as the pressure transmitting liquid, directly connected via a high-pressure control network with the cell interior. Additionally, the temperature in the pressure cell can be regulated by external Peltier devices or alternatively by thermostated metal blocks in the range from 0°C to 80°C. The temperature within the sample cell is measured by an inserted thermocouple, the pressure by analog or digital pressure transducers/sensors within the network system. Temperature/pressure scans and data collection during scattering experiments are completely software controlled.

The large accessible angular range in the reciprocal space makes the cell well suited for scattering/diffraction measurements in the small- (SAXS) and wide-angle (WAXS) region of samples like solid polymers, liquid-crystalline probes and biological model-membrane systems. First static measurements of lipid samples at different pressures showed an excellent signal/noise ratio of the diffraction patterns at exposure times of 10 s.

Alternatively, this system can be used for time-resolved measurements of dynamic processes (pressure-jump relaxation experiments) with a time resolution of the diffraction patterns in the millisecond range and with jump amplitudes up to 3kbar. In these experiments the high-pressure network has two sections separated by a remotely controllable pneumatic valve. For pressure-jumps, the outer section is brought to a different pressure level than the inner one (with the high-pressure cell) and pressure jumps are accomplished by opening fast the connection between both sections. At the same time a trigger signal is sent to the data acquisition electronics. The pressure jump amplitudes are approximately 1 kbar/10 ms in both directions (pressurizing and depressurizing jumps) and diffraction patterns of p-jump induced barotropic phase-transitions of lipid samples could be measured with 5 ms time-resolution.

- (1) K.Pressl, M.Kriechbaum, M.Steinhardt and P.Laggner, *Rev.Sci.Instrum* 68, 4588-4592 (1997).
- (2) M.Steinhardt, M.Kriechbaum, K.Pressl, H.Amenitsch, P.Laggner and S.Bernstorff, *Rev.Sci.Instrum.* submitted (1998).

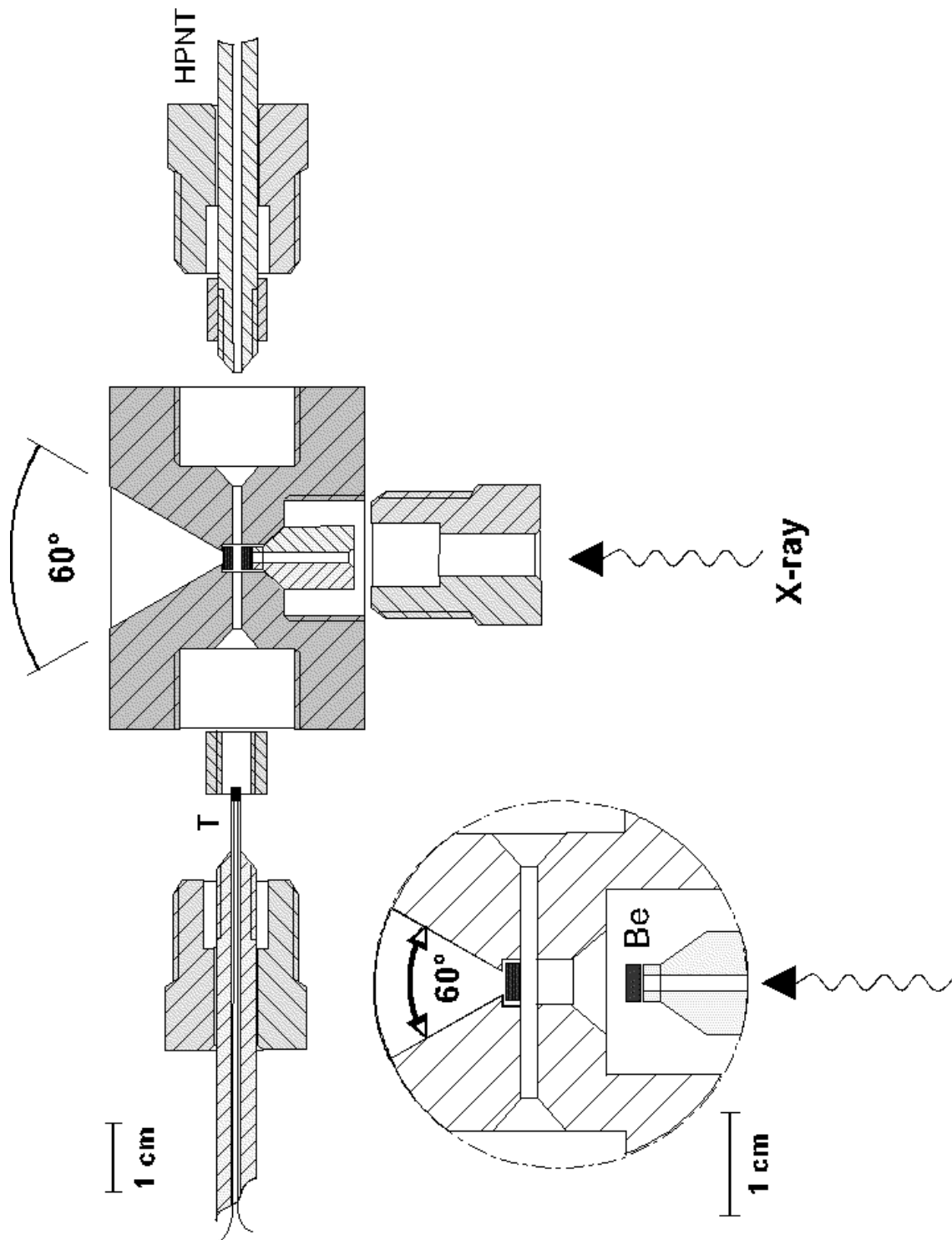


Fig. 1: Schematic view of the high-pressure X-ray cell. (C) high-pressure cell body; (P) sealing part of connection III and support of the X-ray input window; (W) X-ray window (beryllium-discs); (T) iron-constantan thermocouple seated in a stainless steel casing; (N) standard high-pressure network (HPNT) connection; (S) standard support plug; (R) standard sealing collar; (I) connection to the high pressure network N, (II) connection to the thermocouple T, (III) X-ray beam input.

User Contributions

1. Material Sciences

Time-resolved SAXS Study of Crystallization of PEO and PEO/PMMA Blends

J.Baldrian¹, M.Horky², M.Steinhardt¹, P.Vlček¹, H.Amenitsch³, S.Bernstorff⁴

¹Institute of Macromolecular Chemistry, Academy of Sciences of the Czech Republic, Prague

²Faculty of Nuclear Science and Engineering, Czech Technical University, Prague

³Institute of Biophysics and X-Ray Structure Research, Austrian Academy of Sciences, Graz

⁴Sincrotrone Trieste, Basovizza, Trieste

The crystallization of low-molecular fractions of poly(ethylene oxide) (PEO) showed, that chains integrally fold (IF) when incorporated into crystalline lamellae. The most stable crystals are formed by extended chains (EC). Recently it has been reported on the basis of time-resolved synchrotron SAXS results, that nonintegral folded chain crystals (NIF) in pure PEO can be formed in the early stages of crystallization and IF crystals are derived from isothermal thickening or thinning of NIF crystals. The purpose of the measurements has been to study these effects in PEO/poly(methyl methacrylate) (PMMA) blends in comparison with the situation in pure PEO.

Blends of PEO (Mw 3000) with PMMA (Mw 1170) with 80, 60, 40, and 20wt.% of PEO were prepared by dissolving in chloroform and subsequent drying in vacuum oven at 40°C for a week. Time-resolved SAXS measurements were performed on the ELETTRA SAXS beamline with sample-detector distance of 1.75m, wave length $\lambda = 0.154\text{nm}$. The 1.5mm thick samples in special holder were melted at 80°C for 15min. and than quickly inserted into a cell placed in the path of the X rays, maintained at the isothermal crystallization temperature 40°C. Measurements consisted of 256 frames each 10s long. The scattering data were corrected for detector efficiency and background and Lorentz correction was applied. The background was taken to be the scattering curve of the molten sample. The following parameters have been extracted from the data: (1) long period - thicknesses of the lamellae from the positions of SAXS peaks ; (2) peak intensities of SAXS reflections - relative content of different kinds of lamellar crystals. Time development of these structure parameters for blends with 80 and 60 wt.% of PEO are shown on Figs.1 and 2.

It has been found that in early stages of PEO/PMMA blends crystallization a transient nonintegral folding of PEO lamellae in wide range of compositions were formed similarly to the situation in pure PEO. Subsequent transformation of NIF lamellae into the lamellae with integrally folded crystals with one folded (1F) or extended chains has occurred through isothermal thinning and thickening. The amorphous diluent has played a decisive role in structure development. With growing content of PMMA increased induction time of crystal formation, reduced rates of NIF, 1F and EC crystallization and time of start and rate of NIF structure recrystallization. The retardation effect of amorphous diluent to the kinetics of these processes resulted in tendency to create gradually more stable and more perfectly ordered structures.

Research supported by the Grant Agency of the Czech Republic (Grant No. 203/96/1387)

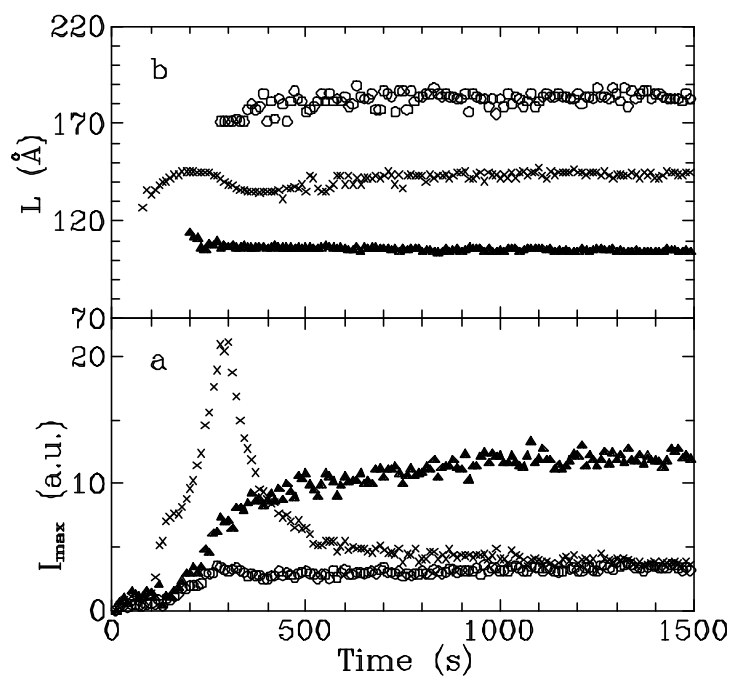


Fig.1.: Changes of peak intensities (a) and crystal thicknesses (b) of NIF (x), 1F (▲) and EC (o) PEO crystals during crystallization of PEO/PMMA 8/2 blend

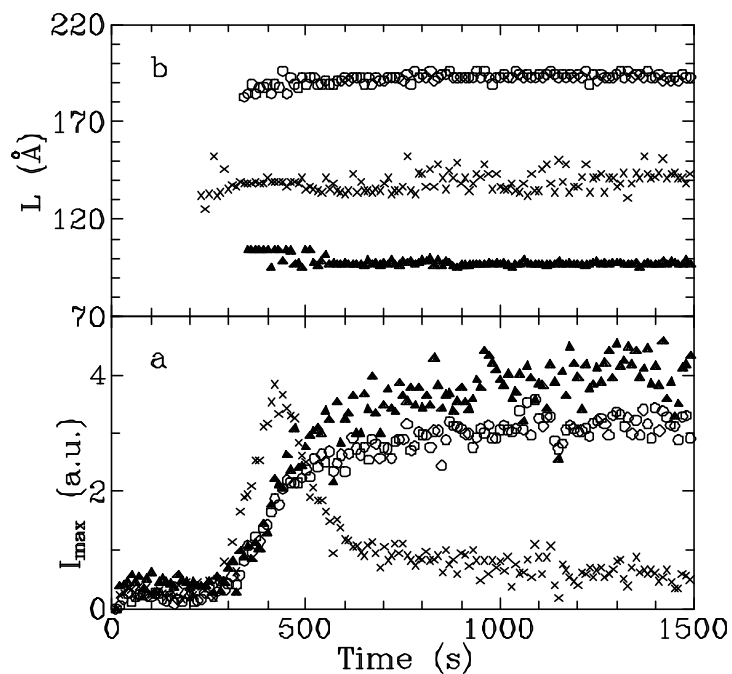


Fig.2: Changes of peak intensities (a) and crystal thicknesses (b) of NIF (x), 1F (▲) and EC (o) PEO crystals during crystallization of PEO/PMMA 6/4 blend

LOCAL DISLOCATION DENSITIES AND INTERNAL STRESSES BY HIGH LATERAL RESOLUTION PEAK PROFILE ANALYSIS IN PLASTICALLY DEFORMED POLYCRYSTALLINE NICKEL [1]

E.Schafner¹), M. Zehetbauer¹), I.Kopacz¹), B.Ortner²), S.Bernstorff³), H.Amenitsch⁴), and T. Ungár⁵)

¹) Institute of Materials Physics, University of Vienna,
A-1090 Wien, Strudlhofgasse 4, Austria

²) Erich Schmid Institute for Materials Science, Austrian Academy of
Sciences, A-8700 Leoben, Jahnstraße 12, Austria

³) Sincrotrone ELETTRA, I-34012 Trieste, Basovizza, Italy

⁴) Institute of Biophysics and X-Ray Structure Research,
Austrian Academy of Sciences, A-8010 Graz, Steyrergasse 17, Austria

⁵) Institute for General Physics, Eötvös University Budapest,
H-1088 Budapest, Muzeum körút 6-8, Hungary

In recent experiments at the SAXS-Beamline at ELETTRA, the method of X-ray Peak Profile Analysis in connection with high intensity Synchrotron radiation (Synchrotron X-ray Peak Profile Analysis, SXPA) has been successfully developed [1, 2], in order to measure the distribution of dislocation densities and internal stresses within individual grains of cold rolled f.c.c. metals by a lateral resolution down to 10 μm . Similar to previous studies in equally deformed Cu [2, 3], the measurements in Ni [1] exhibited rather homogeneous distributions of dislocations/internal stresses at low strains, but increasingly heterogeneous ones at higher strains (see standard deviation bars in Figs. 1 & 2). In the case of Cu this has been attributed to a transformation of cell walls from a dipolar dislocation structure (PDW) to a tilted one (PTW) [2, 3]. In approaching high deformation degrees in Ni, however, the average dislocation density showed a maximum followed by a marked decrease (Figs. 1 & 2 [1]), in contrast to the behaviour in cold worked Cu. This effect seems to be a direct consequence of the higher stacking fault energy of Ni in combination with the iterative character of rolling deformation, allowing for recovery processes to take place between the steps of a fast deformation of pure metals [4]. Because of this situation, the increasing heterogeneity of dislocation structure cannot be conclusively related to the PDW-PTW transformation as it is the case for Cu. Therefore further SXPA measurements are planned on samples which are to be continuously deformed to different deformation degrees. For this the torsional deformation seems to be the best since it also allows for a direct measurement of deformation dependent stress which can be well related to the microstructural features.

References

1. Proposal 088/97 at Sincrotrone ELETTRA, in preparation for Scripta mater. (1998)
2. M.Zehetbauer, R.Kral, T.Ungar, A.Borbely, B.Ortner, S.Bernstorff, H.Amenitsch, ELETTRA News 8 (1996), and submitted to J.Appl.Phys.
3. T. Ungar, M. Zehetbauer, Scripta Mater. 35, 1467 (1996)
4. M.Zehetbauer, D.Trattner, Mater.Sci.Eng. 89, 93 (1987)

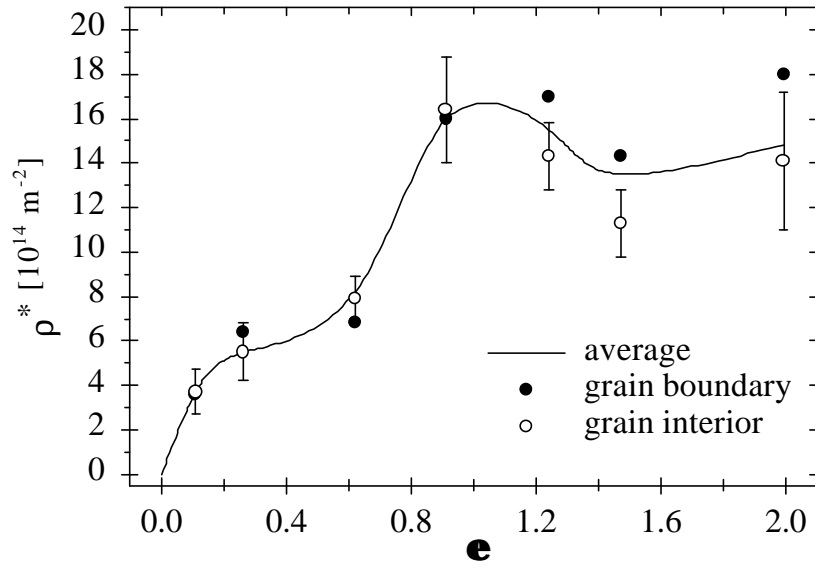


Fig.1: The dislocation density as a function of true strain e in pure Ni deformed by rolling deformation at room temperature. Each bar represents the standard deviation from all measurements in grain interiors.

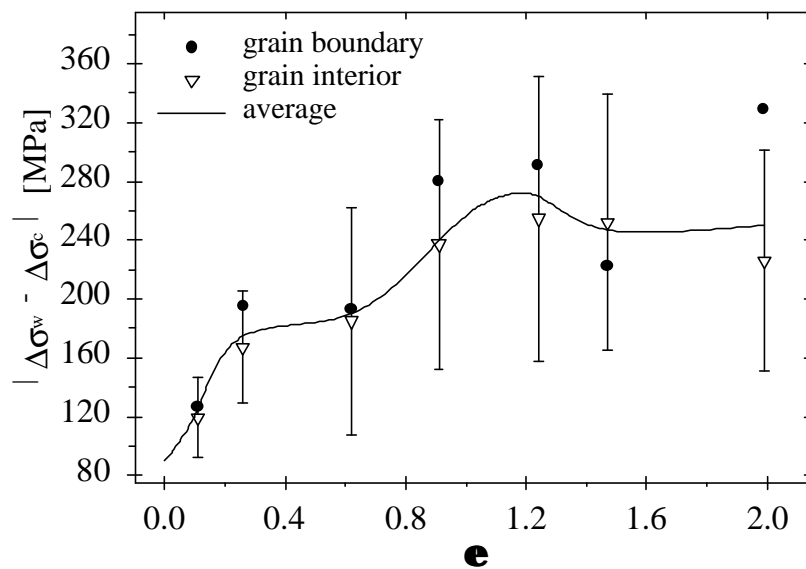


Fig.2: The long range internal stresses as a function of true strain e in pure Ni deformed by rolling deformation at room temperature. Each bar represents the standard deviation from all measurements in grain interiors.

Scanning Wide-Angle Micro Diffraction: the first material science experiment at the new Austrian SAXS beamline

M. Zehetbauer, R. Kral

Institute of Material Physics, University of Vienna, A-1090 Wien, Strudlhofg. 4, Austria

T. Ungar, A. Borbely

Institute for General Physics, Eotvos University Budapest, H-1088 Muzeum krt. 6-8, Budapest, Hungary

B. Ortner

Erich Schmid Institute for Solid State Physics, Austrian Academy of Sciences, Jahnstr. 12, A-8700 Leoben, Austria

S. Bernstorff

Sincrotrone Trieste, Strada Statale per Basovizza 14 km 163.5, 34012 Trieste, Italy

H. Amenitsch

Institute for Biophysics and X-ray Structure Research, Austrian Academy of Sciences, Steyrerg. 17, 8010 Graz, Austria

In April 1996 the first external user group performed material science experiments successfully with the 8 keV high flux beam of the new Austrian SAXS beam line.

Plastic deformation produces microstructures usually heterogeneous on the micron scale. In pure crystalline materials dislocation cell structures are typical. Cell wall regions with high dislocation densities enclose cell interior regions where only few dislocations are present. Long experience has shown that the dynamic nature of dislocation structures, especially long-range internal stresses and dislocation arrangements can be well studied by X-ray line profile analysis. In polycrystalline materials the grain boundaries are a special heterogeneity in which the dislocation arrangement is certainly different from that in the grain interior.

According to theory the line profiles of dislocated crystals can be characterised by two parameters: i) the line width (Fig. 1.), and ii) the line shape (Fig. 2.) which can especially be observed in the tails of the intensity distributions. The two parameters correspond to the average dislocation density, ρ , and the outer effective cutoff radius of dislocations, R_e . The values of R_e are small or large if the intensity in the tails of the profiles drops weaker or stronger, respectively. The differences of the dislocation densities and arrangements in the grain boundary and in the grain interior can only be determined with a fine X-ray beam of the order of a few tens of a micron with sufficient intensity. This kind of a beam is only available at a synchrotron source.

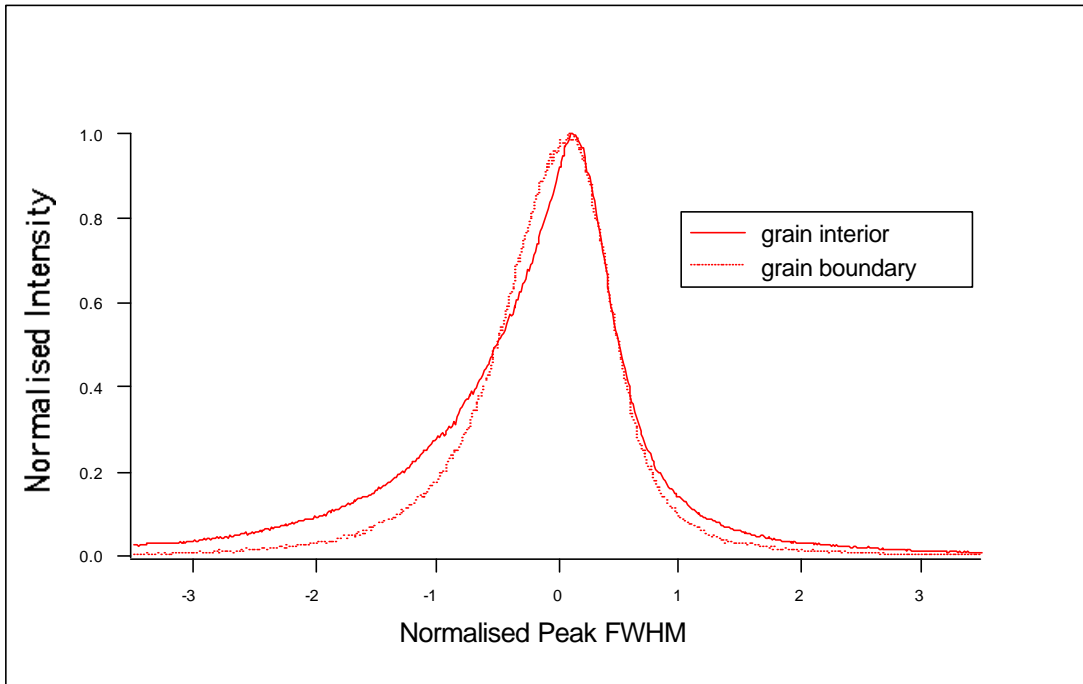


Fig. 1. Typical line profiles of the (002) reflection of polycrystalline pure copper, plastically deformed to 8.6%, obtained with a beam of 50 micron diameter. The broad profile corresponds to the grain boundary region with high dislocation density, and the narrow one to the grain interior region with smaller dislocation density, respectively.

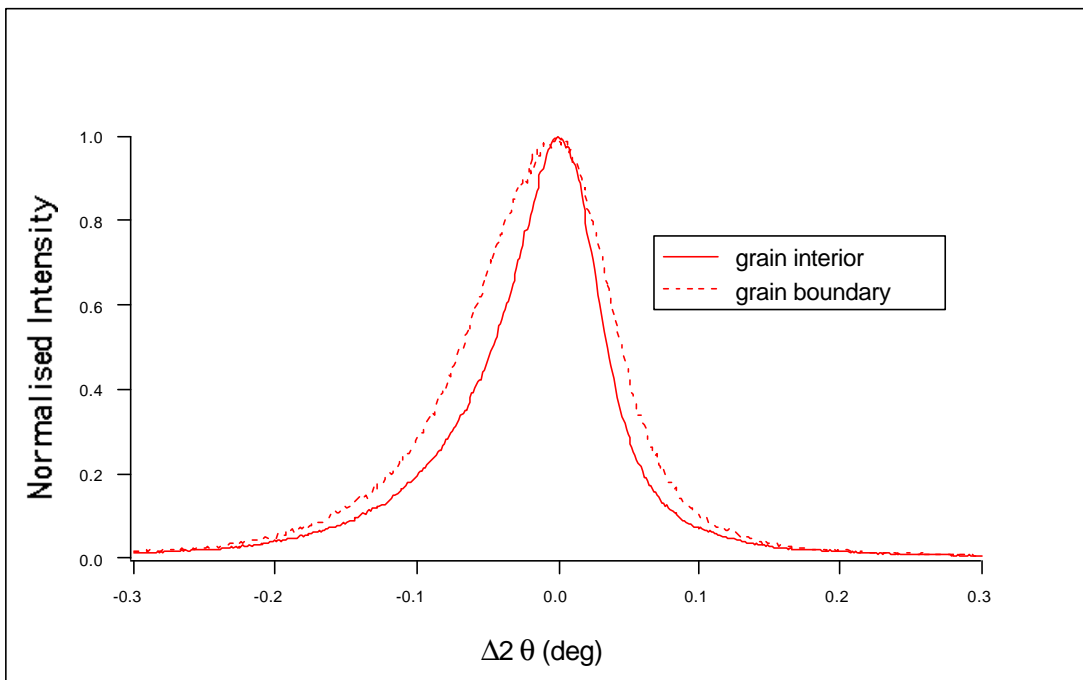


Fig. 2. Two profiles normalised to maximum intensity and FWHM corresponding to the grain boundary and grain interior region, respectively. The profiles with strongly decaying tails belong to the grain boundary and indicate that the dislocation arrangement is considerably more random than in the grain interior region.

SCANNING DIFFRACTION PROFILE ANALYSIS OF LARGE STRAIN DEFORMED CU BY SYNCHROTRON RADIATION [1]

M. ZEHETBAUER ¹⁾, T. UNGÀR ²⁾, R. KRAL ¹⁾, A. BORBÉLY ²⁾, E. SCHAFLER ¹⁾, B. ORTNER ³⁾, H. AMENITSCH ⁴⁾, S. BERNSTORFF ⁵⁾

¹⁾ Institute of Materials Physics, University of Vienna,
A-1090 Wien, Strudlhofgasse 4, Austria

²⁾ Institute for General Physics, Eötvös University Budapest,
H-1088 Budapest, Muzeum körut 6-8, Hungary

³⁾ Erich Schmid Institute for Materials Science, Austrian Academy of
Sciences, A-8700 Leoben, Jahnstraße 12, Austria

⁴⁾ Institute of Biophysics and X-Ray Structure Research,
Austrian Academy of Sciences, A-8010 Graz, Steyrergasse 17, Austria

⁵⁾ Sincrotrone ELETTRA, I-34012 Trieste, Basovizza, Italy

Local variations of the dislocation density and the long-range internal stresses have been measured by scanning X-ray diffraction profile analysis and Synchrotron radiation, as a function of plastic deformation with a spatial resolution of 50 μ m. The scanning experiments were carried out across individual grains from grain boundary to grain boundary of polycrystalline copper samples.

In stage III of deformation, the dislocation density and the long-range internal stresses were obtained to be larger in regions close to the grain boundaries than in the grain interior regions (Fig. 1). In stage IV these differences between grain boundary and grain interior regions disappeared, however, large singular fluctuations of these quantities in the grain interior regions were observed (Fig. 2): at the beginning of stage IV the fluctuation of the dislocation density is positive whereas that of the residual stresses is negative. At larger strains, well in stage IV, the situation is reversed (Fig. 3): the fluctuation of the dislocation density is negative whereas that of the residual stresses is positive. No such singular fluctuations were observed in stage III.

Recently it has been shown that the dislocation cell structure changes drastically from stage III to stage IV [2-4]: In stage III dislocations agglomerate into thick walls which separate untilted dislocation free regions; in stage IV the dislocation walls fundamentally rearrange: they become thin and separate strongly misoriented regions. In [3,4] it has been shown that the thick untilted walls, called polarised dipolar walls (PDW), correspond to relatively lower dislocation densities and larger internal stresses, whereas the thin tilted walls, called polarised tilt walls (PTW), are related to larger dislocation densities and lower internal stresses. The positive singular fluctuations at the beginning of stage IV indicate the nucleation of the PTW structure, whereas the negative singular fluctuations at larger strains correspond to the PDWs left within the almost completely transformed PTW structure.

References

1. ELETTRA News vol. 8, May 17th (1996), and submitted for publication in: J.Appl.Phys.
2. D. A. Hughes, Proc.16th RISO Int. Symp. Mater. Sci. Microstr. Cryst. Asp. Recryst.,ed. N. Hansen et al., Riso Nat. Lab. Roskilde, Denmark, p. 63 (1995)
3. T. Ungar, M. Zehetbauer, Scripta mater. 35, 1467 (1996)
4. E. Schafner, M. Zehetbauer, A. Borbely, T. Ungar, Mater.Sci.Eng. A 234-236, 445(1997)

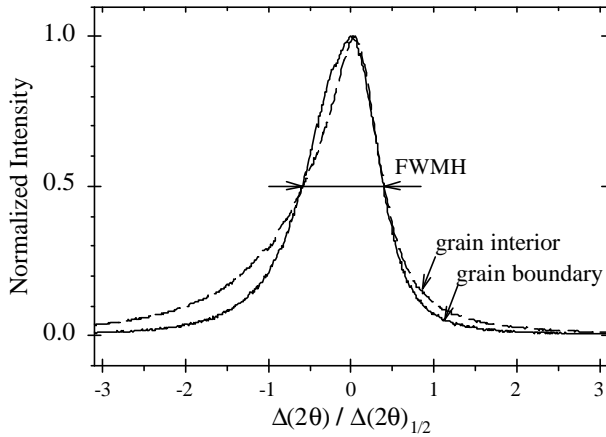


Fig.1:

X-Ray Bragg profiles from grain interior and grain boundary area of a Cu-sample cold rolled to $\epsilon=0.086$, normalized to maximum intensity and FWHM. The strongly decaying tail of grain boundary profile indicate that dipolar dislocation arrays prevail in the grain boundary as compared with the grain interior area.

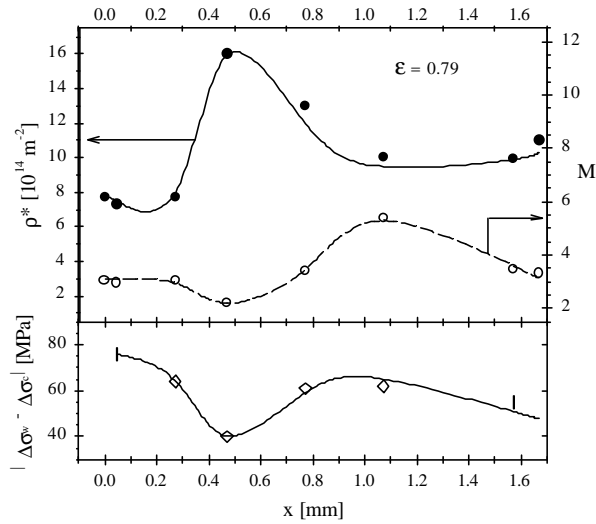


Fig.2:

Formal dislocation density ρ^* , long range internal stresses $|\Delta\sigma_w - \Delta\sigma_c|$ and dislocation arrangement parameter M , measured along a spatial grain scan in Cu cold rolled to $\epsilon=0.79$ (onset of deformation stage IV). Note the strong fluctuations occurring in parallel with all three parameters.

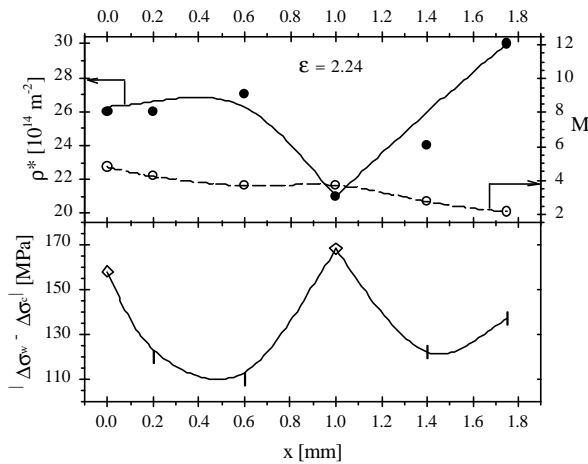


Fig.3:

Same experiment as shown in Fig.2, but for Cu cold rolled to $\epsilon=2.24$ (deformation stage IV). Note the reversal of fluctuations in ρ^* and $|\Delta\sigma_w - \Delta\sigma_c|$ as compared with Fig.2 (onset of stage IV).

Smectic Ordering in Porous Glasses: A Small Angle X-Ray Scattering Study

A. Zidansek^{1,2}, H. Amenitsch³, M. Rappolt³, S. Bernstorff¹, S. Kralj^{4,2,5}, G. Lahajnar² and R. Blinc^{2,5}

¹ Sincrotrone Elettra SCpA, SS14 per Basovizza, I-34012 Trieste, Italy

² J. Stefan Institute, Jamova 39, 1000 Ljubljana, Slovenia

³ Institute of Biophysics and X-Ray Structure Research, Austrian Academy of Sciences, Steyrergasse 17, A-8010 Graz, Austria

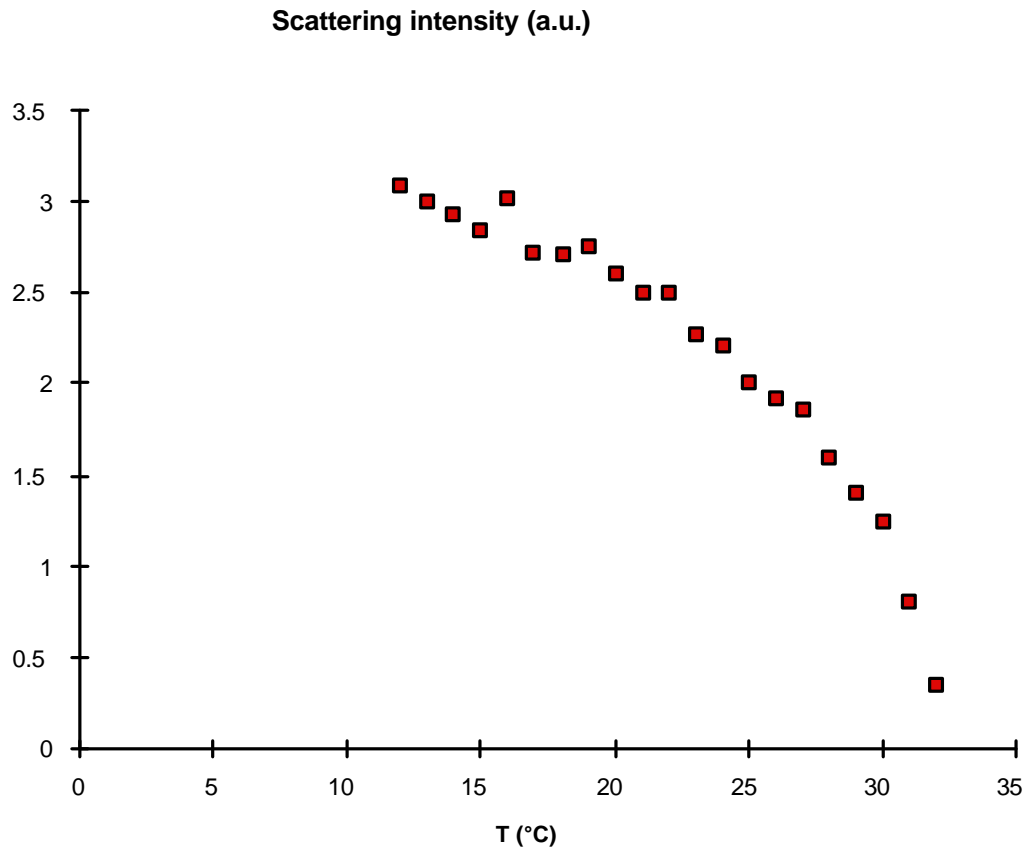
⁴ Department of Physics, Faculty of Education, University of Maribor, Koroska 160, 2000 Maribor, Slovenia

⁵ Department of Physics, Faculty of Mathematics and Physics, University of Ljubljana, Jadranska 19, 1000 Ljubljana, Slovenia

We have studied the nematic to smectic A (N-A) phase transition of the 4-cyano-4'-octylbiphenyl (8CB) liquid crystal confined to the controlled pore glass [1] (CPG) matrix of pore diameter 400 nm via small angle X-ray scattering (SAXS). We find that the smectic ordering in CPG is similar as in the bulk, with a rather sharp transition close to the bulk N-A transition temperature. Smectic ordering is much stronger than for 8CB in aerogel [2] and also the smectic correlation length is about three times larger than in aerogel, which indicates that the smectic layers are perpendicular to the cylindrical pore axes. The smectic layer spacing decreases from 3.2 nm at the N-A transition to 3.18 nm 20 K below the transition which is close to the layer spacing in bulk 8CB. The crystalline ordering in CPG is suppressed, and no crystalline peaks were observed even 8 K below the bulk smectic A-crystal phase transition temperature.

[1] A. Zidansek, S. Kralj, G. Lahajnar, S. Zumer and R. Blinc, *Mol. Cryst. L iq. Cryst.* 299, 307-320 (1997).

[2] N.A. Clark, T. Bellini, R.M. Malzbender, B.T. Thomas, A.G. Rappaport , C.D. Muzny, D.W. Schaefer and L. Hrubesh, *Phys. Rev. Lett.* 71, 3505-3508 (1993)



Scattering intensity of the octylcyanobiphenyl (8CB) liquid crystal confined to the controlled pore glass (CPG) is proportional to the smectic order parameter. A continuous phase transition was observed at 33 °C. Temperature dependence of the smectic correlation length and smectic interlayer distance was also measured.

2. Life Sciences

Structure determination with SAXS measurements of various modified P70S6kinase at very low concentrations

H.Amenitsch¹, M.Rappolt¹, P.Laggner¹ and Ch.Kühne²

1. Institute of Biophysics and X-Ray Structure Research, Austrian Academy of Sciences, Steyrerg. 17, A-8010 Graz, Austria.

2. ICGEB - International Centre for Genetic Engineering and Biotechnology, AREA Science Park - Padriciano 99 - 34012 Trieste - ITALY

Biological active human p70S6k and its various types of mutants were produced from insect cell cultures (Sf9-cells). This allowed the isolation of native p70S6k at concentrations of 0.2 mg/ml. The radiation damage was analysed for protein integrity in western blots and in addition kinase activities were compared before and after measurements. As an outcome, lowering of the temperature to 10 °C proved to be essential for recovery of the input kinase activity.

Aggregation problems observed in the first set of experiments mainly due to detergents in the buffers have been solved by optimisation of the protein purification, including the dialysis procedures for the following experiments. This time consuming trails established a protocol to measure an intact p70S6k at very low protein concentrations described previously as very low for SAXS experiments.

Diffraction patterns obtained are shown in Fig. 1. Single amino acid substitutions at the N-terminus results in a significant change of the calculated Guinier Radius (see tab.1). This correlates with the observed different electrophoretic mobilities for an active versus inactive p70S6k [1]. Moreover the outcome of these series of experiments proofs for the first time a structural difference of an active (wild type, SEED/DEED) in comparison to an inactive (SEED/AEED) p70S6k. Beside the p70S6k this should be relevant for many other kinases involved in signalling, whose electrophoretic mobilities vary in response to their activation.

[1] H.Edelmann H., Kühne Ch., Petritsch C., and Ballou L.M. (1996) J.Biol.Chem **271**, 963.

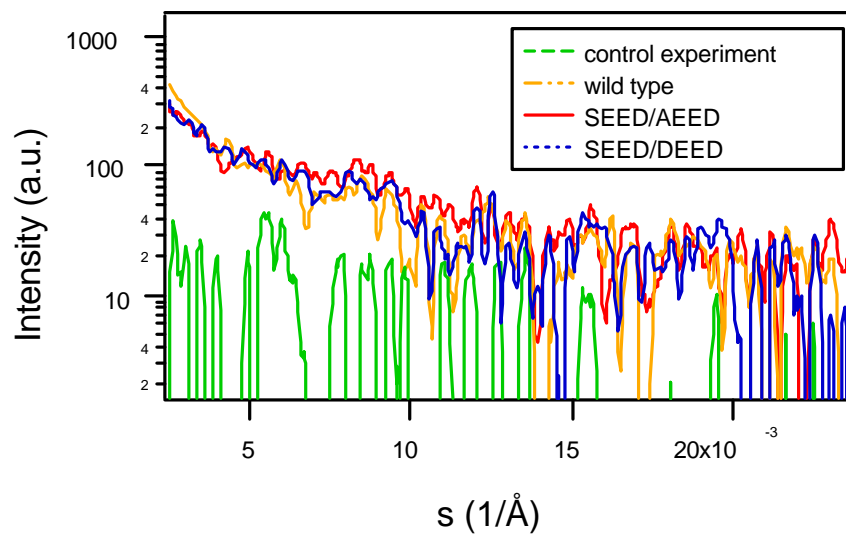


Fig.1 SAXS diffraction pattern of a biological active p70S6k protein modification is compared to its respective structural mutants (wild type, substitution mutant (SEED/DEED) and substitution mutant (SEED/AEED)). The control experiment represents the measurement of a mock sample preparation.

Sample	$R_g/\text{\AA}$
wild type	40.3 (18)
SEED/AEED	29.5 (25)
SEED/DEED	37.3 (22)

Tab.1 Guinier Radius calculated from the data in Fig 1.

D-Periodicity in Intramuscular Collagen

H. Amenitsch¹, S. Bernstorff², A. Bigi³, N. Roveri³ and J. S. Shah⁴

1. *Institute for Biophysics and X-ray Structure Research, Austrian Academy of Sciences, Steyrergasse 17, A-8010 Graz, Austria.*

2. *Sincrotrone Trieste, ELETTRA, Strada Statale 14 km 163.5, Trieste, Italy*

3. *Dip. di Chimica "G. Ciamician", Università di Bologna, Via Selmi, 2 Bologna, Italy.*

4. *University of Bristol, H.H. Wills Physics Laboratory, Royal Fort, Tyndall Avenue, BS8 1TL Bristol, UK*

The dependence of chemical, mechanical and thermal properties of collagenous tissues such as tendons and ligaments on the d-periodicity of collagen is well established with a view to explain how these tissues work in the human and animal. However, very little attention is paid to intramuscular collagen in spite of the fact that the properties of intramuscular collagen are very different to those of tendons and ligaments. Furthermore muscle is not only important from the viewpoint of the biomechanical in-vivo function; but it also plays a vital part in determining the properties of meat, such as texture and toughness when used as food. We studied the changes in the d-periodicity of the intramuscular collagen with hydration and thermal treatment. Intramuscular collagen is a very weak diffracting material but it was possible to observe several orders of diffraction arising due to the d-periodicity of collagen using the small angle scattering station at the Elettra synchrotron Radiation facility. The observations show that

- (1) the d-periodicity of hydrated intramuscular collagen is significantly different to that of the wet rat tail tendon (RTT) and dry RTT. The table below shows the different values:

Specimen	d-value (nm)
Dry RTT	~64.0
Wet RTT	~66.9
Wet Intramuscular	~65

This is highly significant since the d-value of other hydrated uncalcified collagenous tissue like Turkey tendon and annulus fibrosus does not differ significantly from that of the wet RTT.

- (2) The intramuscular collagen is more susceptible to radiation damage (as gauged by the deterioration in the diffraction pattern) than the wet RTT.
- (3) Structural damage does occur on thermal treatment. It has been observed that the D-periodicity does not gradually change with temperature but that it is destroyed within a narrow temperature range (~5 degree) in the vicinity of the denaturation temperature of the protein collagen. This is an important observation since it shows that destruction of d-periodicity may be due to the process of denaturation. Generally speaking, time taken for destruction decreases with increasing temperature. Comparison of the results suggest that the d-periodicity in the wet RTT is more robust than that in the intramuscular collagen. Destruction of the pattern is quicker and at a lower temperature in intramuscular collagen than in RTT collagen.

Time-resolved X-ray diffraction studies on intact single muscle fibres using the newly commissioned SAXS beamline at Elettra

G. Cecchi, M.A. Bagni, H. Amenitsch*, S. Bernstorff**, C.C. Ashley# and P.J. Griffiths#

Dipartimento di Scienze Fisiologiche, Università di Firenze, Italy

* Institute of Biophysics and X-ray Structure Research, Steyrergasse 17, 8010 Graz, Austria.

** Sincrotrone Elettra, Trieste, Italy,

University Laboratory of Physiology, Oxford, U.K.

Structural changes which accompany the 'power stroke' of the cycling cross-bridge in a contracting muscle occur in the submillisecond time domain. These structural changes may be synchronised by a length perturbation, in the form of either a step or a sinusoidal oscillation. The mechanical response to a length change is best studied in a single cell preparation, where the viability of the preparation is immediately apparent, interfibre variability in a cell population is eliminated, and sarcomere length can be monitored and controlled. However, because a single fibre preparation provides only a relatively small diffracting mass for structural investigations using X-ray diffraction, the time resolution of such studies is limited by both the intensity of the X-ray reflection under investigation and the strength of the X-ray source.

We have used the SAXS beamline at Elettra to investigate its suitability for time-resolved X-ray diffraction studies on single, intact, skeletal muscle fibres of the frog (*Rana temporaria*). Using the wiggler source tuned to 8keV, we obtained well resolved equatorial X-ray diffraction patterns within 250ms exposure to the beam from a single fibre from the tibialis anterior muscle.

On activation, the 14.3nm reflection intensity fell by 50% (Fig. 1). This is thought to be a consequence of broadening of this peak in the equatorial plane, and not a true reduction in total intensity. However, on application of a step length change, the intensity of the reflection fell still further. This fall in intensity is unrelated to reflection broadening, and indicates a true fall in total intensity. Using SAXS, these changes could be followed at 5ms time resolution in a single fibre. During the rise of tetanic tension, an increase in 14.3nm spacing to 14.5nm occurred, with a similar time course to the rise of isometric tension. However, the discharge of tension during a quick release did not restore the original spacing, indicating that the bulk of this spacing change is due to a structural rearrangement in the muscle protein myosin, and not filament compliance. When exposed to small amplitude sinusoidal length oscillations at 1kHz, the activated muscle responds with a sinusoidal force response which leads the imposed length changes. This phase lead is thought to arise from rate of the synchronised power stroke response to the length oscillation. We detected a 14.5 nm reflection intensity change accompanying the length oscillations at 0.05 ms time resolution, confirming a cross-bridge conformational change occurs during a sinusoidal cycle.

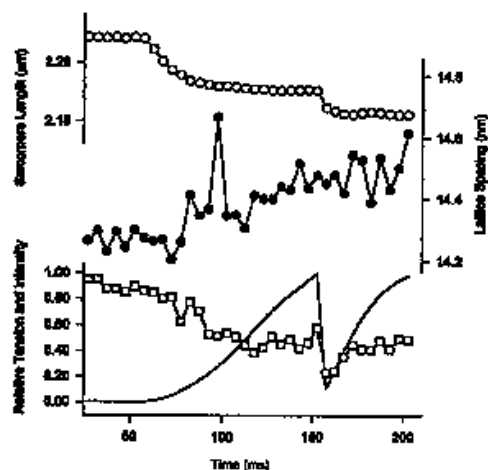


Fig. 1 Intensity (squares) and spacing (filled circles) changes of the 14.3 nm meridional reflection during tetanic tension development (continuous line), and quick sarcomere length (open circles) change.

THERMAL TREATMENT INDUCED ORDER IN PROTEIN LANGMUIR-BLODGETT FILMS AS REVEALED BY SMALL-ANGLE SCATTERING OF SYNCHROTRON RADIATION

Victor Erokhin, Sandro Carrara, Claudio Nicolini
Institute of Biophysics - University of Genoa - Italy
contact: erokhin@ibf.unige.it

Langmuir-Blodgett (LB) technique allows to form complex structures of different materials with a molecular resolution in one direction. The method is also useful for the formation of protein layers[1]. Unfortunately, the films are practically amorphous in the most of cases.

At the same time, it was shown, that proteins in LB films are extremely heat-proof - their secondary structure is preserved till 200° C, while the thermal stability of functional activity depends upon the type of the protein, but in any case several tens of degrees more with respect to that in the solution. On the other hand, there is a possibility to improve the ordering of the film performing the thermal treatment of it, analogue to the crystals annealing. Applicability of this approach was already demonstrated on the LB films of immunoglobuline G (IgG)[2].

The aim of the work, thus, was to study, how general is the suggested approach. For these reasons, LB films of different proteins were deposited and studied, namely, IgG, thioredoxin and cytochrome P450. The choice of the proteins was determined by the fact that they are very different in terms of molecular weight and structure. They are different also from the functional point of view: first is antibody, second is enzyme and third is a metalloprotein.

Films were deposited on MDT Langmuir trough. The subphase was water (purified with Milli-Q, resistance is 18.2 cm) for IgG and cytochrome P450, and 1M KCl for thioredoxin. In the case of thioredoxin, the film was washed with water after depositing each layer in order to remove the residual salt. Films were transferred with horizontal lift technique. Thermal treatment was performed in a usual oven at 150°C for 10 minutes after depositing each successive layer.

Structural measurements were performed in the small-angle station of Elettra. Samples were rotated with respect to the incident beam and the intensity was recorded with linear position-sensitive detector.

Similar results were obtained for all three protein films. For example, samples with LB films of thioredoxin deposited without any thermal treatment give no Bragg reflections, indicating that the film structure is rather amorphous. (Data not shown). The situation was different for the films prepared with thermal treatment of the layer after layer. X-ray pattern obtained from the LB film thermally treated is shown in the Fig. 1. The pattern contains rather wide Bragg reflections, indicating that the film order was really improved. It is interesting to note, that the same results were obtained for all three studied proteins - the order was significantly improved in a case of thermally treated proteins. Improvement of the in-plane structure of LB monolayer of photosynthetic reaction centres from *Rhodobacter sphaeroides* after similar thermal treatment was studied by STM measurements and was already reported[3]. Comparison of all these data allows to conclude that improvement of the film order after thermal treatment is a general phenomenon which is connected with the molecular rearrangement during heating.

Bibliography

- [1] Yu. Lvov, V. Erokhin, and S. Zaitsev "Langmuir-Blodgett protein films", *Biol. Mem.*, **4(9)**, 1477-1513 (1991).
- [2] V. Erokhin, P. Facci and C. Nicolini "Two-Dimensional Order and Protein Thermal Stability: High Temperature Preservation of Structure and Function", *Biosensors and Bioelectronics*, **10**, 25-34 (1995).
- [3] P. Facci, V. Erokhin and C. Nicolini "Scanning tunnelling microscopy of a monolayer of reaction centres", *Thin Solid Films*, **243**, 403-406 (1994).

Acknowledgement

The authors thank Sigrid Bernstorff, Heinz Amenitch, Michael Rappolt for their collaboration during the experiments on Trieste.

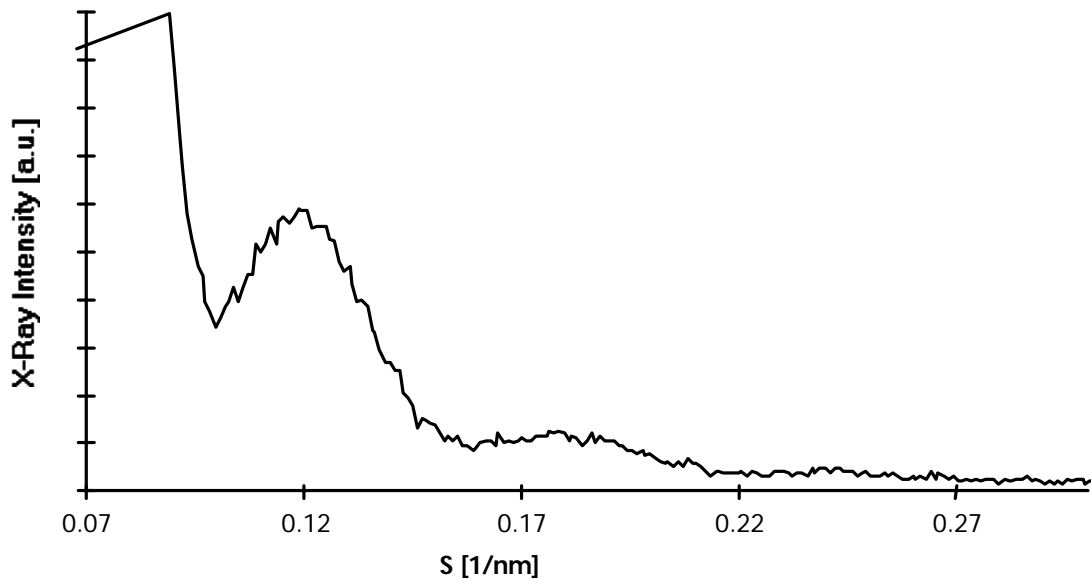


Figure 1: X-ray spectra of a 10 multilayer LB film of thioredoxin heated layer by layer presenting clear Bragg reflections. The same measurements on the same kind of LB films but not thermally treated has shown no reflections.

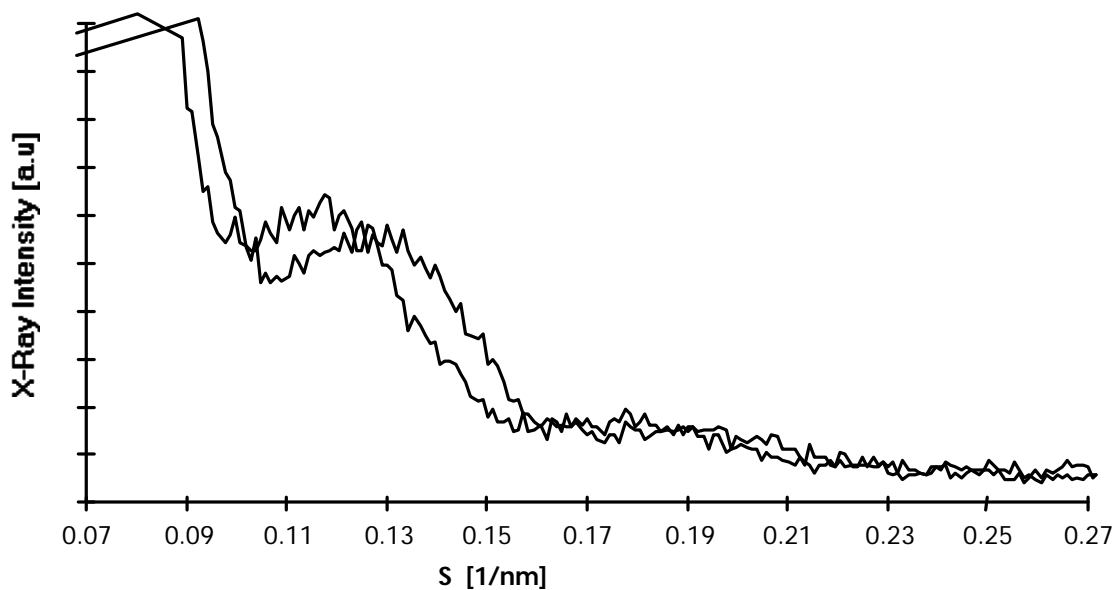


Figure 2: X-ray spectra of 10 multilayer LB film of P450 presenting clear Bragg reflections. The measurement on the LB films thermally treated (heavy line) shows reflections shifted with respect to the film not treated (weak line). This fact should reflect an increase of the films structural order.

In-situ synchrotron x-ray scattering study of the tensile properties of collagen

PETER FRATZL¹, KLAUS MISOF, IVO ZIZAK

*Materials Physics Institute and Ludwig-Boltzmann Institute of Osteology,
Univ. Wien, Strudlhofgasse 4, A-1090 Wien, Austria*

GERT RAPP

European Molecular Biology Laboratory Outstation, Notkestr. 85, 22603 Hamburg, Germany

HEINZ AMENITSCH

*Institute of Biophysics and X-Ray Structure Research, Austrian Academy of Sciences,
Steyrerg. 17, A-8010 Graz, Austria*

AND SIGRID BERNSTORFF

Sincrotrone Trieste, Strada Statale 14 - Km. 163.5, 34012, Basovizza, Trieste, Italy

The outstanding mechanical properties of collagen are due to its structure at various levels of hierarchical organisation. To study the relation between tensile properties and structure at the fibrillar level, we have developed a device for *in-situ* synchrotron x-ray scattering investigations under mechanical tension [1]. Tendons from the rat tail were kept in a humid atmosphere and tension was applied by increasing the length continuously. Both the force and the elongation of the tendons were measured at the same time as the equatorial and the meridional x-ray scattering. Fig. 1 shows the meridional peaks as a function of stress on the tendon measured at the SAXS beamline [2] of ELETTRA.

At lower strains, we had previously found that the intensity of the diffuse equatorial scattering increases linearly with the strain, corresponding to an increase in the degree of lateral ordering in the fibrils. This could be reproduced quantitatively by a model [1] where kinks of the molecules (occurring mostly in the gap-region of the fibrils, case A in Fig. 2) are straightened out due to stretching (case B). This also explains the upwards curvature of the stress-strain curve (dark part in Fig. 2) by an entropic mechanism [1].

At larger strains, the force increases linearly with the elongation of the tendon (grey part in the right of Fig.2) and further elongation leads to a dramatic change in the relative intensities of the meridional diffraction orders (see Fig. 1). In particular, the intensity ratio of second to third order increased, which can be interpreted [3,4] as a parallel gliding of the molecules (case C in Fig. 2). In addition, we found that all higher diffraction orders vanished gradually with increasing stress, which may be explained by an increasing fuzziness of the interface between gap and overlap region. As shown in the Fig. 2 (C), this would occur when neighbouring molecules glide randomly by slightly different amounts [4].

Finally, it was found that the axial periodicity (defined by the peak spacing in Fig. 1) changes less than the total length of the tendon under stress. This points towards some mechanism of interfibrillar gliding which is still very poorly understood [4].

Work supported by the Fonds zur Förderung der Wissenschaftlichen Forschung (P11762-PHY).

¹ Present address: Erich Schmid Institute of the Austrian Academy of Sciences and University of Leoben, Jahnstr. 12, A-8700 Leoben, Austria. E-mail: fratzl@unileoben.ac.at

References:

- [1] K. Misof, G. Rapp, P. Fratzl (1996) *Biophys. J.* 72:1367-1381.
- [2] H. Amenitsch, S. Bernstorff, P. Lagner (1995) *Rev. Sci. Instr.* 66:1624-1626.
- [3] W. Folkhard et al. (1986) *Int. J. Biol. Macromol.* 9:169-175.
- [4] P. Fratzl, K. Misof, I. Zizak, G. Rapp, H. Amenitsch, S. Bernstorff (1998) *J. Struct. Biol.* (in press)

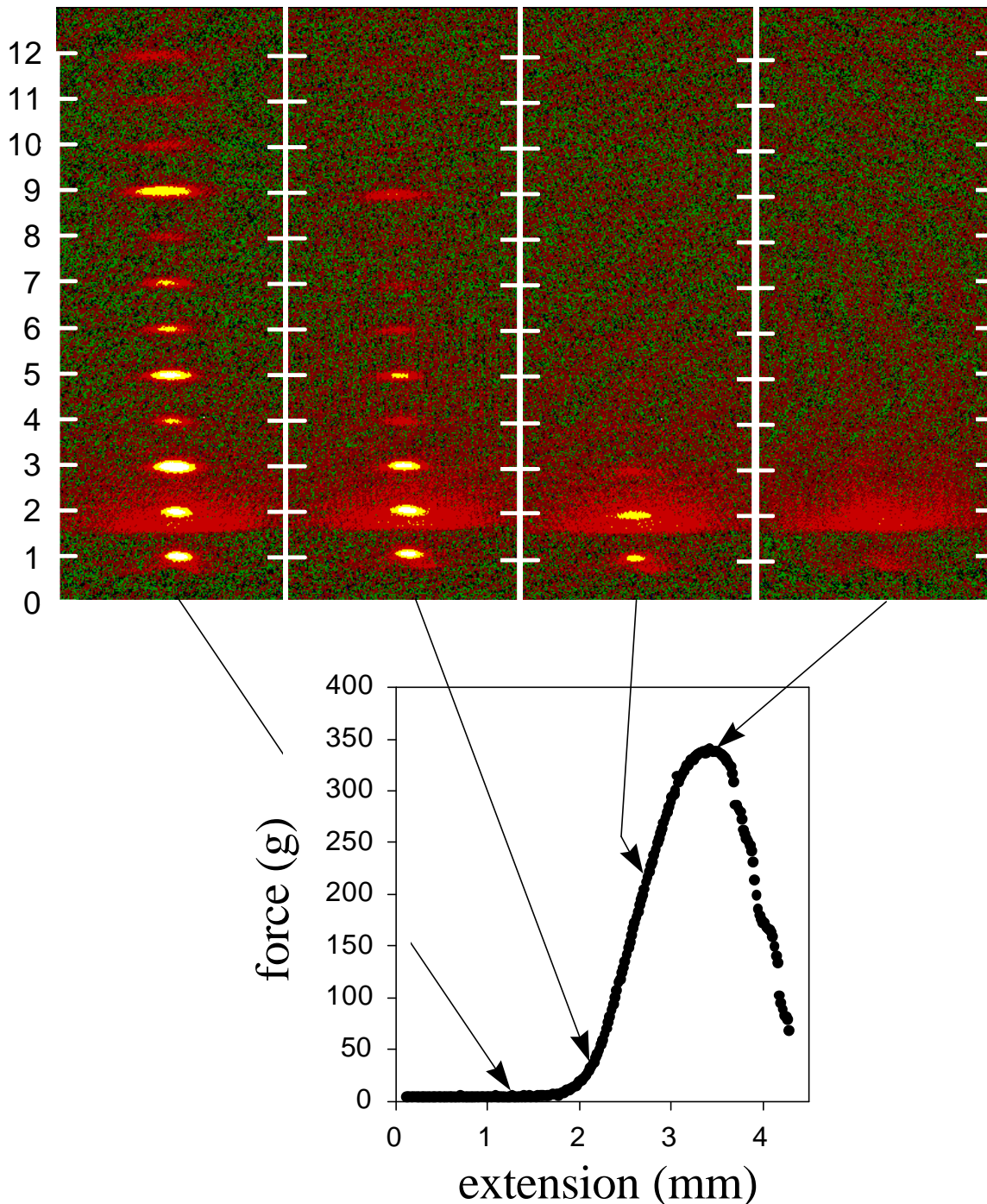


Fig. 1: Meridional reflections of collagen from stretched rat tail tendon measured with a CCD camera as area detector (AXS, Karlsruhe) at the SAXS beamline [2] at ELETTRA. Each of the four spectra were collected during a constant strain rate experiment at different moments during the extension of the fibre.

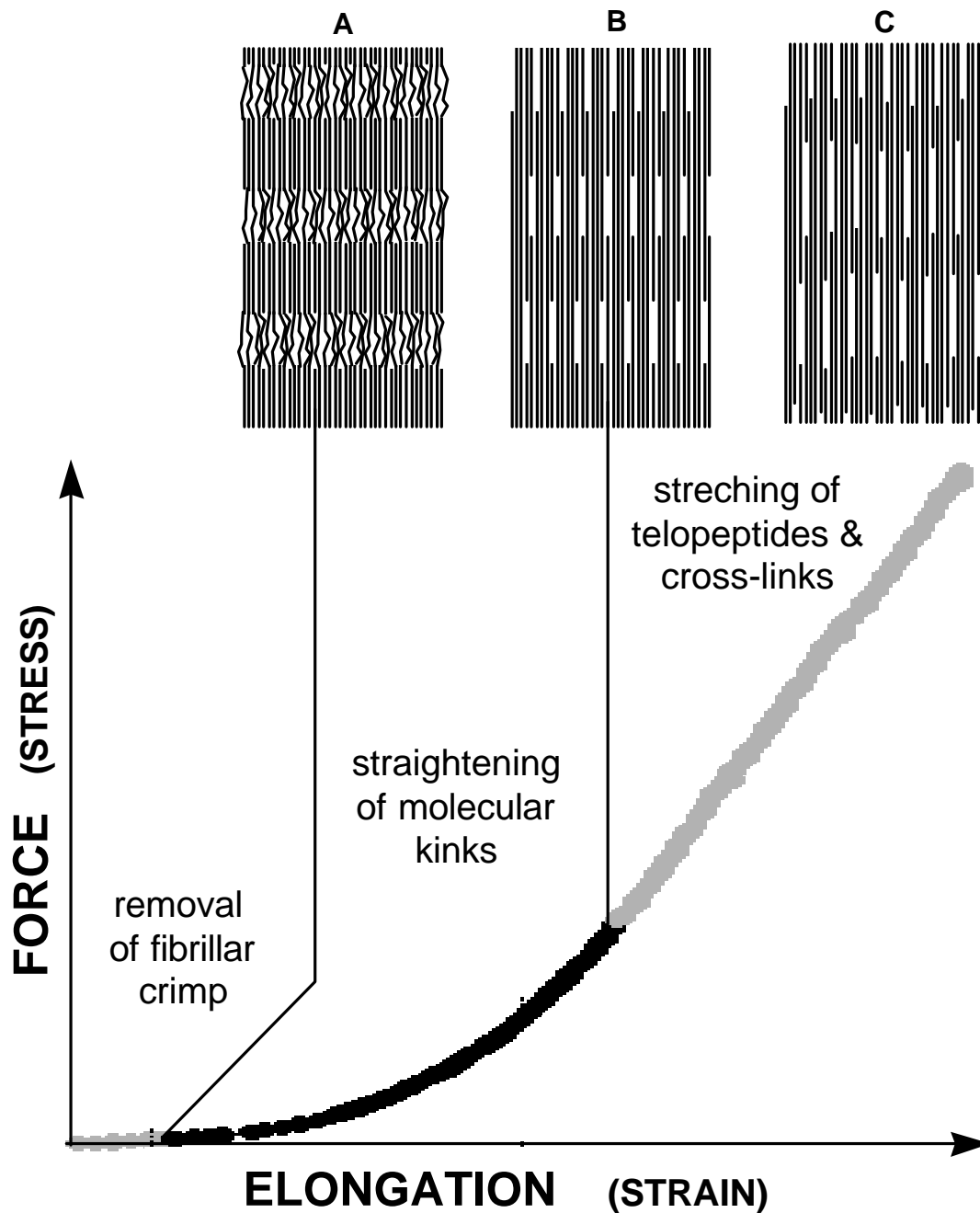
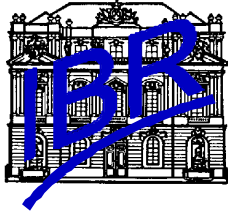


Fig. 2: Model for the stress induced changes in the fibrils at the molecular level (from [4]). At small strains, molecules are kinked inside the gap-region of the fibril structure. At intermediate strains, molecular kinks are straightened out, leading to entropic elasticity [1]. At large strains, molecules glide parallel to each other [3] and the interface between gap and overlap regions is getting increasingly fuzzy [4].



Human Low Density Lipoproteins (LDL)-Microphase Separation

M. Gailhofer, H. Amenitsch, S. Bernstorff*, P. Laggner (282/96)

Institute of Biophysics and X-Ray Structure Research

Austrian Academy of Sciences, Steyrergasse 17, 8010 Graz, Austria

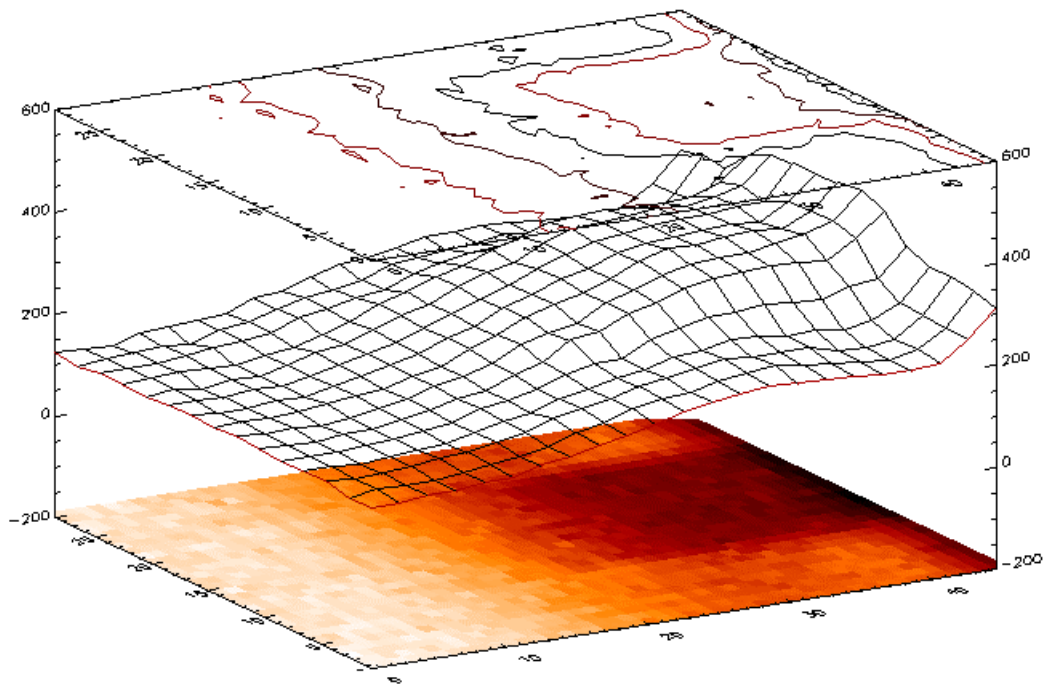
* Sincrotrone Trieste, Trieste, Italy

Low density lipoproteins (LDL), the major carriers of cholesterol in circulating blood and intimately involved in atherogenesis, are complex supramolecular assemblies of various classes of lipids and a single copy of the protein Apo-B₁₀₀.

The structure of LDL can be described, in general terms, by a quasispherical core-shell model, in which the apolar constituents (esterified cholesterol and triglycerides) form a core of about 150 Å diameter, which is surrounded by amphiphilic lipids (phospholipids, unesterified cholesterol) and the protein. LDL shows a very special physical feature, which makes it unique among all structural elements of blood: It undergoes a major structural transition of the apolar core closely below physiological body temperature. One of the key questions yet to be answered is whether the triglycerides and cholesteryl esters are subject to a microphase separation within the apolar core at lower temperatures, or not. This issue is of immense interest, because the transition has a major impact on many biochemical processes, such as enzyme activity, susceptibility to oxidation or solubility of vitamins or drugs. Furthermore nothing is known about the time scale in which this core-transition occurs. By elucidating this matter we would gain information on biological and medical (atherosclerosis) relevance of the core-transition.

Structural knowledge so far originates mainly from SAXS data. To reach the objective of gaining more detailed structural information, as outlined above, we made use of the high precision SAXS in the range of $5 \cdot 10^{-3} < h < 0.3 \text{ \AA}^{-1}$ at ELETTRA. Native and chemically modified LDL samples were measured. To get a wider range of LDL with different chemical compositions of the core, we produced in vitro triglyceride-enriched LDL in our laboratory. In addition, by introducing organo-lead compounds we were able to achieve a pronounced enhancement in contrast, especially in the low-contrast zone of the inner core.

First attempts were made towards time-resolved measurements in combination with temperature jumps. First results are very encouraging and suggest that this approach is worth continuing.



Small angle X-ray and neutron scattering profiles of chloroplast thylakoid membranes determined by the aid of magnetic alignment. Nature of irreversible structural changes induced by intense light

G. Garab¹, T. Jávorfí¹, H. Amenitsch², Z. Cseh^{1,3}, L. Mustárdy¹, S. Borbély⁴, L. Rosta⁴ and P. Laggner²

1Institute of Plant Biology, Biological Research Center, Hungarian Academy of Sciences, Szeged; Hungary

2Institute for Biophysics and X-ray Structure Research, Austrian Academy of Sciences, Graz, Austria

3Department of Biological Physics, Eötvös University, Budapest

4Institute of Solid State Physics, Central Research Institute for Physics, Budapest, Hungary

Small angle X-ray and neutron scattering (SAXS/ELETTRA and SANS/Budapest) experiments were carried out on randomly oriented and magnetically aligned isolated chloroplast thylakoid membranes in order to study their structure and the nature of the rearrangements provoked by changes in the osmotic pressure, ionic strength, or induced by light. In this type of multilamellar system, probably due to a polydispersity, hardly any characteristic scattering profile can be detected when measured in random suspension. Following the alignment of the membranes in a magnetic field of about 1 T, an alignment of membranes with their planes preferentially parallel with the beam, SAXS and SANS exhibited well discernible peaks: a band in real space of approximately 40 Å, which is characteristic to the membrane thickness, and some other peaks (around 80 and 150-200 Å) which originate from different repeat distances between layers (and aqueous phases), the origin of which are yet to be determined. SAXS and SANS was applied on magnetically aligned thylakoids to study the effect of the irreversible structural rearrangements induced by prolonged exposure of the thylakoids to intense light. The structural changes were earlier detected as the loss of circular dichroism bands given rise by the long range chiral of chromophores in thylakoids [1]. We show that illumination of chloroplasts does not affect the thickness of the membranes, and our data strongly suggest that the irreversible structural change in intense light is confined to a lateral disorganization of the initially highly ordered particles/pigment-protein complexes.

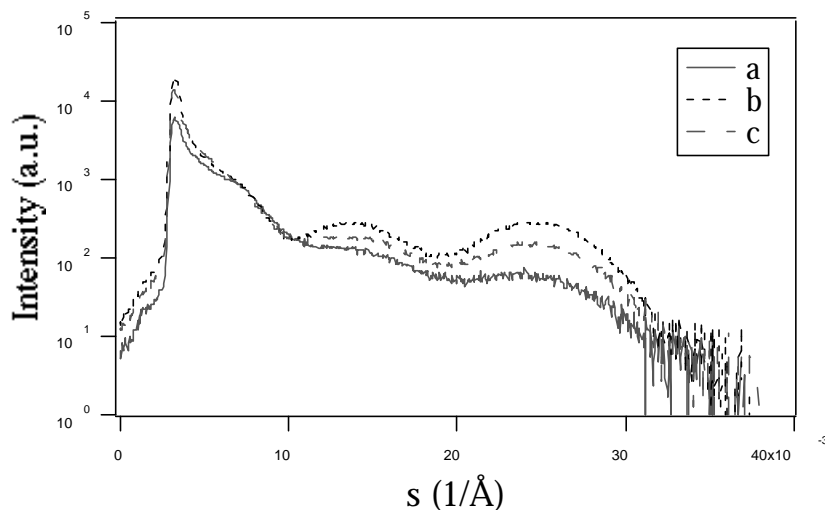


Fig. 1 Small angle scattering of X-ray by randomly (a) and magnetically (b) oriented chloroplasts. (For magnetic orientation a field of 1T was applied which aligned the membranes perpendicular to the field vector and parallel with the beam.) Curve c shows the same chloroplasts in magnetic field after 45 min preillumination with white light of 1000 W/m².

[1] Gussakovskiy et al., 1997, Photosyn. Res. 51, 11

Time-resolved SAXS study of the solubilization of POPC lipid bilayers by the nonionic detergent C₁₂E₈

Thomas Gutberlet¹, Heiko Heerklotz^{1,2}, Burghard Madler¹, Gotthard Klose¹,
Heinz Amenitsch³, Michael Rappolt³

¹ Institut fur Experimentelle Physik I, Universitat Leipzig, Linnestr. 5, 04103 Leipzig,
Germany

² Department of Biochemistry, McMaster University Health Sciences Centre, Hamilton, ON
L8N 3Z5, Ontario, Canada

³ Sincrotrone Trieste, S.S. 14, km 163.5, Area Science Park, 34012 Basovizza / Trieste, Italy

The modification of biological model membrane systems by interaction of phospholipid membranes with detergents is of great importance for studying basic membrane properties [1,2]. Recently we have studied the thermodynamic behaviour of the ternary model system POPC/C₁₂E₈/H₂O in respect of the solubilization of the lipid bilayers upon addition of the micelle-forming detergent (3). As the concentration and temperature dependent phase boundaries of the vesicle-to-micelle transformation on addition of detergent to the lipid bilayer were established, three different structural regimes were found. At first the detergent is incorporated into the lipid bilayer up to saturation of the bilayer with detergent around a mole fraction $X^{\text{sat}} = 0.35$ (at 25°C). Secondly on further increase in concentration of detergent, mixed micelles appear in coexistence with the detergent saturated lipid bilayer.

Above $X^{\text{sol}}_x = 0.65$ all bilayers have disappeared and only micelles are present.

The thermodynamic approach yields a very accurate measure of the phase boundaries and gives a detailed insight into the intermolecular forces controlling the stability of the different types of aggregates. However, it gives no information about the structure of the different aggregates. Note that the local energetic conditions of a molecule in a lamellar arrangement do not depend on whether it is situated in a large (almost no local curvature) unilamellar vesicle, or, for example, in a large lamellar sheet or cup-shaped vesicle. Thus, to establish the structural arrangements present, it cannot even be ruled out definitely that the coexistence of lamellar and micellar arrangements corresponds to the plane and the edge of lamellar sheets, the ratio of which varies with size. Hence, structural information from SAXS must be considered an essential, complementary information.

Using SAXS we now have investigated the structural changes and process of aggregation between large unilamellar vesicles and micelles, occurring during the investigated solubilization process. The nucleation and growth of the particles during the process and the kinetic of it are important information to understand the interaction between the phospholipid membrane and the detergent.

In our first series of measurements mixtures of POPC and C₁₂E₈ at $x = 0.1, 0.3, 0.35, 0.6, 0.7$ and 0.85 were prepared under the same conditions as in the ITC experiments (3) and investigated at the SAXS beamline at ELETTRA under equilibrium conditions at temperatures between 10 and 60 °C. Unfortunately, higher lipid concentrations than in the calorimetric experiments had to be used to obtain sufficient signal intensity, preventing the preparation of unilamellar vesicles.

In Fig. 1 recorded diffraction patterns for POPC/C₁₂E₈, $x = 0.35$ at different temperatures are shown. The Bragg peak of the lamellar bilayer phase shifts to lower q -values on increasing the temperature, indicating a decrease in the concentration of the detergent incorporated in the phospholipid bilayer. Bragg peaks were found only in the lamellar phase of the ternary system as result of the presence of multilamellar vesicles. In the intermediate region and the micellar phase only diffuse scattering was observed. Similar results were obtained in the ternary systems of POPC/C₁₂E₅/H₂O and POPC/C₁₂E₃/H₂O.

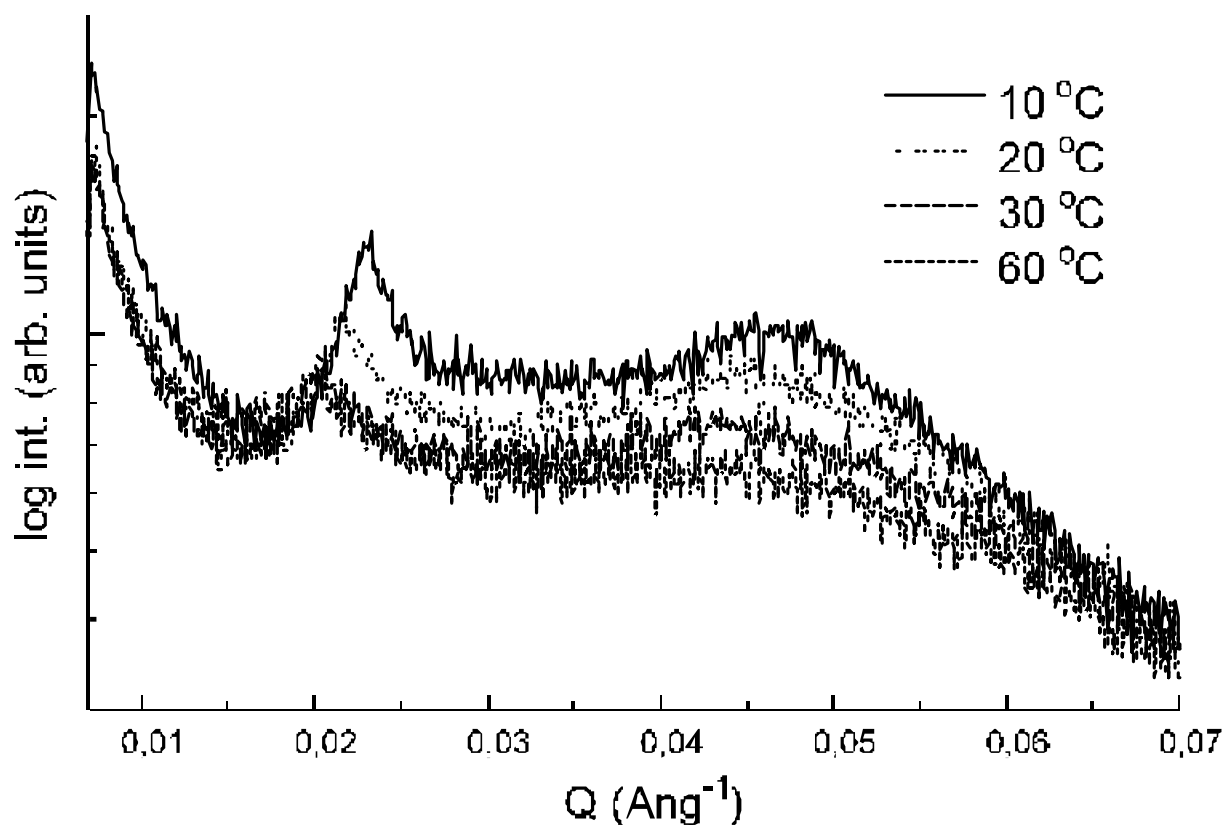


Fig. 1: SAXS diffraction pattern of POPC/C₁₂E₈, 95 mM, $x = 0.35$, at various temperatures

The ITC experiments had given rise to a number of hypotheses concerning the structural pathway of the obtained phase transitions, i.e. the non-equilibrium states facilitating the structural transformation. In order to check these suggestions, a newly constructed mixing chamber was used and Bragg peaks were found only in the lamellar phase of the ternary system. In the intermediate region and the micellar phase only diffuse scattering was observed. Similar results were obtained in the ternary systems of POPC/C₁₂E₅/H₂O and POPC/C₁₂E₃/H₂O.

Another important issue is the pathway of these phase transitions, i.e. the non-equilibrium states facilitating the structural transformation. Note that a biological membrane is far apart from thermodynamic equilibrium, focusing the interest on kinetically entrapped non-equilibrium states. The time resolved mixing heats had given rise to a number of hypotheses. In a second step we started to investigate the structural behaviour of our system during the mixing process of the phospholipid and the detergent. In contrast to the stepwise injections used by the titration calorimetry approach, equal amounts of dispersions of the pure lipid and detergent were mixed. Through this chamber known volumes of 90 mM POPC dispersion and 94 mM C₁₂E₈ solution were injected directly into the quartz capillary of the sample holder

and scattering curves were recorded continuously during the mixing procedure at different time regimes. The hypothesis that (i) the dissolution of micelles added to an almost detergent saturated bilayer, (ii) the subsequent incorporation of the detergent in to the lamellae and (iii) the destruction of the lamellar arrangement would be separated in time by the later steps being considerably slower than the earlier ones could not be supported by the SAXS experiment.

When lipid vesicles and detergent micelles were mixed reaching a composition of X^{sol} , i.e., forming lipid saturated micelles, the vesicles were destroyed immediately (i.e., within a few seconds, being the time resolution of the setup used) forming a broad variety of micellar structures. Then, the preferred micellar structure was formed slowly with a rate of about 1/10 min, as indicated by a sharpening of the corresponding peak in the scattering curve. Hence, this optimization process of the micellar shape and size rather than a slow vesicle destruction must be considered to account for the slow kinetics found in the mixing calorimetry experiments. The obtained scattering curves obtained by mixing 90mM POPC and 94 mM C12E8 (yielding a sample in the coexistence range) did not show any Bragg peaks of multilamellar arrangements as found in the static measurements, even after waiting up to 30 min. In order to gain a detailed time-resolved picture of the incorporation of detergent into lipid bilayers and the particular structural parameters of all the equilibrium and non-equilibrium aggregates formed by these mixtures, transformation of vesicle to micellar structures a complete analysis of the scattering curves recorded at different time intervals is in progress.

The measurements allowed a number of important conclusions and promoted a refinement of the evaluation and interpretation of the thermodynamic data as well. Subsequent SAXS experiments have to be performed using unilamellar vesicles, requiring an about five-fold intensity gain (20 mM POPC instead of 100mM). The stopped flow experiments could be improved by a faster time resolution of the mixing apparatus employed and should be accompanied by monitoring the respective transitions after a T-jump and/or pressure jump.

- 1.) M.T. Paternostre et al., *Biochemistry*, 1988, 27, 2668
- 2.) B. Mädler et al., *Chem. Phys. Lipids*, 1994, 71, 1
- 3.) H. Heerklotz et al., *J. Phys. Chem.*, 1996, 100, 6764

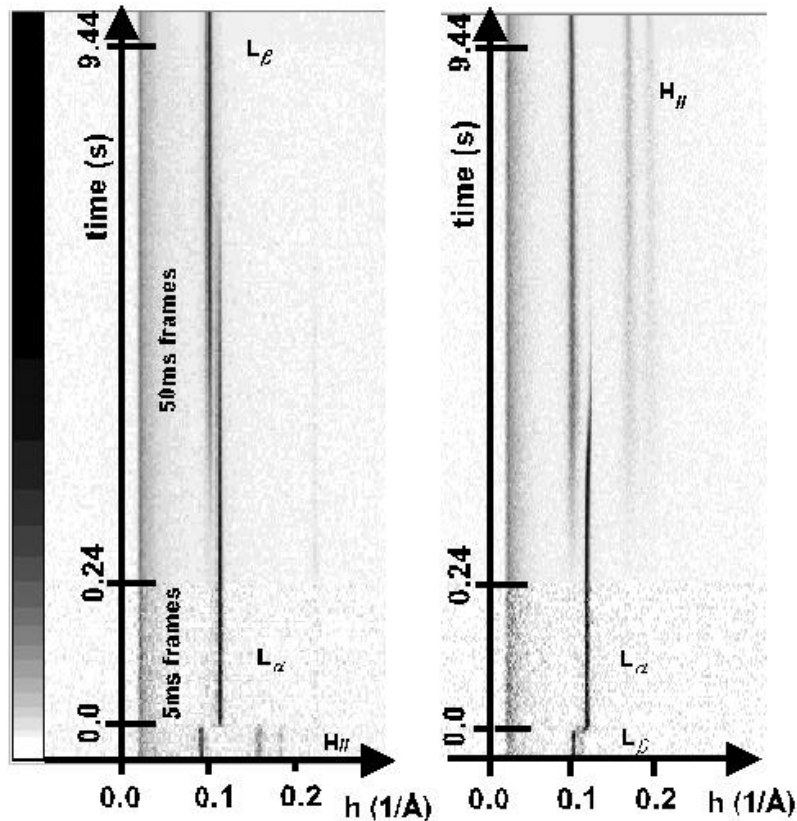
Time-Resolved Small-Angle X-Ray Scattering Studies of Pressure-Jump Induced Barotropic Phase Transitions of Lipids.

M. Kriechbaum, M. Steinhart, P. Laggner, H. Amenitsch and S. Bernstorff*

Institute of Biophysics and X-Ray Structure Research, Austrian Academy of Sciences, Graz, AUSTRIA, * Sincrotrone Trieste, Basovizza, ITALY.

Time-resolved jump relaxations experiments on biological samples like phospholipids in aqueous solutions are a suitable method to elucidate the kinetics and dynamics governing the structural rearrangements during a phase transition. We have applied this technique using pressure-jump on barotropic phase transitions of lipids monitored by time-resolved small-angle X-ray scattering with millisecond time resolution on the SAXS-beamline at ELETTRA.

Barotropic phase transitions were investigated with a high-pressure X-ray cell using jump amplitudes up to 3 kbar (0.3 GPa) within 10 ms. In particular, pressure jump induced phase transitions of the phospholipid DOPE within the temperature region of 5-70°C and a pressure region of 1-3000 bar were performed. Within this T and p region DOPE exhibits two lamellar (gel and liquid-crystalline) and a non-lamellar hexagonal-inverted phase. In the following figure two examples of such time-resolved p-jump SAXS-experiments are shown.



Time-resolved SAXS patterns of barotropic phase transitions of DOPE initiated by pressure-jumps. Each image consists of 256 time-sliced one-dimensional diffraction patterns in a two-dimensional reciprocal space versus time contour plot (intensity bar to the left) with h being the magnitude of the scattering vector. The exposure time increases from initially 5 ms to 50 and 100 ms. The left part shows a pressurizing jump from 0.015 to 0.229 GPa at 20°C. The right part shows a de-pressurizing jump from 0.25 GPa to the atmospheric pressure at 30°C. The respective phases (lamellar L_a and L_b , inverted hexagonal H_{II}) are written next to the corresponding diffraction pattern.

Time-Resolved Small-Angle X-Ray Scattering of Stopped-Flow Experiments of Protein Denaturations.

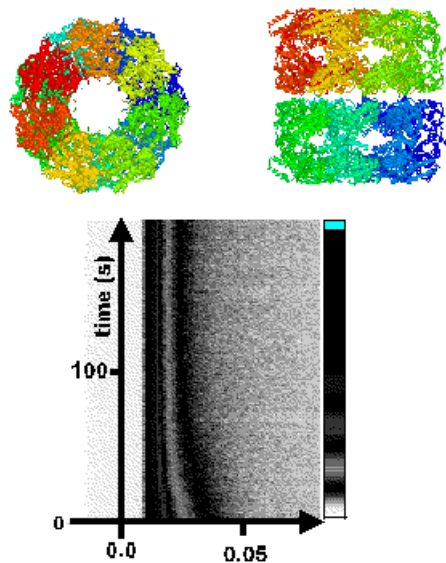
M. Kriechbaum, P. Laggner, Y. Hiragi(*), H. Amenitsch and S. Bernstorff(+), Institute of Biophysics and X-Ray Structure Research, Austrian Academy of Sciences, Graz, AUSTRIA, (*) Institute for Chemical Research, Kyoto University, Kyoto, JAPAN, (+) Sincrotrone Trieste, Basovizza, ITALY.

Time-resolved jump relaxations experiments on biological samples like proteins are a suitable method to elucidate the kinetics and dynamics governing the structural rearrangements during folding/refolding caused by temperature, pressure or chemical denaturation. We used the stopped-flow technique to study the unfolding of the protein GroEL by the chemical denaturant guanidine hydrochloride monitored by time-resolved small-angle X-ray scattering with (milli)second time resolution on the SAX-beamline at ELETTRA.

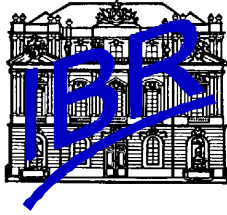
The stopped flow apparatus we used is available at UNISOKU Scientific Instruments, Osaka, Japan. It consists of two reservoirs (4 ml each) containing the solutions to be mixed. Each reservoir is connected to a (commonly) pneumatically driven syringe with a volume of 0.3 ml for each shot. When actuated by an electronic trigger signal both solutions are injected into the X-ray mixing chamber (dead time less than 1 ms). The X-ray cell is contained in a ceramic block (1 x 1 x 1 cm) with an optical path length of 1 mm between 2 sapphire windows of 0.05 mm thickness each.

GroEL in aqueous buffer solution was rapidly mixed (< 1ms) with 3-6 M guanidine hydrochloride and the denaturation was followed by time-sliced X-ray diffraction patterns. Depending on the admixture of various ligands and ions the denaturation (dissociation of the heptamer and unfolding of the monomers) had different time constants.

[1] H.Kihara, J.Synchrotron Rad., 1, 74-77 (1994)



Protein denaturation of GroEL (with K/Mg-ATP) by admixing 5M guanidine HCl in the stopped flow cell (<1 ms) recorded in time-sliced X-ray diffraction patterns (intensity bar to the right, units of the reciprocal scattering vector h in $1/\text{\AA}$) with an exposure time of 1 s per frame. The top shows the top and side view of GroEL, which as a chaperonin protein assists in protein folding. It consists of 14 identical subunits which are assembled as 2 identically heptameric rings, stacked back to back, forming roughly a hollow cylinder (length ~ 14.6 nm, outer diameter ~ 13.7 nm) with a hollow cavity of ~ 4.5 nm in diameter.



Effects of Antimicrobial and Hemolytic Peptides on the Phase Behavior of Biomembranes

A. Latal, E. Staudegger, H. Amenitsch & K. Lohner (250/96)
Institute of Biophysics and X-Ray Structure Research
Austrian Academy of Sciences, Steyrergasse 17, 8010 Graz, Austria

Small antimicrobial and hemolytic peptides of around 20-40 amino acids play an important role in the primary defense mechanisms of organisms. They act by perturbing the barrier function of cell membranes. It has been suggested that the specific membranolysis, i.e. some are toxic for humans while others kill bacteria, is in part related to the different architecture of bacterial and mammalian cell membranes. In order to get insight into the mechanism of membrane damage studies on membrane model systems have been initiated. Thereby, liposomes composed of negatively charged phosphatidylglycerol (PG) and zwitterionic phosphatidylethanolamine (PE) were used to mimic bacterial cell membranes. The thermotropic behavior of fully hydrated mixtures of dipalmitoyl-phosphatidylethanolamine (DPPE) and -phosphatidylglycerol (DPPG) was studied by calorimetry indicating a phase separation for samples containing >90 mol% DPPE.

X-ray scattering revealed that DPPG/DPPE mixtures showed a single bilayer transform up to 90 mol% DPPE, representative for unilamellar vesicles as found for pure DPPG. In contrast pure DPPE formed multilamellar liposomes as evidenced by the sharp Bragg reflections. The coexistence range of uni- and multilamellar liposomes was studied by synchrotron X-ray diffraction at the SAXS-Beamline ELETTRA, Trieste. The first appearance of a fraction of multilamellar vesicles was found for mixtures of DPPG/DPPE 7.5/92.5 mol/mol. At this lipid ratio a very sharp diffraction peak with a d-spacing of 61 Å was superimposed to the single bilayer transform. Increasing the amount of DPPE led to an increase of the multilamellar fraction within these mixtures (Figure 1). Above a molar ratio of DPPG/DPPE 2.5/97.5 predominantly multilamellar aggregates were detected. These findings are in excellent accordance with the calorimetric data obtained for these mixtures.

Our results can be explained by the different molecular properties of the individual lipid components which show that the miscibility properties of DPPE/DPPG mixtures are determined by the nature of the phospholipid headgroups. It can be expected that the constraints in the packing properties of these phospholipids will lead to defects in bilayers being of importance in the interaction with membrane-active peptides. This is of particular interest for the rationale design of peptide antibiotics which should lyse selectively bacterial cell membranes but not erythrocyte membranes predominantly composed of choline phospholipid.

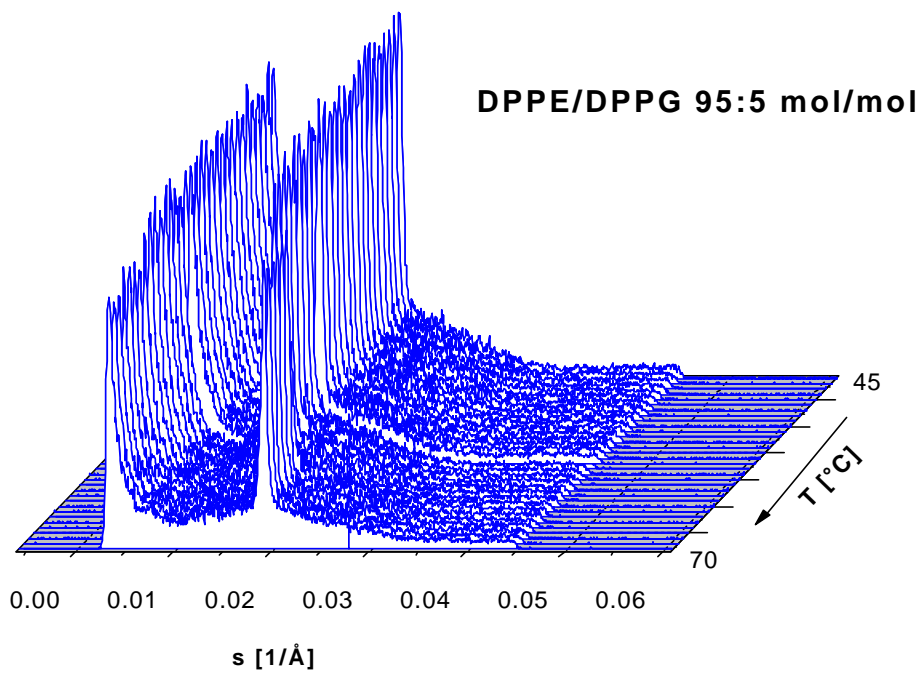
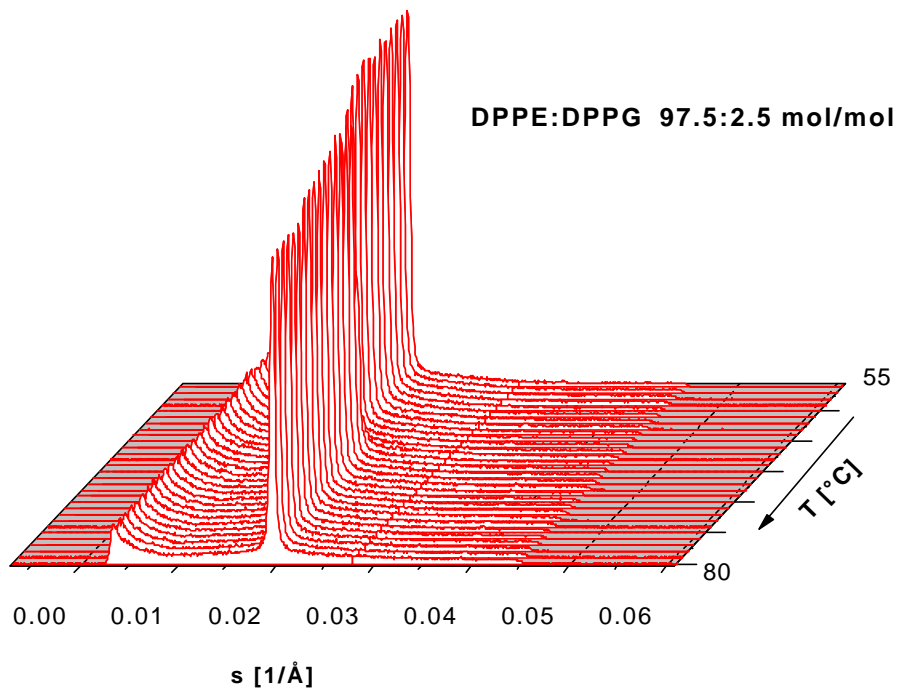


Figure 1: SAXS data of DPPE/DPPG mixtures in 10mM Na-phosphate buffer pH 7.4, the molar ratio is indicated in the panel ($s=1/d=2\sin\theta/\lambda$, 2θ =scattering angle, λ =wavelength).

Structural changes accompanying development of force in single muscle fibres: combined mechanical and X ray diffraction study on the molecular aspects of muscle contraction

V. Lombardi¹, H. Amenitsch², S. Bernstorff³, M. Linari¹, L. Lucii¹, G. Piazzesi¹
and M. Reconditi¹

¹ Dipartimento di Scienze Fisiologiche, Università di Firenze, Viale G.B. Morgani, 63, Firenze, Italy

² Institute for Biophysics and X-ray Structure Research, Austrian Academy of Sciences, A-8010 Graz, Austria

³ Sincrotrone Trieste, ELETTRA, Strada Statale per Basovizza 14 km 163.5, Trieste, Italy

The aim of the combined mechanical and X-ray diffraction experiments on single muscle fibres performed at the SAXS beamline of ELETTRA is to study how the number of diffractors (the fraction of myosin heads attached to actin to form the molecular motors or cross-bridges) and the form factor (the conformation of cross-bridges) modulate the reflection intensities in the diffraction pattern.

In the experiments done in the period 19-25.05.97 (proposal 155/96) we recorded with the gas-filled linear detector available at the SAXS beamline the effects of physical and pharmacological agents on the third order meridional reflection, M3, generated by the 14.5 nm repeat of myosin heads along the filament axis.

Single muscle fibres, freshly dissected under a stereomicroscope at the beamline, were horizontally mounted in the experimental trough between the lever arms of a capacitance gauge force transducer (Huxley & Lombardi, *J. Physiol.* 305, 15-16P, 1980) and a servocontrolled loudspeaker motor used to impose step and ramp length perturbations to the fibre. The linear detector was mounted at 2.5 m from the sample, parallel to the fibre axis so that meridional reflections could be recorded. To avoid detector saturation the dimensions of the beamstop were increased to allow to record only the M3 reflection. Tetanic contraction was induced at 4 °C by electrical stimulation at the frequency of 15-30 Hz. The intensity of M3 reflection was recorded with 500 ms frames at rest, at the isometric tetanus plateau and during the steady state force response to lengthening at the velocity of 0.1 µm/s per half-sarcomere, a condition that makes the cross-bridges to redistribute towards an early stage of the force-generating process (Piazzesi et al. *J. Physiol.* 445, 659-711, 1992; Piazzesi & Lombardi, *Biophys. J.* 68, 1966-1979, 1995). Measurements were done either in physiological solution (normal Ringer) or in a test solution containing 1 mM 2,3 butanedione monoxime (BDM), a drug that lowers the force by inhibiting the actin-myosin interaction (Horiuti et al. *J. Muscle Res. Cell Motility* 9, 156-164, 1988). Data were analysed by means of Sigmaplot (Jandel Scientific) software. The integrated intensity of the M3 reflection at rest was about 600 counts/s, a value comparable to that obtained at ID2, ESRF after attenuation of beam intensity to minimise the radiation damage and avoid detector saturation.

In agreement with previous results (Huxley et al. *J. Mol. Biol.* 158, 637-684, 1982) the spacing of the reflection was 14.33 (0.04 nm (mean (SD, data from 9 fibres) at rest and 14.51 (0.05 nm at the isometric tetanus plateau (force, T, = T₀). The addition of 1 mM BDM (data from 5 fibres) did not alter significantly the spacing in the two conditions. In BDM-Ringer the isometric tetanus plateau force decreased by 24 %, while the M3 reflection intensity, normalised by its value at rest, decreased by 44 %. Taking into account that, with no change in the form factor and in the axial dispersion of the cross-bridges, the reflection intensity changes proportionally to the square of the number of the diffractors, these results indicate that in BDM-Ringer the number of attached cross-bridges decreases by 25 %. This conclusion agrees with the estimate of the fraction of attached cross-bridges obtained with stiffness measurements.

In the experiments done to determine the effect of the stretch on M3 reflection, lengthenings of about 5 % of the fibre length at the velocity of 0.1 $\mu\text{m/s}$ per half-sarcomere were imposed at the plateau of isometric tetanus. Force increased up to a quasi-steady value of about 1.6 T_0 while the M3 intensity decreased by about 60 % (Fig. 1, data from 5 fibres). The reduction of M3 intensity calculated with a structural simulation (Piazzesi et al. *Pflügers Arch.* 434, R57, 1997), based on the atomic model by Rayment et al. (*Science* 261, 58-65, 1993) and assuming that the steady lengthening induces in the cross-bridge the conformation characteristic of the initial state in the force-generating process, is about 25 %. This discrepancy is explained if we take into account the further M3 intensity reduction during steady lengthening expected from the larger axial dispersion of the cross-bridge population (Huxley, *Prog. Biophys. Biophys. Chem.* 7, 255-318, 1957; Piazzesi et al. 1992; Piazzesi & Lombardi, 1995). From these results it is evident that from the changes in intensity of only one reflection it is not possible to evaluate correctly the form factor, when other factors (axial dispersion, number of diffractors) affect the reflection. Moreover with a linear detector the intensity of the reflection cannot be corrected for the radial dispersion factor when, in the different conditions, the register between filament changes (Huxley et al. 1982).

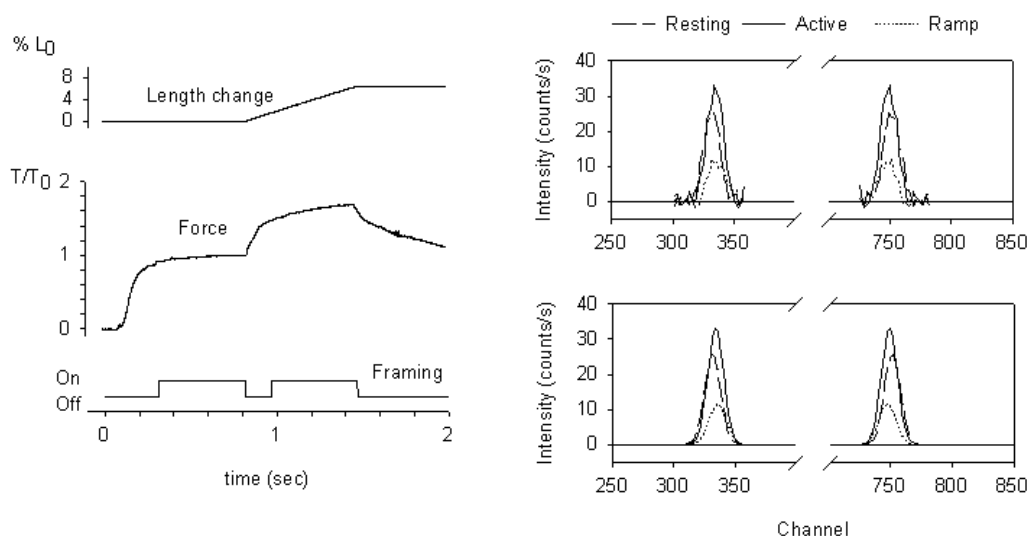


Figure 1. *Left panel.* Experimental protocol: a steady lengthening at about 0.1 mm/s per half-sarcomere was imposed at the isometric tetanus plateau in normal Ringer. The origin of the abscissa is the start of the stimulation. Scale on the ordinates: upper trace, per cent of fibre length (L_0); middle trace, tension relative to the isometric plateau tension. *Right panel.* Top: intensity distribution for the M3 reflection after mirroring and background subtraction (5 fibres, 12 s total exposure time in each condition); bottom: gaussian fit on the experimental data.

STRUCTURAL PROPERTIES OF **β** -LACTOGLOBULIN

(November, 10-14, 1997)

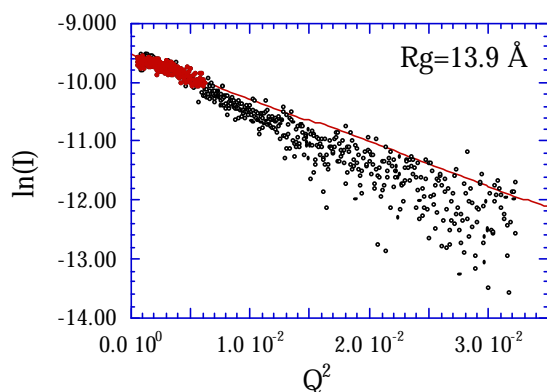
Elisabetta MACCIONI, Paolo MARIANI, Francesco SPINOZZI

INFN - Istituto di Scienze Fisiche, Università di Ancona,

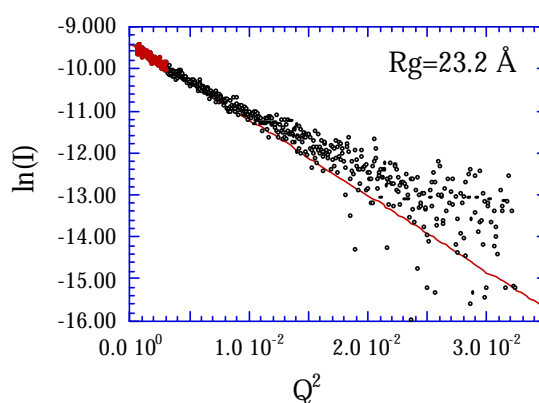
Via Ranieri, 65 - 60131 Ancona (I)

β -lactoglobulin (β -LG) is an 18400 D molecular weight globular protein. Even if the biological function is unknown, this protein shows a three dimensional structure very similar to that of plasma retinol binding proteins and it was evidenced that it can bind many hydrophobic molecules; consequently it has been included in the family of protein transporters called lipocalins [1]. The three dimensional structure of β -LG has been determined by X-ray diffraction studies of more than one crystal form: it is a barrel of eight strands of antiparallel β -sheets [2]. In the native form and at neutral pH, the protein is a dimer [3,4], but the structural properties of β -LG have been observed to be strongly sensitive to pH, temperature and ionic strength: in particular, at acid pH where the protein is highly charged the quaternary structure is lost, yielding two monomers, which show an ordered tertiary structure. However, the dissociation is expected to be influenced by the ionic strength of the solution, which should modulate the electrostatic interactions. The knowledge of the structural behavior and of association/dissociation phenomena, when the β -LG is submitted to pH variations or to changes in the ionic strength of the solution is very important, as these phenomena simulate the β -LG conditions before the transfer through biological membranes. The folding process in fact, seems to involve a passage from an essentially helical structure to the β -sheet structure, as suggested from CD measurements at 220 nm [5]. In order to have information on structural changes, and to detect some important events, Small Angle X-ray Scattering (SAXS) measurements have been performed at Elettra, using the SAS camera on the 5.2 L beam-line.

β -LG scattering behavior has been measured in dilute solution at acidic pH with different salt concentrations, ranging from 6 mM up to 100 mM NaCl. Protein was dissolved in a phosphate buffer (pH 2.3) at concentration ranging from 2 to 10 mg/ml and measured in 1 mm quartz capillaries. The scattering from a buffer capillary was subtracted from the data after correction for absorption and detector sensitivity. Only relative scattering intensities were obtained. Two typical spectra are reported in the figure, in the form of Guinier plots. Guinier plots showed different radii of gyration and different intensity scattered at zero angle for different salt conditions, confirming the dependence of the aggregation mechanism on ionic strength, as previously observed by Static and Dynamic Light Scattering measurements [Beretta S., Chirico G., Baldini G. unpublished data,]. It results that increasing the ionic strength, the radius of gyration continuously increases from 14 (measured at 10 mM NaCl) to about 23 Å (measured at 100 mM NaCl), indicating that the increased electrostatic screening influences the monomer-dimer equilibrium, increasing the concentration of dimers.



10 mM NaCl



100 mM NaCl

The analysis of the observed radii of gyration has been performed using very simple models. The protein volume (that one which excludes the solvent) has been derived from the amino acid composition and the corresponding aminoacid volumes, as reported by Jacrot and Zaccai [6]. The volume of the monomer results 22600 \AA^3 . From the volume, and assuming a spherical shape for the monomer and a dumbbell structure for the dimer [3], a radius of gyration of 13.6 \AA and 22.1 \AA have been calculated, respectively. These values are in perfect agreement with the radii of gyration experimentally measured at very low and very high ionic strengths. Moreover, by multipole expansion, using the original method developed by Stuhrmann [7] and recently improved introducing maximum entropy and group theory [Spinuzzi F., Carsughi F., Mariani P., submitted], the shape of the scattering particle was reconstructed: the result confirms the presence of dimers and monomers in the investigated samples.

- (1) Akerstroem B. and Loegdberg L., 1990, *TiBS*, 15, 240-243.
- (2) Monaco H.L., Zanotti G., Spadon P., Bolognesi M., Sawyer L. and Eliopoulos E.E., 1987, *J.Mol.Biol.*, 167, 695-706;
- (3) Witz J., Timasheff S.N., Luzzati V., 1963, *JACS*, 86, 168-173.
- (4) Molinari H., Ragona L., Varani L., Musco G., Consonni R., Zetta L., Monaco H., 1996, *Febs Letters*, 381, 237-243
- (5) Hamada D., Segawa S., Goto Y., 1996, *Nature Structural Biology*, 3, 868-873.
- (6) Jacrot B. and Zaccai, G., 1981. *Biopolymers*, 20, 2413-2426
- (7) Stuhrmann, H.B., 1970, *Z. Phys. Chem.* 72, 177-184, 185-198

Time resolved investigation of protein dynamics - working native F₁ATPase

Thomas Nawroth¹, Iris Lauer¹, Manfred Rößle², Hermann Heumann²,
Sigrid Bernstorff³ and Heinz Amenitsch⁴

1. Institute of Biochemistry, Gutenberg-Universität, Becherweg 30, D-55099 Mainz, Germany
2. Max-Planck Institute of Biochemistry, Membrane-Biophysics, D-82152 Martinsried, Germany
3. Sincrotrone Trieste, Strada Statale 14, km 163.5, I-34012 Basovizza / Trieste, Italy
4. IBR, Austrian Academy of Science, Steyrergasse 17, 8010 Graz, Austria

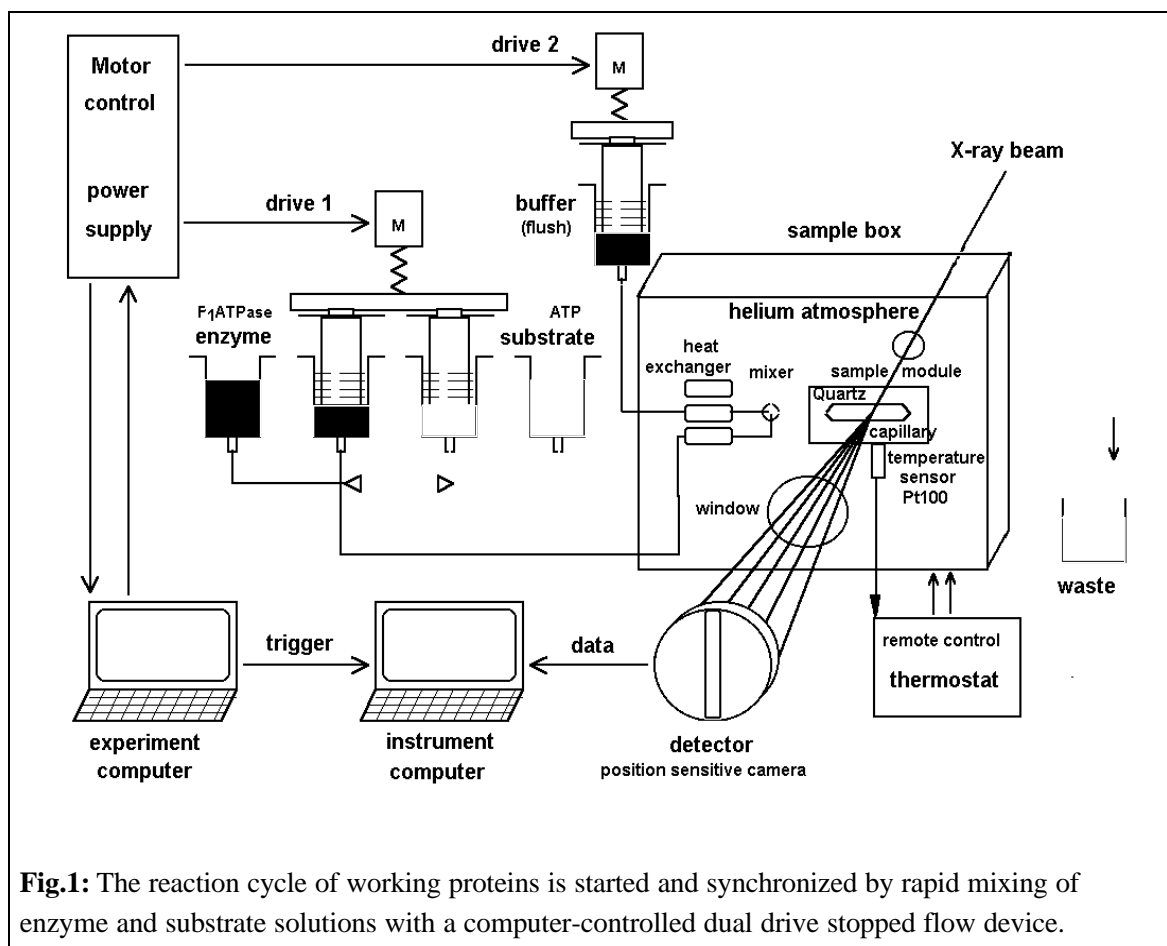


Fig.1: The reaction cycle of working proteins is started and synchronized by rapid mixing of enzyme and substrate solutions with a computer-controlled dual drive stopped flow device.

The reaction cycle and the molecular regulation of several large multidomain proteins depends on structural changes of the protein complex. This is suggested indirectly by enzyme kinetics, thermodynamic studies and time resolved spectroscopic studies of enzymes, e.g. bacteriorhodopsin, photosynthetic proteins, cytochrome oxidase and ATP-synthase or its catalytic F₁-fragment (F₁ATPase) [1]. In some cases the protein structures have been estimated before and after the enzymatic catalysis by X-ray crystallography, e.g. with the proteins hexokinase, ras and EF-Tu. Nevertheless the online analysis of structural dynamics during protein activity requires the

unrestricted flexibility and accessibility of the protein to diffusion of substrate and products. This is in most cases only possible with protein solutions, which can be structurally investigated by time resolved small angle scattering.

At the SAXS beamline of ELETTRA a novel experimental setup for the investigation of transient structural changes of working protein solutions was installed. As shown in Fig.1, the setup consists of 3 devices: i) a computer controlled stepping motor driven dual drive rapid mixing device (stopped flow), which delivered enzyme, substrate and flush-buffer solutions at selectable volume, speed and repetition rate; ii) a sample environment box with a flow-through

quartz capillary (1.1 mm diameter), tefzel mixer, 3-branched heat exchanger, Pt100 temperature sensor and helium atmosphere; and iii) a remote control thermostat connected to the sensor at the sample module inside the box. After the first experiment series the box was additionally equipped with a helium jet fan blowing on the irradiation point at the capillary and then used for experiments at ELETTRA and ESRF. The beam heating was less than 0.2 K/min with 2×10^{12} photons/s (8 keV) in an irradiated area of 0.8×1.5 mm (negligible). The radiation damage of the proteins was suppressed by degassing (removal of oxygen) and addition of a radical scavenger (10 % glycerol) in 1000 fold molar excess with respect to the protein concentration (5g/l, i.e. 10 μ Mol/l with ATP-synthase; M=500.000).

$$I_p(q) = [(I_{ps}/B_{ps} - I_d/B_d)/T_{ps} - (I_e/B_e - I_d/B_d)/T_e] - [(I_s/B_s - I_d/B_d)/T_s - (I_e/B_e - I_d/B_d)/T_e]$$

When protein and solvent experiments were done within one day, the empty cell correction was omitted. The scattering vector (momentum transfer) was expressed as $q = 4\pi/\lambda \sin\theta$ where q is the half scattering vector.

ATP-synthase is a membrane protein of cell energy metabolism, that transfers the energy of respiration by synthesizing the energy rich chemical compound ATP to other biologic systems, e.g muscle [1].

In Fig.2 the X-ray small angle scattering of the catalytic head fragment F₁ATPase (10 g/l) obtained at the SAXS beamline in 1000s with an 1-dimensional gas-detector is shown as Guinier representation. The plot yields the averaged size of the molecule of $R_g = 45.8 \pm 0.28 \text{ \AA}$, which is suggested to change during the catalytic reaction [2] as well as upon the molecular regulation [3]. The result fits well the properties obtained with long-time scattering experiments at the DESY synchrotron obtained in 4x3 h with a 2d-camera [4]. Stopped flow experiments showed that an acceptable error ($R_g < 1\text{ \AA}$) is obtained with the 1d-camera in 20 shots of 2 s time resolution. Thus we have started the investigation of the interaction of the catalytic sites by comparison of azide-inhibited [5] and native F₁ATPase and ATP-synthase, where we see a 3-fold expansion of the molecule during action.

Due to the high stability and reproducibility of the sample geometry, the experiments were each done as a series of four subexperiments with scattering of: 1) protein solution I_{ps} ; 2) solvent I_s ; 3) empty dry cell I_e ; and 4) dark (intransparent) sample I_d . As dark sample we used saturated RbBr solution, which is the equivalent to the Cd-probe in neutron scattering for X-rays. In the evaluation the contribution I_d was subtracted from each of I_{ps} , I_s , and I_e after normalization to the incoming beam monitor $B = \int I(t) dt$, whereas the scattering contribution of the protein I_p was estimated by subtraction of the components after additional normalization with the sample transmission T , estimated with a pin diode:

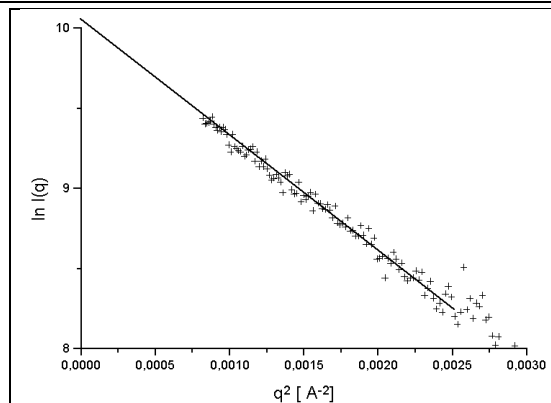


Fig.2: X-ray small angle scattering of native F₁ATPase (10g/l) as Guinier representation, which yields the average size of the molecule of $R_g = 45.8 \pm 0.28 \text{ \AA}$.

1. Junge, W., Lill, H.; Engelbrecht, S. (1997) Trends Biol. Sci, 22, 420-423 (review)
2. Neidhardt, A.; Nawroth, T.; Hütsch, M.; Dose, K. (1991) FEBS Lett. 280, 179-182
3. Nawroth, T., Neidhardt, A.; Dose, K.; Conrad, H.; Munk, B.; Stuhmann, H.B. (1989) Physica 156 & 157 B, 485-488
4. Nawroth, T. et al. (1996) DESY-HASYLAB report 1996, vol.II, 157-158
5. Nawroth, T. et al. (1997) DESY-HASYLAB report 1997, vol .I, 655-656

Infrared-Laser T-jumps with 10^4 K/sec at the SAXS beamline

G. Pabst, H. Amenitsch, C. Krenn, M. Rappolt and P. Laggner

Institute of Biophysics and X-Ray Structure Research, Austrian Academy of Sciences,
Steyrergasse 17, A-8010 Graz, Austria

S. Bernstorff

Sincrotrone Trieste, Experimental Division, Strada Statale 14, 163.5 km
I-34012 Basovizza (Trieste), Italy

The fastest temperature-jump (T-jump) facility presently world-wide available for time resolved X-ray diffraction studies on aqueous disperse systems, as e.g. liquid crystals or polymer solutions, has been installed recently at the SAXS beamline at ELETTRA. This system features as core element an Erbium glass infrared laser which is commercially available from Dr. Rapp Optoelektronik, Hamburg, Germany. This laser can be triggered to emit 1-2 kJ pulses for durations of about 1 ms. Using suitable crystal optics the laser pulse can be deposited onto a capillary sample holder for SAXS such that temperature jumps of 10-20 °C are made in 1 ms time, which corresponds to heating rates of 10^4 K/sec. For the investigation of liquid crystalline phase transitions which frequently span a transition range of 0.1 °C or less, this means that the transition can be triggered within tens of microseconds.

In a first experimental session, the formation of a short-lived intermediate, designated as L_{α^*} , during the pretransition of DPPC (Dipalmitoyl-lecithin) has been investigated by time-resolved X-ray small angle diffraction. The results show that the transition proceeds in at least two steps, if conducted in a strongly non-equilibrium fashion: In the first step, the appearance of a discrete reflection at $1/58 \text{ \AA}^{-1}$ (compared to the 63 \AA lamellar repeat distance of the initial $L_{\beta'}$ gel phase) indicates the production of a thin liquid crystalline bilayer phase. This new phase which is not seen under equilibrium conditions is designated as L_{α^*} . The lifetime of this intermediate, which coexists with variable amounts of the initial gel phase structure, can be varied by changing the power of the laser beam, and the chemical composition of the system. In the second step, which has a characteristic time scale of seconds, the L_{α^*} phase structure gradually relaxes into the stable ripple phase structure $P_{\beta'}$ (see schematic model) [1, 2].

Research is now directed to the identification of factors which may prolong the life-time of the intermediate structures. On the one hand, this will facilitate the detailed structural analysis of the intermediate and thereby provide a point of entry for a full understanding of the mechanism of this and other, related phospholipid phase transitions. On the other hand, this may lead to interesting nanostructures which are not accessible under equilibrium conditions.

Table 1: Lifetime of the L_{α^*} intermediate depending on the concentration of the NaCl in the solvent. T_0 is the temperature of the sample before the T-jump. The lifetime is given by the inflection-point of the mean d-spacing curves in the L_{α^*} to $P_{\beta'}$ transition.

NaCl-Concentration	T_0	Lifetime [s]
0 M	27.4	11.63
0.5 M	26	11.23
1 M	26	10.22

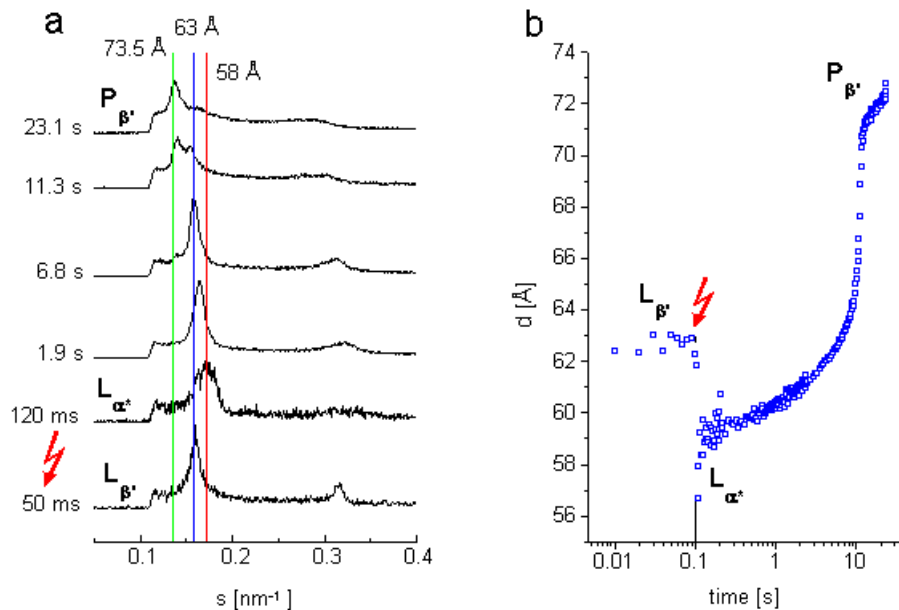


Figure 1: The pretransition in the SAXS regime of an aqueous dispersion of dipalmitoylphosphatidylcholine (0.5 M NaCl), which had been induced by a T-jump.

a) The stack-plot shows six characteristic diffraction patterns: one before the laser shot ($L_{\beta'}$), three during the lifetime of the intermediate (L_{α^*}), one in the mid of the L_{α^*} to $P_{\beta'}$ transition and one in the pure ripple phase ($P_{\beta'}$). The flash indicates the laser shot.

b) Shows the mean d-spacing of the existing phases during the transition (versus elapsed time).

References

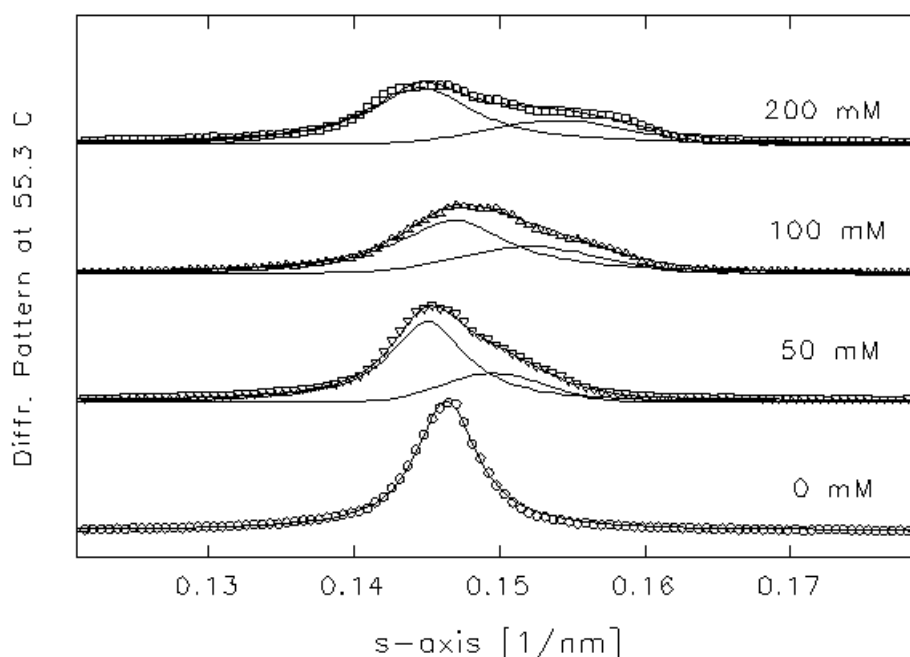
- [1] P. Lagner, M. Kriechbaum and G. Rapp. Structural intermediates in phospholipid phase transitions. *J. Appl. Cryst.* **24**: 836-842, 1991.
- [2] M. Rappolt. *Zeitaufgelöste Röntgenbeugung zur Untersuchung von Phasenübergängen an Modellmembranen*. PhD thesis, Universität Hamburg, 1995.

Time-Resolved Small Angle X-ray Scattering Studies on the Liquid Crystalline Phase of Lecithins under the Presence of Salt

Michael Rappolt¹, Karin Pressl¹, Heinz Amenitsch¹, Sigrid Bernstorff² and Peter Laggner¹

1. Institute of Biophysics and X-ray Structure Research, Austrian Academy of Science, Steyrergasse 17, 8010 Graz, Austria.
2. Sincrotrone Trieste, Experimental Division, SS14, 163.5 km, 34012 Basovizza (Trieste), Italy.

Under natural salt conditions the liquid crystalline phase of lecithins consists of a lamellar lattice type, depending on the chain length with a lamellar repeat of 6-7 nm [1]. However, providing higher salt concentrations of, e.g., NaCl or KCl, the lattice type of the superstructure changes. The figure below gives an example, where the first order diffraction Bragg-peaks of distearoyl phosphatidylcholine (DSPC) are shown for different KCl concentrations. Without salt a single peak is visible indicating a flat lamellar membrane bilayer, whereas with increasing KCl concentrations a further reflection rises with a d-spacing clearly smaller than the original one.



This particular salt effect, the formation of an additional thinner lamellar phase has most favorable to do with the altered molecular organization of bound water at the bilayer surface. Such an interpretation is supported by the facts that the thinning also depends on the ionic strength of the salt.[2].

[1] Cevc, G. and Marsh, D. (1987): Phospholipid bilayers. Wiley, New York.

[2] M. Rappolt, K. Pressl, G. Pabst & P. Laggner (1998) BBA in Press.

COLLAGEN FIBRIL STRUCTURE IN NORMALLY LOADED AND UNLOADED REGIONS OF ARTICULAR CARTILAGES: A SAXS STUDY.

R. Rizzo¹, S. Bernstorff², M. Rappolt³, H. Amenitsch³, and F. Vittur¹

¹*Dip. Biochimica, Biofisica e Chimica delle Macromolecole-Univ. Trieste, via L. Giorgieri 1, I-34127 Trieste, Italy;* ²*Sincrotrone Trieste, SS 14, Km 163.5, I-34012 Basovizza (TS), Italy;* ³*Inst. for Biophysics and X-ray Structure Research, Austrian Academy of Sciences, Steyrerg.17, 8010 Graz, Austria.*

Magnetic resonance (MR) microimaging of articular cartilage shows a laminar structure which is different for the *in vivo* loaded and *in vivo* unloaded regions of the tissue. It was demonstrated by means of MRI and biochemical studies that the laminar appearance could be related both to orientation and to the amount of collagen fibrils present in the different zones of the tissue. In addition to this, a different arrangement of the collagen fibres in the two regions cannot be ruled out. To investigate this problem, a SAXS study was performed at the 5.2L beam line of Elettra.

Cylindrical plugs (5 mm diameter) were excised from the loaded and unloaded regions of the proximal head of pig humerus and imaged by magnetic resonance microscopy (T2 weighted images). Thin slices (1-1.5 mm thick) were cut from cartilage plugs and fixed in 3% formaline. Samples were stored in a physiological saline solution for SAXS experiments; a home-made thermostatable cell, provided with two mylar windows, was employed to maintain samples in a wet state during diffraction experiments. Samples of the loaded and unloaded cartilage regions were scanned with a X-ray beam of 200x500 microns from articular surface to the subchondral bone. Images were taken at a sample to detector distance of 1.8 m with a 1D delay-line gas detector.

SAXS experiments showed that loaded and unloaded cartilages exhibited different diffraction patterns. In fact, samples from loaded regions gave rise to diffraction patterns characterised by regularly spaced peaks, while those obtained from the unloaded regions did not show any diffraction peak. The analysis of the spacing revealed a periodicity attributable to the typical organization of collagen molecules in fibrils (670 Å period).

According to the MR microimages, SAXS data confirm that the structure of the loaded regions of cartilage is different from that relative to the unloaded ones and suggest that this difference can be attributed to the organisation of the collagen macromolecules.

Time dependent small angle scattering studies on the refolding process of substrate protein mediated by the *E. coli* chaperonin system GroEL-GroES

Manfred Rößle¹, Iris Lauer², Thomas Nawroth², Sigrid Bernstorff³, Heinz Amenitsch⁴ & Hermann Heumann¹

¹ Max-Planck-Institut für Biochemie, Am Klopferspitz 18A, D-82152 Martinsried

² Institut für Biochemie der Universität Mainz, Becherweg 30, D-55099 Mainz

³ Sincrotrone Trieste, Strada Statale 14, 163.5 km, I-34012 Basovizza / Trieste

⁴ Institute for Biophysics and X-Ray Structure Research of the Austrian Academy of Science, Steyrergasse 17/6, A-8010 Graz

Molecular chaperonins like the GroEL-GroES system from *E. coli* are proteins which bind incorrectly folded polypeptides such as denatured protein or proteins in the *statu nascendi*, preventing aggregation and then mediate their refolding in an ATP-dependent process.

The main chaperonin GroEL consists of 14 identical monomers. This monomers are arranged in two heptameric rings stacked together back by back building a cylinder of 15nm height and 14nm diameter. The rings form a cavity in which the refolding of the substrate protein probably takes place. The co chaperonin GroES is a heptamer of identical subunits, building a dome of 3.5nm height and 8nm diameter.

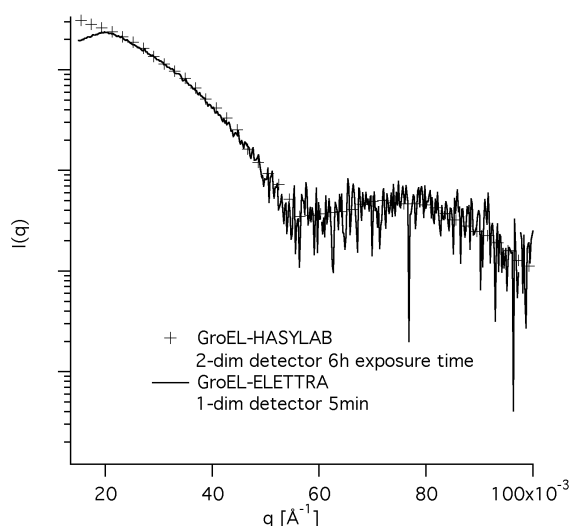


Fig. 1: Scattering function of the main chaperonin GroEL.

During the refolding pathway the GroEL binds to one end of the main chaperonin GroEL and forms an asymmetric GroEL-GroES complex. The binding of a second GroES to the other side of the GroEL can be observed in the presence of high ATP concentrations. The static conformations of this symmetric GroEL-(GroES)₂ complex were observed at HASYLAB's JUSIFA using the non hydrolyzable ATP analogue AMP-PNP.

The resulting radius of gyration for the static structures of the GroEL alone and in complex are shown in table 1.

Tab. 1:

	Nucleotide	Radius of gyration
GroEL without nucleotides	---	65.4 Å ± 0.7 Å
GroEL + GroES 1 : 1 asymmetric complex	ADP	67.7 Å ± 0.6 Å
GroEL + GroES 1 : 2 symmetric complex	30mM AMP-PNP	69.9 Å ± 0.7 Å

The kinetics of the formation of the symmetric GroEL-(GroES)₂ complex was investigated using the SAXS beamline at ELETTRA.

Solutions of GroEL and GroES with ATP were mixed in the presence of ATP by means of a stopped flow apparatus (deadtime 30ms). As a control experiment GroEL was mixed with buffer (without ATP and GroES). The results are presented in Fig. 2 and Fig.3. The control experiment (Fig. 3) shows that the radius of gyration remains stable ($62\text{\AA}\pm 2\text{\AA}$) over 40min. The exposure time for a single experiment was 60s. No protein damaging (aggregation or dissociation) could be observed.

The formation of the symmetric GroEL-(GroES)₂ complex has been followed by measuring the I_0 . Fig. 2 shows that the molecular weight (MW) increases from 860 kDa to 950 kDa for 30min and decreases then back to 850kDa.

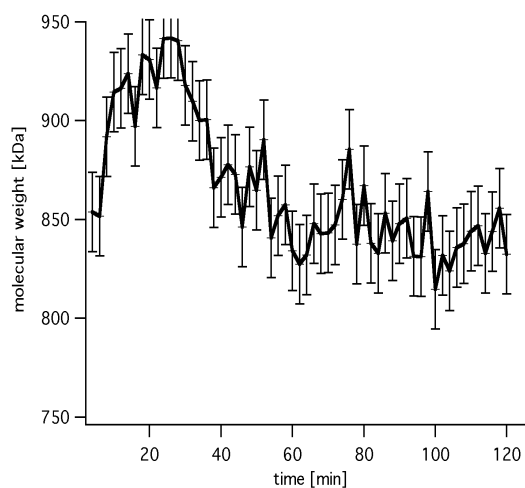


Fig. 2

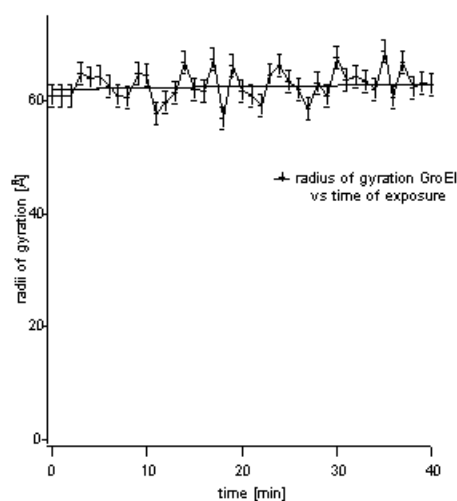


Fig. 3

Interpretation:

The asymmetric GroEL-GroES complex (MW 870kDa) is formed in the first seconds of the reaction cycle with cannot be followed in this experiment. Subsequently the GroEL-(GroES)₂ complex is formed.

The symmetric complex is formed within 30min. Afterwards the complex dissociates into the asymmetric GroEL-GroES complex probably due to depletion of ATP.

3. Physics

Small Angle X-ray Scattering on Thin Films at Grazing Angles

P. Dubcek, A. Turkovic and B. Etlinger
Ruder Boskovic Institute, Bijenicka 54, Zagreb, Croatia

O. Milat
Institute for Physics, Bijenicka 46, Zagreb, Croatia

M. Lucic - Lavcevic
University of Technology, Split, Croatia

H. Amenitsch
*Institute for Biophysics and X-ray Structure Research, Austrian Academy of
Sciences, Steyrerg. 17, 8010 Graz, Austria*

Nanocrystalline titanium dioxide (TiO₂) thin films, deposited on the flat glass substrate using various techniques, have been investigated at the SAXS beamline at Elettra. Because the film thickness is much smaller than optimal, and because of the unfavourable film to substrate thickness ratio, grazing angle scattering was performed.

The peak corresponding to the totally reflected primary beam is broadened because of the roughness of the film surface, and, also, there are two main contributions to the scattered intensity: scattering from the bulk, and the scattering from the surface. Both could be interpreted as SAXS signals originating from different distribution of the scattering particles.

Because of the increasing effective film thickness, the absorption of the scattered radiation is increasing with decreasing 2Θ . Therefore, the actual particle size resolution depends on the grazing angle magnitude. This high absorption at very low scattering angles is also dependant on the surface roughness.

The results the experiment as well as the data treatment will be presented for different samples and for different grazing angles.

Test Experiment: X-Ray Fluorescence Analysis

K.C. Prince, M. Kiskinova, S. Bernstorff, L. Romanzin, D. Lonza
Sincrotrone Trieste
H. Amenitsch, *Austrian Academy of Sciences*
M. Matteucci, *CNR*, and
R. Rizzo and F. Vittur, *Dip. di Biochimica, Università di Trieste*

The goal of the beam time was to assess the suitability of the beam line for use as a SRXRF (Synchrotron Radiation X-Ray Fluorescence) microprobe. Several standard samples and test objects were analysed with excitation by monochromatic 8 keV radiation, and detection by a Si(Li) energy dispersive analyser.

Experimental. The samples were mounted on the standard mount of the beamline and the analyser was placed with its axis horizontal along the electric vector of the incident radiation, to minimise Compton scattering. The analyser was first mounted in vacuum with a Mylar window and low vacuum; later some tests were performed in a windowless arrangement with the sample and detector in a He atmosphere.

The samples consisted of:

1. Standard sample "Peach Leaves", from the NIST, Maryland, USA.
2. Diluted peach leaves.
3. Geological samples, consisting of: lead sulphide from Broken Hill, Australia and Bulgaria; gold from Ballarat, Australia; and pyrite from Spain.
4. Archaeological samples: "Old" coloured glass; and a shard of medieval pottery.
5. A palaeontological sample, a trilobite of age approx. 550 million years.
6. Two thin films of known composition, consisting of Langmuir Blodgett films of 10 and 100 layers of cadmium arachidate on silicon wafers.

Results. Some initial difficulties were encountered with electromagnetic noise and resolved.

Initially spectra from the "peach leaves" sample were taken with a large spot, approximately 4x1 mm. The sensitivity to light elements is poor as the detector was used with a window. A small spot was created by masking the beam to approx. 350x350 microns; the flux after an Al-filter was 5×10^9 photons/sec. Ba was identified with a signal at least 10 times the background noise level, at a concentration of 124 mg/kg. Later in the run we improved the collection efficiency by roughly an order of magnitude, so with the present instrumentation we can reach a lower detection limit of about 10 ppm. Furthermore we calculate that it would be possible to focus a spot which is 30 times larger than that used into a 20x20 micron spot with 70% efficiency. This would give us 20 times the flux and sub-ppm elemental sensitivity in a 20 micron spot. Detection of $K\alpha$ emission would give a further increase in sensitivity by up to a factor of 5 for elements whose K edges are close to the excitation energy.

Spectra of lead sulphide crystals from Australia and Bulgaria were taken, and the peaks tentatively assigned. The chief point is that the samples from different sources have different chemical fingerprints. This illustrates the application of the technique to identifying the source of objects and artefacts, in this case two mines. In future we wish to apply this to other samples such as archaeological specimens.

Other spectra were taken of pyrite (iron sulphide) and gold. These illustrate two complications when analysis is carried out with fixed photon energy. For pyrite, the excitation was above the iron K edge and so very intense peaks due to iron emission were observed, which mask nearby peaks. With gold, no strong peaks due to the matrix are excited by 8 keV radiation (energy of $L\alpha_1 = 9.7$ keV), and the sample was relatively pure. Again it would be preferable to use a higher energy from a tunable source.

A spectrum taken of a trilobite indicated the presence of Mn and Fe, which are responsible for the dark colour of the fossil.

A spectrum was taken from an ancient ceramic (terra cotta with yellow colouring), and shows the presence of Fe and calcium, as well as Cr and S. A sample of ancient multicoloured glass was examined and Co, Fe, Mn and Ca were found to be present in quantities which changed with the colour of the glass. The signal from Na and Si was very low so that it was not possible to quantify the concentrations by normalising to the intensity from elements of the matrix. Without having access to higher energies it is not possible to state whether these elements give the colour or whether they are fortuitous.

The Langmuir-Blodgett films were examined at grazing incidence, <0.2 degrees grazing angle. The elastic peak was very small as we were working in total reflection. There was a small Fe signal and it is not clear whether this is contamination (we did not use clean room conditions) or due to stray radiation. The minimum detection limit was 100 pg of Cd and it was estimated that a minimum detection limit of about 10 pg was possible if instrumental improvements were introduced. This is for $L\beta$ emission so clearly even lower limits can be detected if $K\alpha$ emission is used.

Conclusions.

The first x-ray fluorescence experiments at Elettra have been carried out.

Using the unfocused beam, we achieved a minimum detection limit of approximately 100 pg of Cd on the surface of a Si wafer. Higher sensitivity can be expected with optimisation and improvement of the experimental set-up.

The present experiments indicate a sensitivity of 10 ppm ($L\alpha$) or 2 ppm ($K\alpha$) can be achieved by simply masking the spot to an area of 350x350 microns.

A range of demonstration data was acquired with a view to raising scientific support and funding resources. Since the experiment, Sincrotrone Trieste has decided to construct a dedicated facility on a bending magnet, with tunable energy.

Acknowledgements. Drs Victor Erokhin and Sandro Carrara, University of Genoa, are thanked for supplying the Langmuir Blodgett films.

SAXS ON TiO₂ THIN FILMS AT GRAZING ANGLES

A. Turkovic, P. Dubcek and B. Etlinger

Ruder Boskovic Institute, Bijenicka 54, Zagreb, Croatia

O. Milat

Institute for Physics, Bijenicka 46, Zagreb, Croatia

M. Lucic - Lavcevic

Faculty of Technology, University of Split, Teslina 10, Split, Croatia

H. Amenitsch

*Institute for Biophysics and X-ray Structure Research, Austrian Academy of Sciences,
Steyrerg. 17, 8010 Graz, Austria*

The TiO₂ thin films, obtained by chemical vapour deposition (CVD) [1] or spray technique [2], were used as intercalation electrodes for Ag/AgI/TiO₂, SnO₂ rechargeable, photosensitive galvanic cells [2]. The Ag⁺ ion diffusion in TiO₂ and thus the kinetics of the electrochemical intercalation reaction are greatly influenced by the properties of oxide electrode. In order to achieve a better understanding the role of TiO₂ in these cells, a series of measurements of the optical and electrical properties of TiO₂ thin films in different environments, as well as X-ray diffraction, Raman spectroscopy, Thermally stimulated currents (TSC), Photoresistance in wavelength range of 250 to 350 nm, Fourier transform infrared (FTIR), X-ray photoelectron spectroscopy (XPS), and UV-VIS absorption were performed [3 - 9].

In 1991 Grätzel and co-workers [11] made a breakthrough in preparing an efficient dye sensitised cell, which was made of relatively non-pure material by using a cheap preparation procedure achieving energy conversion efficiencies ranging from 7 to 12%. All previous attempts to produce a stable electrochemical cell from semiconductors with adequate energy gap for solar light absorption have failed because of photocorrosion effect. Photo-generated minor charge carriers at the semiconductor electrolyte boundary act as oxidants and destroy the photoanode. In fact, this new type of solar cell mimics natural process of photosynthesis, being even more efficient in energy conversion. It differs from conventional semiconductor device in that it separates the function of light absorption from charge-carrier transport. It was a great satisfaction to learn that TiO₂ semiconductor electrodes were used in this cell, i. e. the same material that we used in photosensitive galvanic cell [2,3]. Also, in our cell the application of AgI to TiO₂ produced a shift of absorption maximum to the visible region of solar spectrum. This shift is not marked as in the case of dye-coated TiO₂ thin films [11], but the idea of moving absorption edge of anatase (band gap 3.2 eV) to visible region, in order to obtain efficient solar cells or photo batteries is essentially the same. The preparation of TiO₂ thin films in Grätzel work [11] was performed by sol-gel procedure. Parallel to the other groups [13-16], trying to improve properties of Grätzel cell or its components: electrodes, electrolyte and dyes, we have connected our previous work [3-9] and investigated nanosized TiO₂ prepared by our original sol-gel procedure by X-ray and electron diffraction, TEM, HREM, DTA and Raman spectroscopy [17-21].

Nanocrystalline titanium dioxide (TiO₂) thin films, deposited on the flat glass substrate using above mentioned preparation procedures, have been investigated at the SAXS beamline at

Elettra. Because the film thickness is much smaller than optimal, and because of the unfavourable film to substrate thickness ratio, grazing angle scattering was performed. The peak corresponding to the totally reflected primary beam is broadened because of the roughness of the film surface, and, also, there are two main contributions to the scattered intensity: scattering from the bulk, and the scattering from the surface. Both could be interpreted as SAXS signals originating from different distribution of the scattering particles. Because of the increasing effective film thickness, the absorption of the scattered radiation is increasing with decreasing 2θ . Therefore, the actual particle size resolution depends on the grazing angle magnitude. This high absorption at very low scattering angles is also dependant on the surface roughness.

REFERENCES

1. B.Vlahovic and M. Persin, *J Phys D: Appl Phys*, **4** 23 (1990) 1324
2. A.Turkovic and V.Vranesa, *Int .J. of Materials and Product Technology*, **47** (1992) 51.
3. A.Turkovic, M. Ivanda, A. Drasner, V. Vranesa and M. Persin, *Thin Solid Films*,198 (1991)199
4. A.Turkovic and M.Ivanda,*Solid State Ionics*, 50(1992)159
5. A.Turkovic, M.Ivanda, J. Tudoric-Ghemo, N. Godinovic and I. Soric, *Nonstoichiometry in Semiconductors*, Ed. K.J. Bachmann, H.L. Hwang, C. Schwab, Elseiver Science Publisher LTD, 4A3 (1991) 307
6. A.Turkovic, M. Ivanda, V. Vranesa and A. Drasner, *Vacuum*, 443 (1992) 471
7. A.Turkovic, D. Sokcevic, M. Milun, T. Valla and J. Rukavina, *Fizika*, A 2, I (1993) 23
8. A.Turkovic, D. Sokcevic, *Appl. Surf. Sci.*, 68 (1993) 477
9. A.Turkovic, N. Radic and D. Sokcevic, *Mater. Sci. Eng*, B23 (1994) 41
10. K. Zweibel, *Harnessing Solar Power; The Photovoltaic Challenge*, Plenum Press, New York, 1990.
11. B. O'Regan and M. Grätzel, *Nature*, 353 (1111991)737
12. M.K. Nazeeruddin, A. Kay, I. Rodicio, R. Humphry-Baker, E. Muller, P. Liska, N. Vlachopoulos and M.Grätzel, *J. Am. Chem. Soc.*, 115 (1993) 6382
13. A. Hagfeldt, B. Dirikson, T. Palmquist, H. Lindström, S. Södrgren, H. Rensmo and S-E. Lindquist, *Solar Energy Materials and Solar Cells*, 31 (1994) 481
14. T. Lopez, E. Sanchez, P. Bosch, Y. Meas and R. Gomez, *Mater. Chem. Phys.*, 32 (1992) 141
15. M. Crisan, M. Zaharescu, D. Crisan and L. Simionescu, *Ceramics: Charting the Future*, Ed. P Vincenzini (1995) 2805
16. V. J. Nagpal, R.M. Davis and S. B. Desu, *J. Mater. Res.*, 10,12 (1995) 3068
17. M. Gotic, B. Grzeta, S. Music, S. Popovic, A.M. Tonejc, R. Trojko and A. Turkovic, *Fourth Croatian-Slivenian Crystallographic meeting*, Trakoscan, Croatia, Sept 28-30, 1995. Book of abstracts, p. 16.
18. A. M. Tonejc, M. Gotic, B. Grzeta, S. Music, S. Popovic, R. Trojko, A. Turkovic and I. Musevic, *Mat. Sci. Eng. B40* (1996) 177.
19. M. Gotic, M. Ivanda, A. Sekulic, S. Music, S. Popovic, A. Turkovic and K.Furic, *Mat. Lett.* 28 (1996) 225
20. A. M. Tonejc, A. Turkovic, M. Gotic, S. Music, M. Vukovic, R. Trojko and A. Tonejc, *Mat. Lett.*, in press.
21. A. M. Tonejc, A. Turkovic, M. Gotic, B. Grzeta, S. Music, S. Popovic and R. Trojko, *International Symposium on Metastable Mechanically Alloyed and Nanocrystalline Materials*, ISMANAM-96, Rome, Italy, May 20-24, 1996, P-D-5.

4. Chemistry

Relationships among synthesis, structure and drawability of nascent reactor powders of high molecular weight polyethylene (HMWPE)

E. Ferracini, A. Ferrero, V. Malta and S. Ottani

Centro di Studio per la Fisica delle Macromolecole del C.N.R. and Dipartimento di Chimica "G.Ciamician" dell'Università di Bologna (Italy) - via F.Selmi,2 40126 Bologna.

The first (and only) SAXS measurements have been performed during December 1997; the proposals concerned a morphological study on HMWPE samples obtained in different polymerization conditions (produced by Union Carbide Comp.). The aim was to correlate the polymerization techniques (slurry and gas-phase) and temperatures with the morphology and lastly with the workability of the materials. The technological interest on HMWPE comes out from the possibility of obtaining high-modulus fibers.

The samples were both as-polymerized reactor powders and sintered powders; co-extruded and stretched samples could not be observed being only a 1-D detector available.

All the samples analyzed showed a continuous scattering profile (pure particle scattering without any interference effect); the analysis of the scattered intensities, after correction for the background, has been performed by the generalized Guinier approximation showing all the samples more than one particle dimension. In other words, the iterative Guinier analysis has been applied and the results can be summarized in the following way:

- 1) The "nascent" HMWPE samples show four sets of particle dimensions whose radii (we assume a globular shape) range from 15 Å about for the smaller dimension to 250-300 Å for the largest one, and these results are independent on the polymerization technique and temperature; only the largest dimension is, in our opinion, slightly influenced by the above mentioned parameters.

Our assumption of considering a globular morphology in the nascent HMWPE, although the crystalline and semicrystalline polymers show usually a lamellar morphology, is supported both by our previous studies on nascent isotactic Polypropylene and by the absence of any interference effects in the SAXS profiles. The lamellar-like aggregation gives rise to a "shoulder" also in the not oriented samples; in any case there is no evidence of a regularly stacked lamellar crystals. In the isotactic Polypropylene case the results obtained by the SAXS technique were supported by the experimental evidence of transmission electron microscopy technique.

- 2) The annealing of the nascent samples at 80°C has no practical effects on their morphology and particle dimensions for annealing times till 15 days. A very slight increase of particle dimensions can be observed after annealing at 120°C for 32 days.
- 3) The sintered powders samples (the powders sintering does not involve a strong thermal treatment) do not show any valuable variation in the polymer morphology.

Characterization of the Nanostructures in Liquid Crystalline Mesophases Present in the Ternary System Brij-35 / Dibutylether / H₂O by Small and Wide-Angle X-Ray Scattering

R. Schwarzenbacher¹, M. Kriechbaum¹, H. Amenitsch¹, and P. Lagner^{*1}

¹ Institute of Biophysics and X-ray Structure Research, Austrian Academy of Sciences, Steyrergasse 17, 8010 GRAZ, Austria. Tel.: **43-316-812003; Fax: **43-361-812367; E-mail: fibrlagg@mbox.tu-graz.ac.at.

We investigated the liquid crystalline phase structures and their temperature-dependent dynamics in the ternary system composed of Brij-35 [poly(oxyethylene(-23)laurylether, C₁₂OE₋₂₃], dibutylether (DBE) and 10mM Na/K-buffer. The lyotropic phases in this special system are of current interest as a nanostructured liquid crystal immobilization matrix (LCIM) for enzymes or microorganisms in the field of biocatalysis. To obtain detailed studies with structural data of the LCIM, we established a sequence of schematic ternary phase diagrams at 10, 20, 30, 40 and 60°C, derived from temperature-scanning small- and wide-angle x-ray scattering (SWAX).

In the binary Brij-35 / H₂O system, the amphiphilic component Brij-35, being totally miscible with water, self-assembles as a function of its concentration into a normal micellar solution L₁, a normal packed micellar cubic I₁-phase region, and an extended region of various lamellar structures. These lamellar phases show unit cell dimensions of $a = 179 - 181\text{\AA}$. The cubic I₁ phases show diffraction patterns with Im3m (unit cell parameter $a_{\text{Im3m}} = 85-94\text{\AA}$) and Ia3d ($a_{\text{Ia3d}} = 162-167\text{\AA}$) symmetry. Increasing temperature destabilizes the cubic phases between 15°C and 55°C, depending on the weight ratio of the used components. Within the lamellar region, the phase-transition from L_c- (crystalline lamellar phase) and L_g- (gel lamellar phase), respectively, to an isotropic micellar phase, here denoted as L₂, occurs at temperatures from 15°C to 35°C as a function of the water content. The DBE uptake of these structures is limited to 20 - 50%(w/w), which generates bi-phasic regions at higher DBE amounts, where a DBE excess- phase containing approximately 2%(w/w) H₂O and 0.02%(w/w) Brij-35 is formed. Increasing amounts of DBE lead - with exception of the L_c- phase - to enhanced phase temperature stabilities in the water lean region and induce normal hexagonal H₁- ($a = 68 - 135\text{\AA}$) and various cubic structures. We found the cubic space groups Im3m and Ia3d with unit cell dimensions ($a_{\text{Im3m}} = 83 - 112\text{\AA}$) and ($a_{\text{Ia3d}} = 162 - 195\text{\AA}$) in the cubic I₁- region, and Pn3m ($a_{\text{Pn3m}} = 164\text{\AA}$), Ia3d ($a_{\text{Ia3d}} = 187 - 214\text{\AA}$), as well as Fd3m ($a_{\text{Fd3m}} = 218 - 275\text{\AA}$) in the cubic region with low water contents.

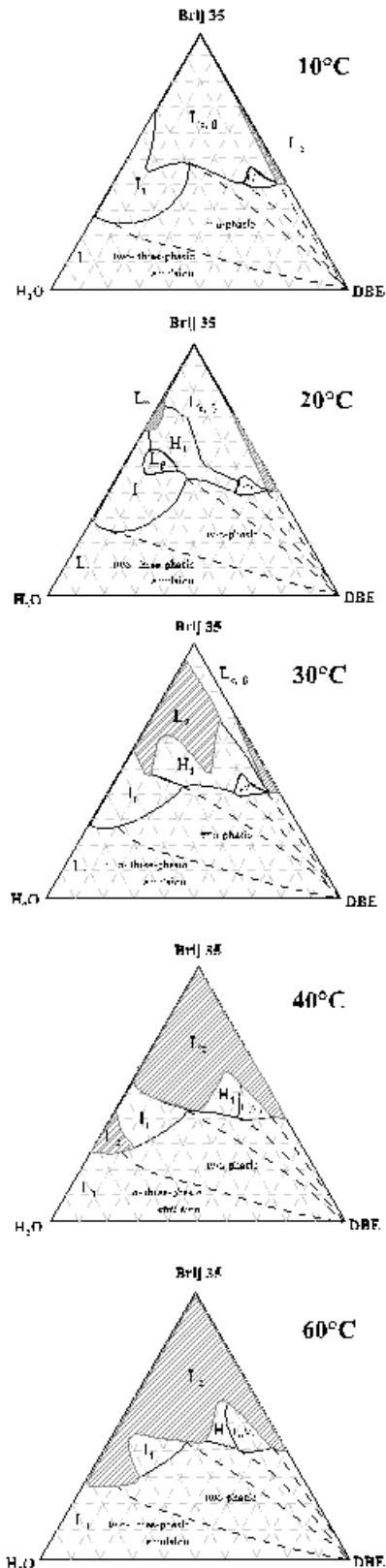


Figure 1: Schematic phase diagrams at five different temperatures, $T_1 < T_2 < T_3 < T_4 < T_5$, illustrating the evolution of the phase equilibria of the ternary non-ionic surfactant/cosurfactant/water system Brij-35, DBE, and H₂O. For the present system the different temperatures correspond approximately to $T_1 = 10^\circ\text{C}$, $T_2 = 20^\circ\text{C}$, $T_3 = 30^\circ\text{C}$, $T_4 = 40^\circ\text{C}$, and $T_5 = 60^\circ\text{C}$. The concentrations are expressed in weight percent. The nomenclature of the various phases is mainly according to the system given in ref. (23); L₁, micellar solution; I₁, cubic phase of close packed spherical micelles; H₁, normal hexagonal phase; V₁, normal bicontinuous cubic phase; L_c, crystalline lamellar phase; L_β, fluid lamellar phase; L₂, isotropic surfactant liquid.

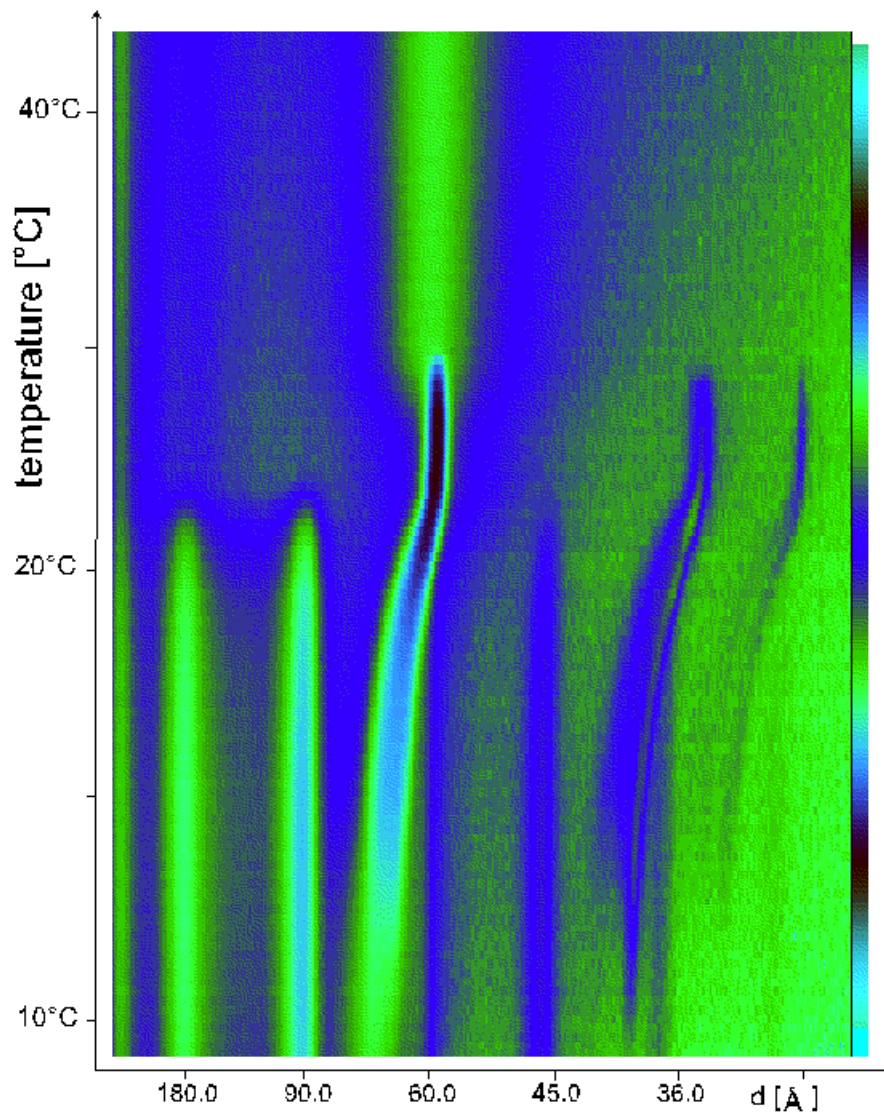


Figure 3: Synchrotron X-ray diffraction patterns of a L_c - H_1 - L_2 - phase transition at a Brij-35/ H_2O /DBE weight composition of 60.0/20.0/20.0 as a function of temperature. The scan rate is $1^\circ\text{C}/\text{min}$ and the acquisition time is 20s/frame.

5. Instrumentation

CCD detector research and development

H. Amenitsch^a, S. Bernstorff^b, P. Ottonello^c, G.A. Rottigni^c, G. Zanella^d, and R. Zannoni^d

^a *Inst. for Biophysics and X-ray Structure Research, Austrian Academy of Sciences, Steyrerg.17, 8010 Graz, Austria*

^b *Sincrotrone Trieste SCpA., Strada Statale per Basovizza 14 km 163.5, 34012 Trieste, Italy*

^c *Dipartimento di Fisica dell'Università di Genova and Istituto Nazionale di Fisica Nucleare, Sezione di Genova, via Dodecaneso 33, 16146 Genova, Italy*

^d *Dipartimento di Fisica dell'Università di Padova and Istituto Nazionale di Fisica Nucleare, Sezione di Padova, via Marzolo 8, 35131 Padova, Italy*

During 1997 a CCD detector was tested which had been developed with support of INFN (SAXS-CCD experiment of “gruppo V”). This detector is optimized for dynamic X-ray diffraction imaging and the tested version had a 2 MCP image intensifier Proxitronic (25 mm diameter, fiber optic input and output, S20 photocatode, P20 output phosphor, 10 ns electronic gate) coupled 1:1 to a CCD Thomson (1024 pixel x 1024 pixel, 28 ms per frame, 4 outputs, 19 μ m x 19 μ m pixel size). The image processor was the Matrox Image board.

The preliminary tests, at room temperature, were addressed to compare the performances of a terbium doped scintillating glass fiber optic plate vs. a Hamamatsu FOS (fiber optic plate coated with Gd₂O₂S:Tb, 30 μ m thick), obtaining the following results. In the case of the diagnostics of an intense X-ray beam of 8 keV (for example measuring of the transverse two-dimensional beam profiles as in Fig.1) only using the scintillating fibers it was possible to obtain a linear response with high spatial resolution without an immediate radiation damage. In contrast, in the case of phosphor insuperable saturation problems appeared.

Using beam images, it was also possible to measure the DQE of the detector as a function of the input signal. In case of acquiring of low intensity (8 keV) X-ray diffraction images, typical for dynamic SAXS-measurements, the lower light yield of the scintillating glasses, as compared to the phosphors, does not permit the use of the scintillating glass fiber optic plates in many applications. In Fig. 2 and 3 we can see a part of the diffraction figure of the dry rat tendon collagen (2D and 3D profile) obtained with the described detector, using 8 keV X-rays and the FOS.

The future version of the detector foresees a 75 mm x 75 mm FOS coupled, through a fiber optic taper, to a 40 mm diameter 2 MCP image intensifier and this last also coupled by a taper to the CCD. The new image processor will be the Matrox Genesis board which permits an on-board 64 MB processing memory with a data transfer rate up to 400 MB/s, useful to follow the dynamic phenomena.

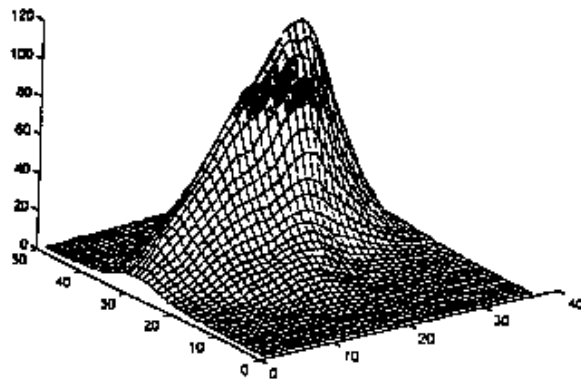


Fig.1. 3D profile of the 8 keV X-ray beam of the SAXS beam line, obtained with a CCD detector (see text) coupled to a scintillating glass fiber optic plate. The intensity of the beam is in arbitrary units and the squared sampling mesh has 95 μm side.

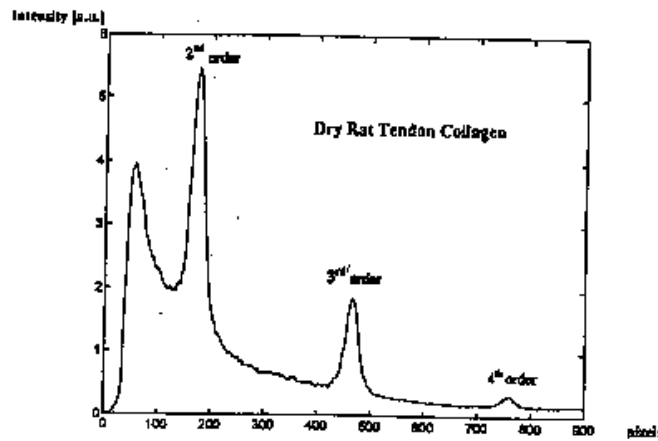


Fig.2. Part of 2D intensity profile of the 8 keV X-ray diffraction image of dry rat tendon collagen, obtained with a CCD detector (see text) coupled to a FOS (a film of $\text{Gd}_2\text{O}_3\text{:Tb}$, 30 μm thick, covering a fiber optic plate). The integration time was of about 10 s at room temperature.

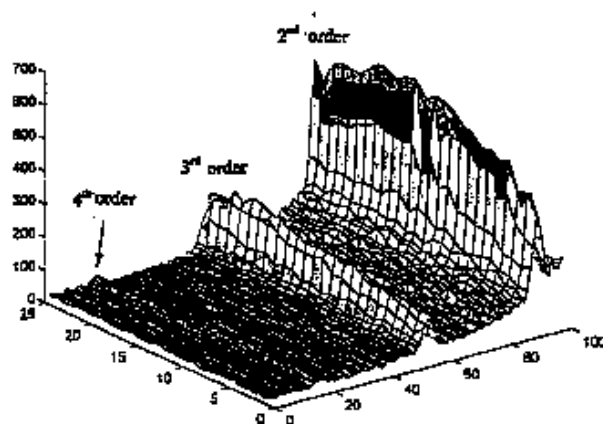


Fig.3. Part of the 3D intensity image pertaining fig.2. The intensity is in arbitrary units and the sampling mesh has 3.5 pixel side.

A fast 1-D detector for time resolved SAXS experiments

R.H.Menk¹, H.Amenitsch², F.Arfeelli¹, S.Bernstorff¹, P.Dubcek¹, G.Pabst², D.Pontoni¹
M.Rappolt², A.Sarvestani³

1. Sincrotrone Trieste, Strada Statale, SS14, km163.5, 34012 Basovizza, Trieste, Italy
2. Institute of Biophysics and X-ray Structure Research, Steyrergasse 17, 8010 Graz, Austria.
3. Universitaet Siegen, Walter Flex Strasse, 57068 Siegen, Germany.

The analysis of Small Angle X-ray Scattering data (SAXS) in the regime of x-rays is widely used in the fields of biological, chemical, medical and material sciences in order to determine the microscopic structure in the range from about 1 to 1000 nm in systems like gels, liquid crystals, (bio) polymers, fibers or amorphous materials. The recent development of high-flux SAXS-stations at third generation synchrotron radiation sources allows additional, to perform time-resolved studies of fast structural transitions in the sub-millisecond time region in solutions and partly ordered systems. Such SAXS-studies require essentially 1D or 2D position sensitive detectors for x-rays in the energy range of 5-20 keV with a position resolution of the order of 0.1-0.2 mm and a high linearity over a large dynamical range. In addition a time resolution of 0.01-1 ms for time dependent measurements is required.

A 1-D test detector on the principle of a highly segmented ionization chamber was developed to evaluate if this kind of detector is suitable for advanced SAXS experiments. Most of the tests and measurements were carried out at the SAXS beam line at Sincrotrone Trieste.

At present this detector consists of a stainless steel cathode above an anode structure, which is arranged in 128 strips each 3 cm long with a pitch of 150mm. Filled with an ArCO₂ gas mixture at 8 bars a quantum efficiency of 80% was achieved. The spatial resolution at this pressure was 3 line pairs /mm (Figure 1). Two custom made VLSIs (64 channels each) in combination with a 16 bit 1MHz ADC are used to obtain the first measurements. The noise performance of these analog integrating devices at 100µs integration time is around 10000 e- which is equivalent to approximately 25 photons of 8 keV. This leads to DQE values of 80% for photon fluxes above 1000 photons per integration time. Fast recording sequences in the order of 200µs are ensured by a shielding grid inserted between anode and cathode. The grid bases on the principle of the recently invented MCAT structure which allows also gas amplification. An energy resolution of 25 % at 8 KeV was observed. The gas amplification mode enables imaging with this integrating detector on a sub photon noise level with respect to the integration time. Preliminary experiments of saturation behavior show that this kind of detector digests a photon flux density up to 10¹² photons / mm² sec and operates still linear (figure 2). All these features show that this type of detector is well suited for time resolved SAXS experiments as well as high flux imaging applications.

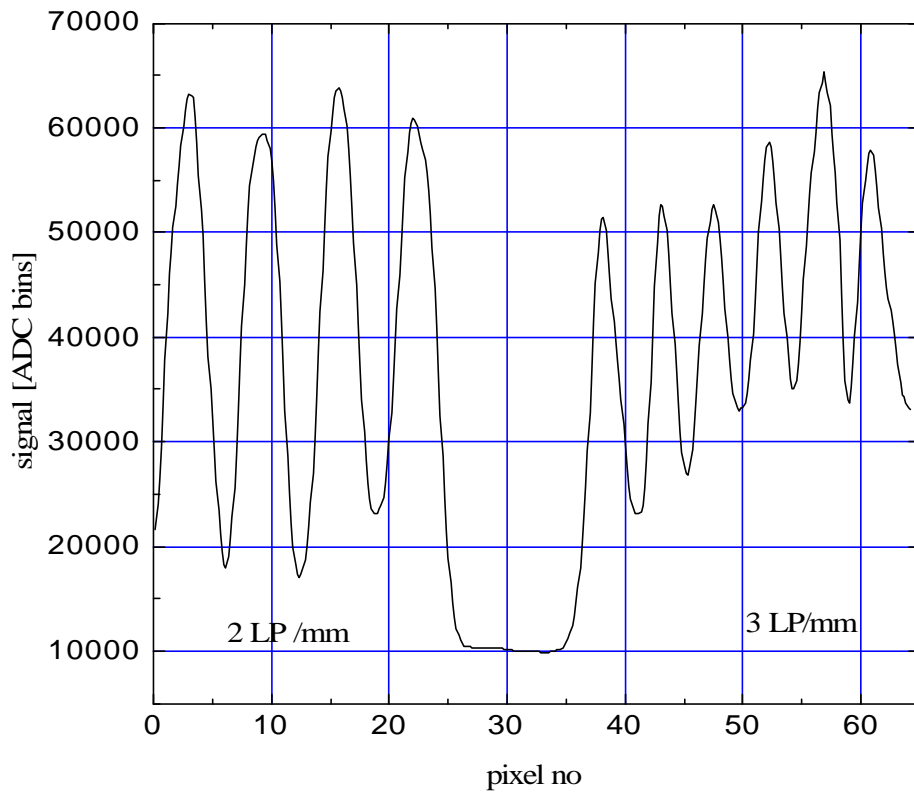


Figure 1: Recorded profile of a spatial resolution phantom showing clearly bar pattern with 2 and 3 LP/mm

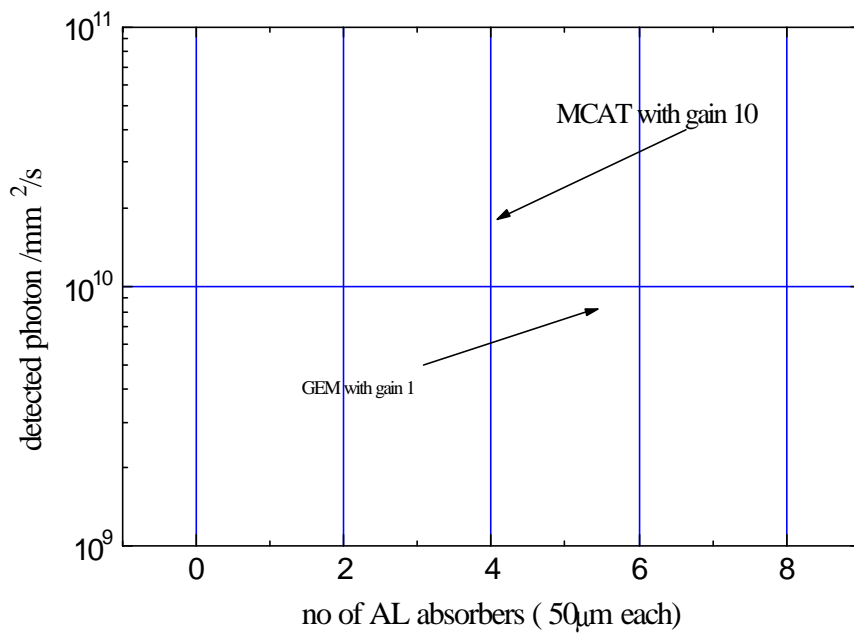


Figure 2: Response of the detector equipped with MCAT (and GEM) structure and operating with gas amplification of 10 (and 1) for different absorber thickness (photon flux densities)

Test of a fast PC-based data acquisition system for gas-filled position sensitive detectors

H.Mio¹, M.Chemloul¹, P.Laggner¹, H.Amenitsch¹, S.Bernstorff², M.Rappolt¹

¹ *Institute for Biophysics and X-ray Structure Research, Austrian Academy of Sciences, Steyrerg. 17, A-8010 Graz Austria*

² *Sincrotrone Trieste, SS 14, Km 163.5, 34012 Basovizza, Trieste, Italy*

The high flux of new generation synchrotron radiation sources requires fast position sensitive detectors with high count rate data acquisition systems capability. Though the local count rate in a gas-filled position-sensitive detector is limited by the space charge effect, the integral rate will increase with the area of the detector. Thus, more than several million events per second can be achieved. Therefore, we developed a new PC-based histogramming and control interface (HCI) with an intrinsic dead time lower than 200 ns for linear and area X-ray detectors for time-resolved measurement applications. During the tests this system has been operating the 1 dimensional delay-line detector (Gabriel-type) at the SAXS beamline. The tests were performed with a rotating tungsten plate positioned in the primary beam path, which generates a variable time structure due to a selectable number of holes in the disc (4, 45, 90 holes, diameter: 1 mm) and the rotating speed of the disc. The maximum rotation speed of the disc was 36000 rpm corresponding to a minimum opening time of 9 μ s.

To simulate a time resolved experiment we placed dry rat tail tendon collagen after the disc and recorded the diffraction pattern produced through the set-up. Therefore we used a disc with 4 holes and additionally we fixed a guard pinhole near to the rotating disk. The rotation speed of the disc was set to 50 rps. A photoelectric beam detection system on the opposite side of the disk produced a trigger signal at each time the hole was passing the synchrotron beam. For synchronisation with the data acquisition system we adjusted a variable delay on the PC-board to be able to start a cycle just before the next aperture was intersecting the beam. In one cycle about 80 frames, each with 10 μ s active and 1 μ s frame switching time, have been accumulated and summed in 1000 cycles. In fig 1 the resulting diffraction pattern of the experiment is shown depicting the effect of two holes passing the beam in one cycle. The exposure time of the sample during a single pass of the hole was calculated to be approximately 360 μ s.

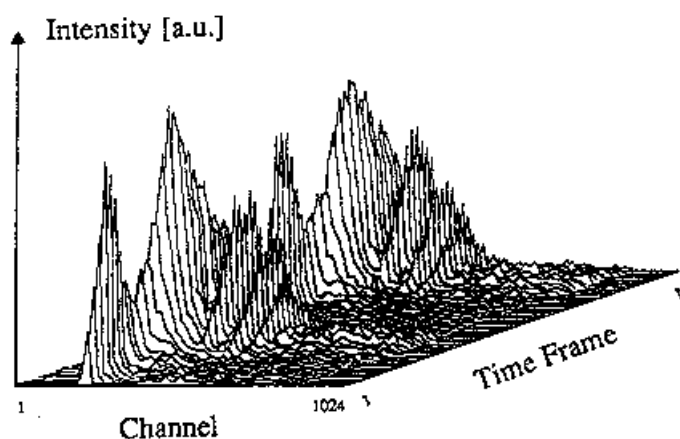


Fig. 1 Practical simulation of a time-resolved experiment with dry rat tail tendon collagen. During the passage of two apertures through the synchrotron beam the sample was exposed for about 360 μ s and several frames, each of 10 μ s recording time and 1 μ s wait time, have been taken.

It has been shown that experiments in the μ s-domain can be performed with a fast PC-based data acquisition system including external trigger facilities. The experiment has been published in [1].

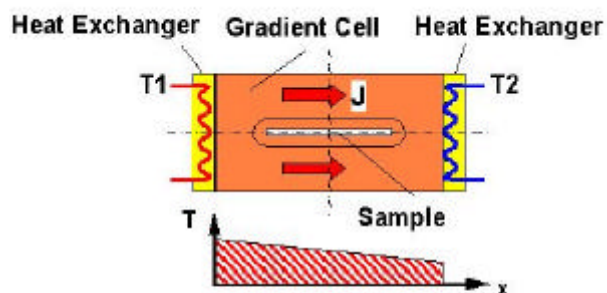
[1] H.Mio, M.Chemloul, P.Laggner, H.Amenitsch, S.Bernstorff, M.Rapplt, *Nucl. Instr. and Meth. A* **392**, (1997), 384-391.

Highly Resolving (< 10 mK) Temperature-Gradient-Cell for X-ray Scattering Studies on Solutions

Michael Rappolt¹, Heinz Amenitsch¹, Sigrid Bernstorff² and Peter Laggner¹

1. Institute of Biophysics and X-ray Structure Research, Austrian Academy of Science, Steyrergasse 17, 8010 Graz, Austria.

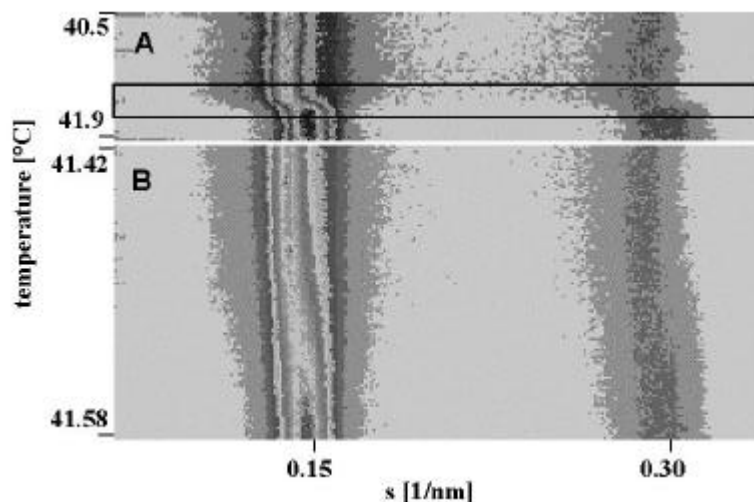
2. Sincrotrone Trieste, Experimental Division, SS14, 163.5 km, 34012 Basovizza (Trieste), Italy.



Gradients: 0.1-10 °C/cm
Scanning Steps: 50 μm
Total Length: 60 mm
Spot Width: 100 μm
Exposure Times: 50 s

A temperature gradient cell for X-ray scattering investigations on the thermal behaviour of soft matter manybody-systems, such as in gels, dispersions and solutions, has been developed. Depending on the adjustment of the temperature gradient in the sample, on the focus size of the X-ray beam and on the translational scanning precision an averaged thermal resolution of a few thousands of a degree can be achieved. This is at least one order of magnitude better than what can be reached in commonly carried out temperature scan experiments using either a thermostated water-circuit or electrical devices such as, e.g., a Peltier element. Moreover, the method guarantees best equilibrium conditions in the sample.

The resolving power has been demonstrated in first pilot experiments on the main transition of lecithin. In the figures A and B the contour plots of this transition display the first two order peaks of the liquid crystalline phase (in each case lower half) and the ripple phase (in each case upper half), respectively. In this experiment the temperature gradient was set to 0.28 °C/cm, the FW of the beam at the sample was 0.2 mm and the translational scanning was carried out in steps of 1 mm over a range of 1.40 °C (A) and in steps of 50 μm over a range of 0.16 °C (B), thus achieving nominal thermal resolutions of 0.028 °C (A) and 0.0014 °C (B), respectively. Simply spoken, figure B shows a zoomed part of A (rectangular box).



Detector Tests with a 2 Dimensional Energy Dispersive X-Ray Pixel Detector with Interpolating Read-Out Structure

A. Sarvestani³, R.H. Menk¹, H. Amenitsch², F. Arfelli¹, S. Bernstorff¹, P. Dubcek¹, W. Meissner³, G. Pabst², M. Rappolt²

- 1.) *Sincrotrone Trieste, Strada Statale, SS14, km163.5, 34012 Basovizza, Trieste, Italy.*
- 2.) *Institute of Biophysics and X-ray Structure Research, Austrian Academy of Science, Steyrergasse 17, 8010 Graz, Austria.*
- 3.) *Universität Siegen, Walter Flex Straße, 57068 Siegen, Germany.*

A two dimensional area detector based on a gas filled single photon counter was developed at the Universität Siegen and tested at the SAXS beam line at Sincrotrone Trieste. Among all possible applications for this kind of device, protein crystallography and small angle x-ray scattering experiments demand for the highest requirements. In particular, the ability of high count rates, good position resolution and high dynamic range have to be combined. Currently, no existing detector, neither integrators nor single photon counters, provide all three aspects simultaneously. The development of this new detector covers a wide range, including simulations, gas gain structures, two dimensional position encoding, high pressure effects and multi channel R/O-electronics.

The entrance window of the detector, through which incoming photons pass, works also as a drift electrode. Inside the gas region the photons are converted into primary electrons, drifting along the vertical drift field towards the gas gain structure. This structure is called MCAT and provides a gas gain $10^4 - 10^5$, depositing this on the read out structure below. This encoding structure contains a periodical arrangement of read out nodes with each one connected to an electronic channel (amplifier, FADC, etc.). The position of a single event is calculated by interpolation, using the charge distribution on the read out nodes surrounding the deposited charge. Compared to a pure pixel counter with the same sensitive area, this interpolating method provides a reduction of read out channels by a factor of 100 to 400.

The main focus of the experiments carried out at the SAXS beam line were the determination of the spatial resolution and the double spot discrimination utilizing a micro spot beam in combination with a multi purpose moving stage.

Depicted in figure 1 is the detector response of the collimated direct beam. For this measurement the detector was filled with a XeCO₂ (75/25) gas mixture at 1 bar pressure. The black area represents the entire photon-sensitive area of 1.4*1.4 cm² that consists of 49 read out pads or interpolation cells and 36 read out nodes, respectively. The beam is visible as a grey-scaled spot right in the middle of that area. Overlaid is a 3-d plot that corresponds to one interpolation cell with a size of 2 x 2 mm². Each pixel in this plot has a size of 100 x 100 μm². Even substructures of the direct beam are visible.

Figure 2 shows a recorded image of a double spot generated by a hole mask and the direct beam. The center to center pitch of both spots -that can be clearly distinguished- is 0.3mm. Utilizing a scatter foil it was possible to generate a homogenous illumination and to obtain images using a "SAXS"-shaped mask placed directly in front of the detector. The spots below are from 5 different holes (500μm diameter) with transparencies of 100%, 51%, 26%, 7% and 0.5% (using different aluminum foils for the attenuation). This measurement was carried out using a XeCO₂ (60/40) gas mixture at 1.2 bar.

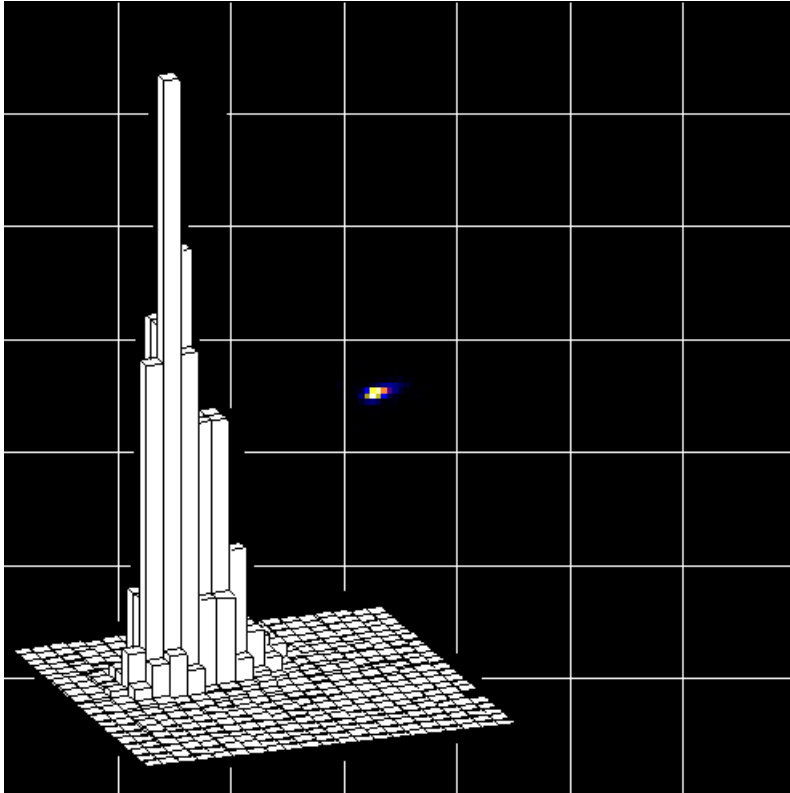


Figure 1

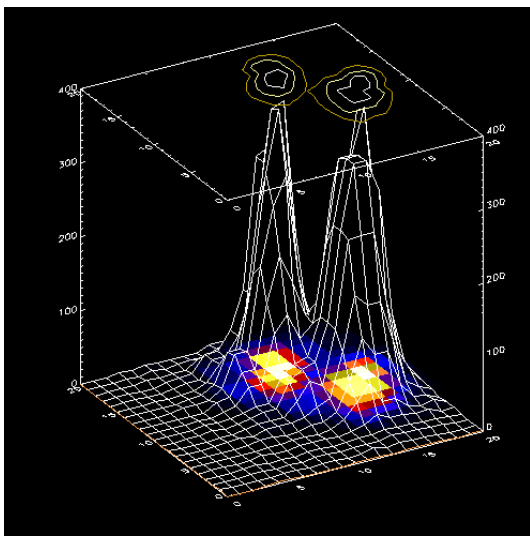


Figure 2.

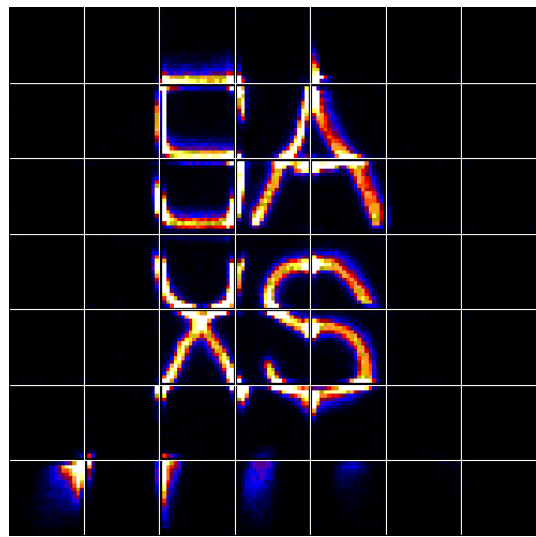


Figure 3

Publications

Publications in Papers in 1995

H. Amenitsch, S. Bernstorff and P. Laggner
High Flux Beamline for Small Angle X-Ray Scattering at ELETTRA
Rev. Sci. Instrum. 66, 1624-1626 (1995)

H. Amenitsch, B. Hainisch, P. Laggner and S. Bernstorff
The Potential of Asymmetric Monochromator Crystals for use in High-Power Insertion-Device Beamlines
Synchrotron Radiation News 8.4, 22-27 (1995)

Publications in Papers in 1997

H.Amenitsch, S.Bernstorff, M.Kriechbaum, D.Lombardo, H.Mio, M. Rappolt and P.Laggner
Performance and First Results of the ELETTRA High-Flux Beamline for Small Angle X-ray Scattering
J. Applied Crystallography 30, 872-876 (1997)

K. Pressl, M. Kriechbaum , M. Steinhart and P. Laggner
High Pressure Cell for Small- and Wide-Angle X-Ray Scattering
Rev. Sci. Instrum. 68 (1997) 4588-4592

G Margaritondo, A. Savoia, S. Bernstorff, M. Bertolo, G. Comelli, F. De Bona, W. Jark, M. Kiskinova, G. Paolucci, K. Prince, A. Santaniello, G. Tromba, R. Walker and R. Rosei
The Ultrabright Synchrotron Source ELETTRA: First Period of Operation
Acta Physica Polonica A91, 631-640 (1997)

H. Mio, M. Chemloul, P. Laggner, H. Amenitsch, S.Bernstorff and M. Rappolt
Fast PC-based Data Acquisition System for Gas-filled Position Sensitive Detectors
Nuclear Instrum.&Methods A 392 (1997) 384-391

Publications in Papers until May 1998

H.Amenitsch, S.Bernstorff, M. Rappolt, Kriechbaum, H.Mio and P.Laggner
First Performance Assessment of the SAXS Beamline at ELETTRA
J. Synchrotron Rad. 5 (1998) 506-508

H. Amenitsch, C.C. Ashley , M.A. Bagni , S. Bernstorff, G. Cecchi , B. Columbini and P.J. Griffiths
Meridional X-ray diffraction intensity changes during sinusoidal length oscillations in skeletal muscle fibres of Rana temporaria
J.Physiol. 505 (1998) 88

M.Zehetbauer, P.Les
Micromechanisms of Plastic Deformation in Metals
Metallic Materials 36 (3) (1998)

Publications in Papers, submitted

H. Amenitsch, S. Bernstorff, A. Bigi, N. Roveri and J. S. Shah
D-Periodicity in Intramuscular Collagen
Connective Tissue Research, in preparation.

H.Amenitsch, M. Kriechbaum, D. Lombardo, H. Mio, G. Pabst, M.Rappolt, P.Laggner and S.Bernstorff
The Small Angle X-Ray Scattering Beamline at ELETTRA: A New Powerful Station for Fast Structural Investigations on Complex Fluids with Synchrotron Radiation
Nuovo Cimento, in press

Baldrian J., Sikora A., Steinhart M., Vlèek P., Horky M., Amenitsch H., Bernstorff S.,
Time-resolved SAXS Study of Crystallization of Poly (ethylene oxide) / Poly (methyl methacrylate) Blends
Polymer, in press

S. Bernstorff, H. Amenitsch and P. Laggner
The High Throughput Double Crystal Monochromator of the SAXS Beamline at ELETTRA
J. Synchrotron Rad., in press

V. Erokhin, S. Carrara, S. Bernstorff, H. Amenitsch and C. Nicolini
Semiconductor Nanoparticles for Quantum Device
Nanotechnology, in press

P. Fratzl, K. Misof, Ivo Zizak, G. Rapp, H. Amenitsch and S. Bernstorff
Fibrillar Structure and Mechanical Properties of Collagen
J. Struct. Biol., in press

P.J. Griffiths, H. Amenitsch, C.C. Ashley, M.A. Bagni, S. Bernstorff, G. Cecchi, B. Colombini and G. Rapp
Studies on the 14.5 nm meridional X-ray reflection during length changes of intact frog muscle fibres
Proceedings of Symposium on: "Mechanism of Work Production and Work Absorption in Muscle", Hakone, Japan, 27-31 October 1997, Plenum Press, New York, in press

T. Javorfi, Z. Cseh, I. Simidjiev, S. Borbely, H. Amenitsch, P. Laggner and G. Garab
Structure and dynamics of thylakoid membranes and lamellar aggregates of LHCII
in prep.

M. Linari, M. Reconditi, L. Lucii, H. Amenitsch, S. Bernstorff, G. Piazzesi and V. Lombardi
Modulation of intensity of the M3 reflection by pharmacological and mechanical means in tetanized single fibres from frog skeletal muscle
Pflügers Arch. 1998, in press

M.Lucic-Lavcevic, P.Dubcek, O.Milat, B.Etlinger, A.Turkovic, D.Sokcevic and H.Amenitsch,
Nanostructure of sol-gel TiO₂ thin films on glass substrate measured by small angle scattering of synchrotron light,
Materials Letters, in press

M.Lucic-Lavcevic, A.Turkovic, D.Sokcevic, P.Dubcek, O.Milat, B.Etlinger, P.Laggner and H.Amenitsch,
Small angle scattering of synchrotron radiation onnanosized TiO₂ thin films obtained by chemical vapour deposition and spray method,
Fizika, submitted

R.H. Menk, F. Arfelli, S.Bernstorff, A.Sarvestani, H.J.Besch, A.H.Walenta
A fast 1-D detector for imaging and time resolved SAXS experiments
Nucl. Instrum., submitted

M. Rappolt, K. Pressl, G. Pabst and P. Laggner
L_α-Phase Separation in Phosphatidylcholine-Water Systems Induced by Alkali Chlorides
BBA, in press

E.Schafler, M.Zehetbauer, I.Kopacz, B.Ortner, S.Bernstorff, H.Amenitsch, T.Ungar
Local Dislocation Densities and Internal Stresses by High Lateral Resolution Peak Profile Analysis in Plastically Deformed Polycrystalline Nickel
Scripta Mater., in preparation

M. Steinhart, M. Kriechbaum, K. Pressl, H. Amenitsch, P. Laggner and S. Bernstorff
High-Pressure Instrument for Small- and Wide-Angle X-ray Scattering. II: Time-Resolved Experiments
Rev. Sci. Instrum., submitted

A.Turkovic, M.Lucic-Lavcevic, A.Drasner, P.Dubcek, O.Milat, B.Etlinger, D. Sokcevic, H.Amenitsch and M.Rappolt
Small angle X-ray scattering studies of nanophase TiO₂ thin films at ELETTRA Materials Science & Engineering B, submitted

M. Zehetbauer, T. Ungar, R. Kral, A. Borbely, E. Schafler, B. Ortner, H. Amenitsch and S. Bernstorff
Scanning X-ray Diffraction Peak Profile Analysis in Deformed Polycrystals by Synchrotron Radiation
J.Appl.Phys., submitted

International Conferences and Workshops in 1993

H. Amenitsch, S. Bernstorff and P. Laggner
High Flux Beamline for SAXS at ELETTRA
Sincrotrone Trieste, Preprint ST/S-P-93/13 (March 1993)

IXth International Conference on Small-Angle Scattering, Saclay, France, April 27-30, 1993

H. Amenitsch, S. Bernstorff and P. Laggner
High Flux Beamline for SAXS at ELETTRA
First Congress of the European Synchrotron Radiation Society, Grenoble, France,
September 22-23, 1993

International Conferences and Workshops in 1994

P. Laggner, H. Amenitsch, M. Kriechbaum, H. Mio, S. Bernstorff and M. Steinhart
Die Österreichische Hochfluß-Röntgenbeugungsstation bei ELETTRA
Proceedings of the "Österreichische Chemietage 1994", Graz, 28. September 1994

H. Amenitsch, S. Bernstorff and P. Laggner
High Flux Beamline for SAXS at ELETTRA
5th International Conference on Synchrotron Radiation Instrumentierung (SRI94),
Stonybrook, New York, USA, July 18-22, 1994

International Conferences and Workshops in 1995

H.Amenitsch, S.Bernstorff, M.Kriechbaum, D.Lombardo, K.Pressel, H.Mio and P.Laggner
Small Angle X-ray Scattering at ELETTRA - A Powerful Method for Structure Determination in the Submicron Range
Congress "La Ricerca in Fisica nell'Universita' di Trieste", Trieste, Italy, May 10-12, 1995

H.Amenitsch, S.Bernstorff, M.Kriechbaum, D.Lombardo, H.Mio, K.Pressel and P.Laggner
The High-Flux beamline for SAXS at ELETTRA
5th International Conference on Biophysics and Synchrotron Radiation, Grenoble, France,
August 21-25, 1995

H.Amenitsch, S.Bernstorff, M.Kriechbaum, D.Lombardo, H.Mio, K.Pressel and P.Laggner
Status of the High-Flux beamline for SAXS at ELETTRA
Third Congress of SILS (Società Italiana Luce di Sincrotrone), Modena, Italy, September
18-19, 1995

International Conferences and Workshops in 1996

H. Amenitsch, C.C. Ashley, S. Bernstorff, M.A. Bagni, G. Cecchi and P.J. Griffiths
Time-resolved X-ray diffraction studies on intact single muscle fibres using the newly commissioned SAXS beamline at Elettra
4th User's Meeting, Sincrotrone Trieste, Trieste, Italy, December 2-3, 1996

H.Amenitsch, S.Bernstorff, M.Kriechbaum, D.Lombardo, H.Mio and P.Laggner
Layout and Status of the new High-Flux SAXS Station at ELETTRA
X International Conference on Small-Angle Scattering, Campinas, Brazil, July 21-25, 1996

H.Amenitsch, S.Bernstorff, M.Kriechbaum, D.Lombardo, H.Mio, M. Rappolt and P.Laggner
Layout and first results from the new high-flux beamline for Small Angle X-ray Scattering at ELETTRA

International Conference on "New Opportunities for Research at 3rd Generation Light Sources", Lipica, Slovenia, May 25-29, 1996

H.Amenitsch, S.Bernstorff, M.Kriechbaum, D.Lombardo, H.Mio, M. Rappolt and P.Laggner
Performance and First Results of the new ELETTRA High-Flux SAXS beamline
X International Conference on Small-Angle Scattering, Campinas, Brazil, July 21-25, 1996

H. Amenitsch, S. Bernstorff, M. Kriechbaum, H. Mio, M. Rappolt and P. Laggner
SAXS sample stage
4th User's Meeting, Sincrotrone Trieste, Trieste, Italy, December 2-3, 1996

H. Amenitsch, S. Bernstorff, M. Kriechbaum, H. Mio, M. Rappolt and P. Laggner
Elettra's High-Flux Beamline for Small Angle X-ray Scattering: Status and Perspectives
4th User's Meeting, Sincrotrone Trieste, Trieste, Italy, December 2-3, 1996

S.Bernstorff
Requirements for 1D- and 2D-detectors for time-resolved Small-Angle-X-ray Scattering (SAXS) Experiments at third generation synchrotron radiation storage rings
2nd European Workshop on Imaging Detectors, Dublin, Ireland, September 17-18, 1996

S. Carrara, V. Erokhin, P. Facci and C. Nicolini
On the Nanoparticles Structure formed in Langmuir-Blodgett Films
4th User's Meeting, Sincrotrone Trieste, Trieste, Italy, December 2-3, 1996

P. Fratzl
Small-Angle X-Ray Scattering Investigations of Collagen and Bone
4th User's Meeting, Sincrotrone Trieste, Trieste, Italy, December 2-3, 1996

M. Kriechbaum, M. Steinhart, K. Pressl and P. Laggner
Design of a Compact High-Pressure X-Ray Diffraction Cell for Hydrostatic Pressures up to 3000 bar
X.Intern. SAS Conference, Campinas, Brasilien, July 21-25, 1996,

M. Kriechbaum, M. Steinhart, K. Pressl and P. Laggner
Design of a Compact High-Pressure X-Ray Diffraction Cell
XVII. Congress & General Assembly of the Internatl. Union of Crystallography, Seattle, USA, August 8.-17, 1996

M. Kriechbaum, M. Steinhart, K. Pressl, P. Laggner, H. Amenitsch, M. Rappolt and S. Bernstorff
Design and Test of a Compact High-Pressure X-Ray Diffraction Cell for Hydrostatic Pressures up to 3000 bar at the SAX beamline at ELETTRA
4th User's Meeting, Sincrotrone Trieste, Trieste, Italy, December 2-3, 1996

P. Laggner, H. Amenitsch, S. Bernstorff, M. Kriechbaum, M. Rappolt and H. Mio
First performance assessment of the SAXS-Beamline at ELETTRA
4th User's Meeting, Sincrotrone Trieste, Trieste, Italy, December 2-3, 1996

Robert Schwarzenbacher, Heinz Amenitsch, Peter Laggner, M. Rappolt and S. Bernstorff
SAXS- Characterisation of Liquid Crystal Immobilisation Matrices for Biocatalytic Processes
4th User's Meeting, Sincrotrone Trieste, Trieste, Italy, December 2-3, 1996

M.Zehetbauer, R. Kral, T. Ungar, A. Borbely, B. Ortner, S. Bernstorff and H. Amenitsch
X-Ray Diffraction Peak Profile Analysis in Deformed Metallic Polycrystals by Synchrotron Radiation
4th User's Meeting, Sincrotrone Trieste, Trieste, Italy, December 2-3, 1996

International Conferences and Workshops in 1997

H. Amenitsch, C.C. Ashley , M.A. Bagni , S. Bernstorff, G. Cecchi , B. Columbini and P.J. Griffiths
Meridional X-ray diffraction intensity changes during sinusoidal length oscillations in skeletal muscle fibres of Rana temporaria
Meeting of the Physiological Society UMDS (St. Thomas's), London, Great Britain, November 6-8, 1997

H. Amenitsch, S. Bernstorff, P. Dubcek, M. Kriechbaum, R. Menk, H. Mio, G. Pabst, M. Rappolt, M. Steinhart and P. Laggner
Real-Time SWAXS Studies of Superstructural and Molecular Changes in Biological and Synthetical Materials at ELETTRA
Fifth User's Meeting, Sincrotrone Trieste, Trieste, Italy, December 1-2, 1997

H.Amenitsch, S.Bernstorff, M.Kriechbaum, R. Menk, H.Mio, M. Rappolt and P.Laggner
Die österreichische Kleinwinkelstation am Speicherring ELETTRA: Status und Perspektiven
Österreichische Physikertagung, Vienna, Austria, September 22-26, 1997

H.Amenitsch, S. Bernstorff, M. Kriechbaum, D. Lombardo, H. Mio, M.Rappolt and P.Laggner
The Small Angle X-Ray Scattering Beamline at ELETTRA: A New Powerful Station for Fast Structural Investigations on Complex Fluids with Synchrotron Radiation
International Conference on "The Morphology and Kinetics of Phase Separating Complex Fluids", Messina, Italy, June 24-28, 1997

H.Amenitsch, M. Rappolt, M.Kriechbaum, H.Mio, P.Laggner and S.Bernstorff
The Small Angle X-ray Scattering Beamline at ELETTRA: A New Powerful Station for Structural Investigations with Synchrotron Radiation (talk)
Sixth Croatian-Slovenian Crystallographic Meeting, Umag, Croatia, June 19-21, 1997

H. Amenitsch, S. Bernstorff, M. Kriechbaum, H. Mio, M. Rappolt, M. Steinhart and P. Laggner

Submillisecond time-resolved SAXS-experiments at ELETTRA on structural changes induced by rapid variations of external field parameters (e.g. pressure, temperature, tension, mixing)

Satellite meeting (of 6th. International Conference on Synchrotron Radiation Instrumentation (SRI 97)) on "Crystallographic Applications - Time Resolved X-ray Experiments", August 1 - 2, 1997, at Photon Factory, Tsukuba, Japan

H.Amenitsch, S.Bernstorff, M. Kriechbaum, M. Rappolt and P.Laggner

Ein Jahr Nutzerbetrieb an der österreichischen Kleinwinkelstation am Speicherring ELETTRA

Österreichische Physikertagung, Vienna, Austria, September 22-26, 1997

H.Amenitsch, S.Bernstorff, M.Kriechbaum, M. Rappolt and P.Laggner

The Austrian Small Angle X-Ray Scattering Station at ELETTRA: Status and Experimental Perspectives

Quinto Convegno SILS (Società Italiana di Luce di Sincrotrone), Pavia, Italy, July 20-22, 1997

H. Amenitsch, S. Bernstorff, M. Kriechbaum, M. Steinhart, K. Pressl and P. Laggner
Time-resolved X-Ray Diffraction Experiments with a New Developed Compact High Pressure Cell

The 6th International Conference on Synchrotron Radiation Instrumentation (SRI97), Himeji, Japan, August 4-8, 1997

H.Amenitsch, S.Bernstorff, M. Rappolt, Kriechbaum, H.Mio and P.Laggner

First Performance Assessment of the SAXS Beamline at ELETTRA

The 6th International Conference on Synchrotron Radiation Instrumentation (SRI97), Himeji, Japan, August 4-8, 1997

Proceedings: J. Synchrotron Rad., in print

S.Bernstorff, H. Amenitsch, P. Dubcek, M. Kriechbaum, R. Menk, H. Mio, G. Pabst, M. Rappolt and P. Laggner

What's new at the SAXS-beamline in 1997?

Fifth User's Meeting, Sincrotrone Trieste, Trieste, Italy, December 1-2, 1997

S. Bernstorff, H. Amenitsch and P. Laggner

The High Throughput Double Crystal Monochromator of the SAXS Beamline at ELETTRA

The 6th International Conference on Synchrotron Radiation Instrumentation (SRI97), Himeji, Japan, August 4-8, 1997

Proceedings: J. Synchrotron Rad., in print

P.Dubcek, O.Milat, M.Lucic-Lavcevic, A.Turkovic B.Etlinger, and H.Amenitsch

Small Angle X-ray Scattering and X-ray reflection on Thin Films

Book of Abstracts: Sixth Slovenian-Croatian Crystallographic Meeting, 57, Umag, Croatia, June 19-21, 1997.

P.Dubcek, O.Milat, M.Lucic-Lavcevic, A.Turkovic B.Etlinger, and H.Amenitsch
Small Angle X-ray Scattering and X-ray reflection on Thin Films
Fifth User's Meeting, Sincrotrone Trieste, Trieste, Italy, December 1-2, 1997

P. Fratzl, K. Misof, S.Rinnerthaler, I. Zizak, K. Klaushofer, G. Rapp, H. Amenitsch and S. Bernstorff
Kollagen und Knochen - Mesoskopische Struktur und biomechanische Eigenschaften
Statusseminar der Ludwig-Maximilians Univ. München bzgl: "Erforschung kondensierter Materie mit Neutronen, nuklearen Sonden, Ionenstrahlen und Synchrotronstrahlung" im Kloster Seon, Germany, September 14.-17, 1997

M. Gailhofer, H. Amenitsch, S. Bernstorff and P. Laggner
Human Low Density Lipoproteins (LDL)-Microphase Separation
Fifth User's Meeting, Sincrotrone Trieste, Trieste, Italy, December 1-2, 1997

P.J. Griffiths, H. Amenitsch, C.C. Ashley, M.A. Bagni, S. Bernstorff, G. Cecchi, B. Colombini and G. Rapp
Studies on the 14.5 nm meridional X-ray diffraction reflection during length changes of intact frog muscle fibres
Symposium on: "Mechanism of Work Production and Work Absorption in Muscle", Hakone, Japan, October 27-31, 1997

Horky M., Baldrian J., Steinhart M.
Crystallization of poly (ethylene oxide) / poly (methyl methacrylate) mixtures (in Czech)
2nd Seminar: Student and Postgraduate Papers on Crystallography and Structure Analysis, Prague 1997
Mater.Struct.Chem.Biol.Phys.Technol. **4**, 25 (1997) (Abstract)

M.Kriechbaum, M.Steinhart, K.Pressl and P.Laggner
Time resolved X-Ray Diffraction Experiments up to 3000 bar with a New Developed Compact High Pressure X-Ray Cell.
Annual Meeting of the American Crystallographic Association, St.Louis, MO, USA, July 19-25, 1997

M.Kriechbaum, M.Steinhart, P.Laggner, H.Amenitsch, S. Bernstorff and Y.Hiragi
Time-resolved Small-Angle X-ray Scattering of Jump-Relaxation and Stopped-Flow Experiments of Lipids and Proteins
Fifth User's Meeting, Sincrotrone Trieste, Trieste, Italy, December 1-2, 1997

M.Lucic-Lavcevic P.Dubcek, O.Milat, B.Etlinger, A.Turkovic and H.Amenitsch,
Small angle scattering of synchrotron light on nanophase TiO₂ measured at ELETTRA
Book of Abstracts: Sixth Slovenian- Croatian Crystallographic Meeting, 57, Umag, Croatia, June 19-21, 1997

K.Misof, I. Zizak, G. Rapp, S.Bernstorff, H.Amenitsch and P. Fratzl
Elastische Eigenschaften von Kollagen
Österreichische Physikertagung, Vienna, Austria, September 22-26, 1997

G. Pabst, M. Rappolt, H. Amenitsch, S. Bernstorff and P. Laggner
Realtime X-ray Diffraction Studies on the Formation of Intermediates in Phospholipids induced by Laser T-jump
Fifth User's Meeting, Sincrotrone Trieste, Trieste, Italy, December 1-2, 1997

Michael Rappolt, Heinz Amenitsch, Sigrid Bernstorff and Peter Laggner
Highly Resolving Temperature-Gradient-Cell for X-ray Scattering Studies on Solutions
Fifth User's Meeting, Sincrotrone Trieste, Trieste, Italy, December 1-2, 1997

R. Rizzo, S. Bernstorff, H. Amenitsch and F. Vittur
Collagen Fibril Structure in Normally Loaded and Unloaded Regions of Articular Cartilages: A SAXS Study
Fifth User's Meeting, Sincrotrone Trieste, Trieste, Italy, December 1-2, 1997

M. Zehetbauer, T. Ungar, R. Kral, A. Borbely, E. Schafner, B. Ortner, H. Amenitsch and S. Bernstorff
Scanning X-ray Diffraction Peak Profile Analysis (XPA) in Deformed Cu-Polycrystals by Synchrotron Radiation
Österreichische Physikertagung, Vienna, Austria, September 22-26, 1997

M. Zehetbauer, T. Ungar, R. Kral, A. Borbély, E. Schafner, B. Ortner, H. Amenitsch, S. Bernstorff
Local Fluctuations of Dislocation Microstructure in Large Strain Deformed Cu by Scanning Diffraction Profile Analysis
Fifth User's Meeting, Sincrotrone Trieste, Trieste, Italy, December 1-2, 1997

M. Zehetbauer, T. Ungar, R. Kral, A. Borbely, E. Schafner, B. Ortner, H. Amenitsch, S. Bernstorff
Scanning X-ray Diffraction Peak Profile Analysis (XPA) in Deformed Cu-Polycrystals by Synchrotron Radiation
Jahrestagung der Oesterr. Physikal. Gesellschaft, Wien, Austria (Sept. 1997)

A. Zidansek, H. Amenitsch, M. Rappolt, S. Bernstorff, S. Kralj, G. Lahajnar and R. Blinc
Smectic Ordering in Porous Glasses: A Small Angle X-Ray Scattering Study
Fifth User's Meeting, Sincrotrone Trieste, Trieste, Italy, December 1-2, 1997

International Conferences and Workshops until May 1998

H. Amenitsch, G. Balducci, S. Bernstorff, M. Linari, V. Lombardi, L. Lucii and G. Piazzesi
Mechanical and structural evidence for the limited contribution by cross-bridges to the enhanced shortening capability following stretch of single muscle fibres
VI Convegno SILS Padova, 18-20 Giugno 1998

Baldrian J., Horky M., Steinhart M., Sikora A., Vlèek P., Amenitsch H., Bernstorff S.
Time-resolved SAXS/WAXS study of polymer blends crystallization
4th International Workshop on X-Ray Investigations of Polymer Structure XIPS'98, Bialsko-Biala 1998

Horky M., Baldrian J., Sikora A., Steinhart M., Vlèek P., Amenitsch H., Bernstorff S.
Integral and nonintegral folding in poly (ethylene oxide) / poly (methyl methacrylate) blends

18th European Crystallographic Meeting, Prague 1998

R.H. Menk, F. Arfelli, S. Bernstorff, A. Sarvestani, H.J. Besch, A.H. Walenta

A fast 1-D detector for imaging and time resolved SAXS experiments

Symposium on: "Radiation Measurements and Applications", Ann Arbor, Michigan, USA,
May 12-14, 1998

A. Turkovic, M. Lucic-Lavcevic, D. Sokcevic, A. Drasner, P. Dubcek, O. Milat, B. Etlinger
and H. Amenitsch

Studij rasprsenja X-zraka pod malim kutem na nanofaznim TiO₂ tankim filmovima na ELETTRI

Zbornik sazetaka s V. Susreta vakuumista Hrvatske i Slovenije, 20.05.1998., Institut
"Ruder Boskovic", p.15-16

T. Ungar and M. Zehetbauer

Internal Stresses and Microstructure at Large Strains in Cell-Forming Materials

European Research Conference "Plasticity of Materials", Granada, Spain, April 25-30,
1998

M. Zehetbauer

Micromechanisms of Plastic Deformation in Metals

2nd Intern. Coll. "Materials Structure & Micromechanics of Fracture", (MSMF-2), Brno,
Czech Republic, July 1-3, 1998

Non-refereed Publications in 1992

S. Bernstorff

Heat Load and Monochromator Crystals: what can be done ?

Sincrotrone Trieste, Technical Note ST/S-TN-92/10 (1992)

Non-refereed Publications in 1993

H. Amenitsch and S. Bernstorff

Specification of the Double Crystal Monochromator for the SAXS Beamline

Sincrotrone Trieste, Technical Note ST/S-TN-93/63 (1993)

H. Amenitsch and S. Bernstorff

Specification of a Chamber for a Segmented Toroidal Mirror for the SAXS Beamline

Sincrotrone Trieste, Technical Note ST/S-TN-93/45 (1993)

H. Amenitsch, S. Bernstorff and P. Laggner

Study of the Performance of the SAXS-Beamline

Sincrotrone Trieste, Internal Report ST/S-R-93/7 (1993)

Non-refereed Publications in 1994

H. Amenitsch and S. Bernstorff

Specification of an Internally Water-Cooled Cu-Block for the SAXS Beamline at ELETTRA
Sincrotrone Trieste, Technical Note ST/S-TN-94/48 (1994)

Non-refereed Publications in 1995

H. Amenitsch and S. Bernstorff

Asymmetric Monochromator Crystals for High-Brightness Insertion-device Beamlines
ELETTRA News Vol. I, Number 2, November 22nd, 1995

Non-refereed Publications in 1996

M.Zehetbauer, T.Ungar, R.Kral, A.Borbely, B.Ortner, S.Bernstorff, H.Amenitsch
Scanning Wide-Angle Micro Diffraction: The First Material Science Experiment at the
New Austrian Saxs beamline.

ELETTRA News Vol.I, Number 8, May 17th (1996)

S. Bernstorff , H. Amenitsch, M. Rappolt and P. Laggner

The new Austrian beamline for small angle X-Ray scattering reaches design parameters
and goes into user operation.

ELETTRA News Vol. I, Number 12, September 16th, (1996)

Non-refereed Publications until May 1998

G. Pabst, H. Amenitsch, C. Krenn, M. Rappolt, P. Laggner and S. Bernstorff

Infrared-Laser T-jumps with 10^4 K/sec at the SAXS beamline.

ELETTRA News Number II, Number 21, March 31th (1998)

and ELETTRA Highlights (1998)

M. Rappolt, H. Amenitsch, S. Bernstorff and P. Laggner

Highly resolving (<10 mK) Temperature-Gradient Cell for X-ray Scattering Studies on
Solutions

ELETTRA News Number II, Number 23, May 29 (1998)

and ELETTRA Highlights (1998)

M. Kriechbaum, P. Laggner, M. Steinhart, K. Pressl, C. Krenn, H. Amenitsch, S. Bernstorff
and M. Rappolt

300 MPa Jump-Relaxation Studies of Phase Transitions Investigated by Time-Resolved
Small-Angle X-Ray Scattering in the ms range

ELETTRA Highlights (1998)

Peter Fratzl, Klaus Misof, Ivo Zizak, Gert Rapp, Heinz Amenitsch, Sigrid Bernstorff
In-situ Synchrotron X-Ray Scattering Study of the Tensile Properties of Collagen
ELETTRA Highlights (1998)

Doctoral Theses

Klaus Misof
Supramolekulare Struktur und mechanische Eigenschaften von Kollagen und Bindegewebe
Universität Wien, Austria, May 1997

Angelika Latal
Membrane Specificity of Antimicrobial Peptides
TU Graz, Biochemie, Dr. techn. Promotion 5.12.97

Karin Pressl
Röntgenographische Untersuchung von Phasenübergängen in hydratisiertem Diacyl-Phosphatidylcholin als Funktion der Temperatur und des Drucks
TU Graz, Physik, Dr. techn. Promotion 25.7.97

Diploma Theses

M.G. Fantozzi
Il fascio della linea SAXS di Elettra: diagnostica e suo uso nella determinazione della DQE di un rivelatore ad area
Università di Padova, 1997

Robert Schwarzenbacher
Die Untersuchung der flüssigkristallinen Strukturen des ternären Systems Brij35 / Dibutylether H₂O in Hinsicht ihrer Verwendung als Immobilisationsmatrix für eine biokatalytische Umsetzung
TU Graz, Biotechnol., Dipl. Ing. Sponsion 18.7.97

Author Index

AMENITSCH, H.	42 44 46 48 50 53 55 56 59 62 63 64 67 68 69 71 75 77 79 80 81 84 85 87 91 95 97 99 100 101
ARFELLI, F.	97 101
ASHLEY, C.C.	56
BAGNI, M.A.	56
BALDRIAN J.	42
BERNSTORFF, S.	42 44 46 48 50 55 56 59 62 67 68 71 75 77 79 80 81 85 95 97 99 100 101
BIGI, A.	55
BLINC, R.	60
BORBELY, A.	46 48
BORBÉLY, S.	63
CARRARA, S.	57
CECCHI, G.	56
CHEMLOUL, M.	99
CSEH, Z.	63
DUBCEK, P.	84 87 97 101
EROKHIN, V.	57
ETLINGER, B.	84 87
FERRACINI, E.	90
FERRERO, A.	90
FRATZL, P.	59
GAILHOFER, M.	62
GARAB, G.	63
GRIFFITHS, P.J.	56
GUTBERLET, T.	64
HEERKLOTZ, H.	64
HEUMANN, H.	75 81
HIRAGI, Y.	68
HORKY, M.	42
JÁVORFI, T.	63
KISKINOVA, M.	85
KLOSE, G.	64
KOPACZ, I.	44
KRAL, R.	46 48
KRALJ, S.	50
KRENN, C.	77
KRIECHBAUM, M.	67 68 91
KÜHNE, CH.	53
LAGGNER, P.	53 62 63 67 68 77 79 91 99 100
LAHAJNAR, G.	50
LATAL, A.	69
LAUER, I.	75 81
LINARI, M.	71

LOHNER, K	69
LOMBARDI, V.	71
LONZA, D.	85
LUCIC-LAVCEVIC, M.	84 87
LUCII, L.	71
MACCIONI, E.	73
MÄDLER, B.	64
MALTA, V.	90
MARIANI, P.	73
MATTEUCCI, M.	85
MEISSNER, W.	101
MENK, R.H.	97 101
MILAT, O.	84 87
MIO, H.	99
MISOF, K.	59
MUSTÁRDY, L.	63
NAWROTH, T.	75 81
NICOLINI, C.	57
ORTNER, B.	44 46 48
OTTANI, S.	90
OTTONELLO, P.	95
PABST, G.	77 97 101
PIAZZESI, G.	71
PONTONI, D.	97
PRESSL, K.	79
PRINCE, K.C.	85
RAPP, G.	59
RAPPOLT, M.	50 53 64 77 79 80 97 99 100 101
RECONDITI, M.	71
RIZZO, R.	80 85
ROMANZIN, L.	85
RÖBLE, M.	75 81
ROSTA, L.	63
ROTTIGNI, G.A.	95
ROVERI, N.	55
SARVESTANI, A.	97 101
SCHAFLER, E.	44 48
SCHWARZENBACHER, R.	91
SHAH, J.S.	55
SPINOZZI, F.	73
STAUDEGGER, E.	69
STEINHART, M.	42 67
TURKOVIC, A.	84 87
UNGÁR, T.	44 46 48
VITTUR, F.	80 85
VLÈEK, P.	42
ZANELLA, G.	95
ZANNONI, R.	95

ZEHETBAUER, M.	44 46 48
ZIDANSEK, A.	50
ZIZAK, I.	59